Implants à base de PLGA pour la libération oculaire

Corinna Bode

UNIVERSITE DE LILLE
Faculté des Sciences Pharmaceutiques et Biologiques
Ecole Doctorale Biologie-Santé

PLGA IMPLANTS FOR OCULAR DRUG DELIVERY

—

IMPLANTS A BASE DE PLGA POUR LA LIBERATION OCULAIRE

THESE DE DOCTORAT

Soutenu le 30 avril 2019

Par
Corinna BODE

Dirigée par **Prof. Juergen SIEPMANN**

Laboratoire INSERM U1008, Médicaments et Biomatériaux à Libération Contrôlée

Composition du Jury :

Monsieur Juergen SIEPMANN *Professeur à l'Université de Lille*	Directeur de thèse
Madame Aurélie MALZERT-FREON *Professeur à l'Université de Caen*	Président du jury/rapporteur
Madame Béatrice HEURTAULT *Maître de Conférences à l'Université de Strasbourg*	Rapporteur
Monsieur Heiko KRANZ *PhD, Bayer R&D, Berlin*	Examinateur

Remerciements

I want to express my gratitude to those who contributed to the success of this thesis.

*To begin with, I would like to thank Professor **Juergen SIEPMANN**, director of the Inserm U1008 unit, for welcoming me in the laboratory for Controlled Drug Delivery Systems and Biomaterials and for supervising this thesis. Thank you for all the valuable advice, the constant availability and kind encouragement over the last years. Vielen Dank!*

*My sincere gratitude goes to Dr. **Heiko KRANZ** who made this cooperation with Bayer possible in the first place. Thank you so much for the commitment and support!*

*Je remercie Professeur **Florence SIEPMANN** pour son aide, son optimisme et le soutien de nature scientifique et administrative.*

*J'aimerais aussi remercier mes deux rapporteurs, Professeur **Aurélie MALZERT-FREON** de l'Université de Caen et Dr. **Béatrice HEURTAULT** de l'Université de Strasbourg, d'avoir pris le temps nécessaire d'évaluer ma thèse et de faire partie du jury.*

*Merci encore à mes stagiaires, **Astrid FIVES** et **Aleksandra KRUSZKA**, qui m'ont soutenu durant ma thèse par leur travail de valeur et leur bonne humeur.*

*Je voudrais remercier toute l'équipe du laboratoire : **Jérémy VERIN** pour le SEM ; **Susanne MUSCHERT**, **Mounira HAMOUDI-BENYELLES** et **Youness KARROUT** pour leur contribution aux bonnes conditions de travail dans le laboratoire ; **Alexandra MACHADO** pour les commandes et l'administration et **Hugues FLORIN** pour la maintenance des machines au laboratoire.*

Les remerciements particuliers à

***Maria** pour m'avoir fait me sentir bienvenu en France, son aide et sa créativité ; **Ting** pour m'avoir toujours remonté le moral ; **Doha** pour sa fiabilité et son écoute et **Youcef** pour son aide au laboratoire.*

Je suis également reconnaissant pour tous mes camarades qui sont et ont été dans le laboratoire : ***Fahima, Martin, Adam, Kévimy, Lauranne, Céline, Thomas, Julie, Oriane, Ester, Elisa, Federica, Fabiana, Nourhène, Saliha et Sine****. Cela m'a fait plaisir de travailler avec vous !*

Ich bin dankbar für meine Freunde ***Julia und Franzi****. Vielen Dank für die moralische Unterstützung zu jeder Tages- und Nachtzeit!*

Ein ganz besonderer Dank gilt meiner Familie: ***meinen Eltern*** *für ihre unbegrenzte Unterstützung in jeglicher Hinsicht und meinem Bruder* ***Thomas*** *für seine Hilfe und Zuverlässigkeit.*

Table of contents

Abbreviations

AMD	age-related macular degeneration
AREDS	age-related disease study
ATBC	acetyltributyl citrate
BA	bioavailability
BAB	blood-aqueous barrier
BRB	blood-retinal barrier
CME	cystoid macular edema
CNV	choroidal neovascularization
DME	diabetic macular edema
DMSO	dimethyl sulfoxide
DR	diabetic retinopathy
EVA	ethylene vinyl acetate
FA	fluocinolone acetonide
GA	geographic atrophy
HME	hot melt extrudate
HPMC	hydroxy methylcellulose
ISFI	*in-situ* forming implant
Mw	molecular weight
NMP	N-methyl pyrrolidone

PEG	poly (ethylene glycol)
PGA	poly (glycolic acid)
PGF	placental growth factor
PLA	poly (lactic acid)
PLGA	poly(lactic-co-glycolic acid)
PVA	polyvinyl alcohol
RPE	retinal pigment epithelium
RVO	retinal vein occlusion
TA	triamcinolone acetonide
Tg	glass transition temperature
VEGF	vascular endothelial growth factor
VEGF	vascular endothelial growth factor receptor

INTRODUCTION GENERALE

Contexte de la recherche

Les causes principales de déficience visuelle et de perte de vision sont la dégénérescence maculaire liée à l'âge, la rétinopathie diabétique et l'uvéite. La dégénérescence maculaire liée à l'âge (DMLA) existe sous deux formes : la DMLA "sèche" ou atrophique et la DMLA "humide" ou néovasculaire. La première est caractérisée par la présence d'un drusen mou entre la membrane de Bruch et l'épithélium pigmentaire rétinien (EPR). Environ 10 à 15 % des patients souffrant de DMLA sèche développent une DMLA humide qui est déclenchée par des facteurs de croissance endothéliale vasculaire (VEGF) provoquant une croissance anormale des vaisseaux sanguins dans la membrane de Bruch. Cela peut endommager l'EPR et les photorécepteurs et provoquer des fuites de sang et de protéines, endommageant ainsi la vision. Dans la rétinopathie diabétique (RD), l'hyperglycémie persistante peut causer des microanévrysmes qui finissent par briser les jonctions endothéliales serrées dans la barrière hématorétinienne (BHR) et entraîner une fuite de protéines dans le vitré. L'œdème maculaire diabétique (OMD) est une conséquence de la RD. La perméabilité capillaire rétinienne anormale peut entraîner un gonflement extravasculaire de la macula et finalement une distorsion de la vision ou même une perte de vision. L'uvéite est une inflammation interne de l'œil qui peut survenir dans différentes parties de l'œil (antérieure, intermédiaire et postérieure). Dans l'uvéite postérieure, la rétine et/ou la choroïde sont affectées. Une inflammation chronique de l'uvée peut causer des dommages structurels dans l'œil et peut entraîner des complications comme l'œdème maculaire avec un risque élevé de perte irréversible de la vision. Pour ces trois maladies, les corticostéroïdes peuvent être utilisés soit comme traitement de première intention, soit comme traitement complémentaire.

Les corticostéroïdes ont des propriétés anti-inflammatoires et inhibent la synthèse des facteurs de croissance endothéliale vasculaire, des prostaglandines et des cytokines inflammatoires. Ils peuvent également stabiliser les jonctions endothéliales serrées et diminuer la rupture du BRB. Dexaméthasone est cinq fois plus puissant que l'acétonide de triamcinolone. Il a également une solubilité plus élevée. Ainsi, des concentrations intravitréennes plus élevées peuvent être atteintes. De plus, en raison de ses propriétés moins lipophiles, l'accumulation dans le réseau trabéculaire et le cristallin est réduite, ce qui pourrait diminuer le risque de pression intraoculaire élevée souvent associé aux stéroïdes. Malgré ces propriétés favorables de la dexaméthasone, la courte demi-vie vitreuse d'environ 5,5 heures (comparativement à environ 18 jours d'acétonide de triamcinolone) restreint la thérapie. Pour obtenir des concentrations thérapeutiques de dexaméthasone sur de longues périodes de temps, le médicament doit être administré

fréquemment. Cependant, en utilisant des gouttes ophtalmiques, seule une très petite portion (environ 0,001 à 0,0004 %) du médicament administré se trouve à l'intérieur du vitré, ce qui entraîne des concentrations inférieures à la concentration minimale efficace. D'autre part, la barrière rétinienne sanguine limite le transport du médicament dans le vitré après son administration systémique, ce qui nécessite de fortes doses de médicament, ce qui peut entraîner des effets secondaires non désirés. Pour surmonter cet obstacle, la dexaméthasone peut être injectée directement dans l'œil, mais chaque administration comporte le risque d'introduire des infections et d'autres effets secondaires tels que décollement de la rétine, cataracte, hémorragies vitrées et rétiniennes, endophtalmie et pression intraoculaire accrue. Une libération prolongée du médicament réduit la fréquence des injections intravitréennes et peut améliorer l'efficacité du traitement grâce à une libération constante du médicament.

L'acide poly(acide lactique-co-glycolique) (PLGA) est un polymère qui est souvent utilisé pour une administration prolongée de médicaments. C'est l'un des polymères biodégradables les plus courants et il a été utilisé pour la première fois dans les années 1960 comme suture biorésorbable. Il est disponible sur le marché dans de nombreux produits approuvés par la FDA pour la libération contrôlée parentérale et d'autres techniques d'administration. Il est possible de fabriquer différentes formes telles que des membranes, des tiges et des disques en utilisant des techniques de moulage, d'extrusion et autres. Le PLGA est également soluble dans une large gamme de solvants tels que le tétrahydrofuranne, l'acétone, les solvants chlorés et l'acétate d'éthyle, ce qui le rend adapté à une large gamme de techniques de préparation. Le PLGA s'est révélé bien toléré et biocompatible dans les tissus oculaires et non oculaires. Par exemple, l'implant oculaire biodégradable Ozurdex contient de la dexaméthasone dans une matrice PLGA qui n'a pas besoin d'être enlevée chirurgicalement une fois la libération du médicament terminée.

Objectifs de la recherche

Les implants de formation in situ peuvent être injectés avec une petite taille d'aiguille, tandis que les implants préformés évitent l'utilisation de solvants potentiellement toxiques. Afin d'adapter la libération du médicament pour les deux systèmes, les différents mécanismes de libération et le comportement de biodégradation doivent être mieux compris. Ils peuvent dépendre de divers facteurs, tels que la surface totale, la charge de médicament, la solubilité du médicament, le gonflement des polymères, l'autocatalyse, par exemple, les mécanismes exacts qui se trouvent derrière la libération et la dégradation du médicament sont très complexes et ne sont pas entièrement compris.

Le but de cette thèse était le développement et la caractérisation de différents systèmes implantaires contenant de la dexaméthasone et du PLGA pour une libération prolongée du médicament pour administration intravitréenne. Les principaux objectifs sont les suivants :

(i) Préparation et caractérisation des implants de formation in situ en mettant l'accent sur l'impact du volume du milieu de libération, du type et de la concentration du polymère ainsi que de la teneur en médicament des formulations.

(ii) Préparation et caractérisation des implants préformés en mettant l'accent sur la charge de médicament, le type de polymère et l'importance du comportement de gonflement pour la libération du médicament.

(iii) Visualisation de la libération du médicament et de l'absorption d'eau des implants préformés et formés in situ à l'aide de médicaments modèles colorés pour mieux comprendre les mécanismes sous-jacents.

(iv) Étude de l'effet de différentes quantités d'additifs sur les principales caractéristiques des implants formés in situ, en particulier la libération de médicaments, le gonflement des implants, la température de transition vitreuse et la morphologie.

Présentation de ce travail

Le présent ouvrage est composé de quatre chapitres :

I. Le premier chapitre donne un aperçu de la structure de l'œil et des défis qui en résultent pour le traitement des maladies affectant le segment postérieur. Il montre différentes approches d'application de médicaments sur le vitré et met l'accent sur les systèmes d'administration prolongée de médicaments potentiels pour une injection intravitréenne.

II. Le deuxième chapitre énumère les matériaux et les méthodes utilisés pour la recherche de ces travaux.

III. Le troisième chapitre présente les résultats et la discussion. Il est divisé en quatre parties. Chaque partie correspond à l'un des objectifs de recherche décrits ci-dessus. Bientôt, les principaux sujets sont :

    1. Implants PLGA de formation in situ pour l'administration intraoculaire de dexaméthasone

    2. Souvent négligé : Le gonflement PLGA/PLA orchestre la libération du médicament - HME implants

    3. Coloration des implants PLGA pour mieux comprendre les mécanismes de libération du médicament

    4. Implants PLGA de formation in situ : comment les additifs influent le gonflement et la liberation du médicaments

IV. Enfin, la quatrième partie donne une conclusion générale et résume les résultats de cette thèse.

GENERAL INTRODUCTION

Research Context

The major causes for vision impairment and vision loss are age-related macular degeneration, diabetic retinopathy and uveitis. *Age-related macular degeneration* (AMD) exists in two forms: the "dry" or atrophic AMD and the "wet" or neovascular AMD. The first one is characterized by an occurrence of soft drusen between the Bruch's membrane and retinal pigment epithelium (RPE). Around 10-15% of patients with a dry AMD develop a wet AMD which is triggered by vascular endothelial growth factors (VEGF) causing an abnormal growth of blood vessels into the Bruch's membrane. This can damage the RPE and photoreceptors and lead to blood and protein leakage, ultimately damaging the vision. In *diabetic retinopathy* (DR) continuous hyperglycemia can cause microaneurysms which eventually break down the endothelial tight junctions in the blood retinal barrier (BRB) and lead to a protein leakage into the vitreous. Diabetic macular edema (DME) is a consequence of DR. The abnormal retinal capillary permeability can lead to extravascular swelling in the macula and finally a distortion of vision or even vision loss. *Uveitis* is an internal inflammation of the eye and can occur in different parts of the eye (anterior, intermediate and posterior). In the posterior uveitis, the retina and/or choroid are affected. A chronic inflammation of the uvea can cause structural damage in the eye and can lead to complications like macular edema with a high risk of irreversible vision loss. For all three diseases corticosteroids can be either used as a first-line therapy or as an add-on therapy.

Corticosteroids have anti-inflammatory properties and they inhibit the synthesis of vascular endothelial growth factors, prostaglandins and inflammatory cytokines. They can also stabilize endothelial tight junctions and decrease the breakdown of the BRB. Dexamethasone is five times more potent than triamcinolone acetonide. It also has a higher solubility. Thus, higher intravitreal concentrations can be achieved. Additionally, due to its less lipophilic properties, the accumulation in the trabecular meshwork and lens is reduced which might decrease the risk of elevated intraocular pressure often associated with steroids. Despite these favorable properties of dexamethasone, the short vitreous half-life of approximately 5.5 hours (compared to approximately 18 days of triamcinolone acetonide) restricts the therapy. To achieve therapeutic dexamethasone concentrations over prolonged periods of time, the drug has to be administered frequently. However, using eye drops only a very small portion (approximately 0.001 to 0.0004 %) of the administered drug is found inside the vitreous, leading to concentrations below the minimum effective concentration. On the other hand, the blood-retinal-barrier limits drug transport into the vitreous after systemic administration, requiring high drug doses, which can lead to undesired side effects. To overcome this hurdle, dexamethasone can be directly injected

into the eye, but each administration bears the risk of introducing infections and other side effects such as retinal detachment, cataract, vitreous and retinal hemorrhages, endophthalmitis and increased intraocular pressure. A prolonged drug release reduces the frequency of intravitreal injections and can improve the efficacy of the therapy due to a constant drug release.

Poly(lactic-co-glycolic acid) (PLGA) is a polymer that is often used for a sustained drug delivery. It is one of the most common biodegradable polymers and was first used in the 1960s as bioresorbable sutures. It is commercially available in many FDA-approved products for parenteral controlled release and other administration techniques. It is possible to fabricate various forms such as membranes, rods and disc using molding, extrusion and other techniques. PLGA is also soluble in a broad range of solvents such as tetrahydrofuran, acetone, chlorinated solvents and ethyl acetate, which makes it suitable for a wide range of preparation techniques. PLGA was shown to be well tolerated and biocompatible in ocular and non-ocular tissues. For example, the biodegradable, ocular implant Ozurdex contains dexamethasone in a PLGA matrix that does not have to be surgically removed after the drug release is completed.

Research Objectives

In-situ forming implants and pre-formed implants using PLGA can both sustain the drug release and biodegrade over time to avoid any surgical removal after complete drug liberation. In-situ forming implants can be injected with a small needle size, whereas pre-formed implants avoid the use of potentially toxic solvents. In order to adapt the drug release for both systems, the different release mechanisms and biodegradation behavior have to be better understood. They can depend on various factors, such as the total surface area, drug loading, solubility of the drug, polymer swelling, autocatalysis, e.g. The exact mechanisms behind the drug release and degradation are very complex and are not fully understood.

The aim of this thesis was the development and characterization of different implant systems containing dexamethasone and PLGA for a sustained drug release for intravitreal administration. Main objectives include:

(i) Preparation and characterization of in-situ forming implants with emphasis on the impact of the volume of the release medium, polymer type and concentration as well as drug content of the formulations.

(ii) Preparation and characterization of pre-formed implants with focus on the drug loading, polymer type and the importance of swelling behavior to the drug release.

(iii) Visualization of drug release and water uptake of in-situ forming and pre-formed implants using colored model drugs to better understand the underlying mechanisms.

(iv) Investigation of the effect of different amounts of additives on the key features of in-situ forming implants in particular drug release, implant swelling, glass transition temperature and morphology.

Presentation of the work

The present work is composed of four chapters:

I. The first chapter gives an overview of the structure of the eye and its resulting challenges for the treatment of diseases affecting the posterior segment. It shows different approaches to apply drugs to the vitreous and focuses on potential sustained drug delivery systems for an intravitreal injection.

II. The second chapter lists the materials and methods used for the research of this work.

III. The third chapter contains the results and discussion. It is divided into four parts. Each part corresponds to one of the research objectives described above. Shortly, the main subjects are:

    1. In-situ forming PLGA implants for intraocular dexamethasone delivery
    2. Often neglected: PLGA/PLA swelling orchestrates drug release - HME implants
    3. Coloring of PLGA implants to better understand drug release mechanisms
    4. In-situ forming PLGA implants: How additives affect swelling and drug release

IV. Finally, the fourth part gives a general conclusion and summarizes the findings of this thesis.

CHAPTER 1:

INTRODUCTION

1.1 The eye

1.1.1 Anatomy of the eye

The eye can be divided into two segments – the anterior segment including the cornea, conjunctiva, iris, ciliary body and lens and the posterior segment including the sclera, choroid, retina and vitreous (Figure 1.1) [1,2]. The transparent, avascular cornea is directly exposed to the environment and is comprised of five layers: the epithelium, Bowman's membrane, stroma, Descernet's membrane and endothelium. The Bowman's and Descernet's membrane are interface layers, whereas the other three are cellular layers. The cellular layers differ in polarity and act as a mechanical barrier from exogenous substances [2,3]. The conjunctiva is a thin layer that covers the eyelids and sclera. It produces mucus and tears to lubricate the eye. The iris is the colored part of the eye. The circular membrane has an opening in the center, the pupil. Through contraction the pupil can alter the amount of light that enters the eye. The ciliary body produces the aqueous humor and its ciliary muscles control the shape of the lens to focus the vision. The aqueous humor is responsible for supplying nutrients and oxygen to avascular tissues (cornea and lens) and also removes macrophages, blood and waste products found between the cornea and lens. The entire aqueous humor is renewed in approximately 100 min [4]. The aqueous humor leaves the anterior chamber via the trabecular meshwork and canal of Schlemm.

The sclera is commonly called the "white of the eye". It is connected with the cornea and covers around 80% of the eyeball. The middle layer of the posterior segment is the choroid and is comprised of three distinguished layers: suprachoroid, vascular layer and Bruch's membrane (from out to in). The blood vessels in the choroid are lined by endothelial cells, through which molecules can be exchanged between the blood and choroid. The Bruch's membrane acts as a diffusional barrier to macromolecules [5]. The innermost layer is the retina containing the neural retina, which is involved in signal transduction, and the retinal pigment epithelium (RPE). The RPE cells are polarized and the tight junctions in between those cells hinder the diffusion of small molecules from the choroid to the retina. The retina contains photoreceptor cells including rods and cones. These cells convert light into a nerve signal. The macular is part of the retina and is located close to the optic nerve. With its high concentration of photoreceptor cells in the center of the macula (called fovea), it is responsible for high-acuity vision. The posterior segment of the eye is filled with approximately 4 mL vitreous humor. Even though it consists to 98% of water, it has a high viscosity due to collagen type II and hyaluronic acid [6–8].

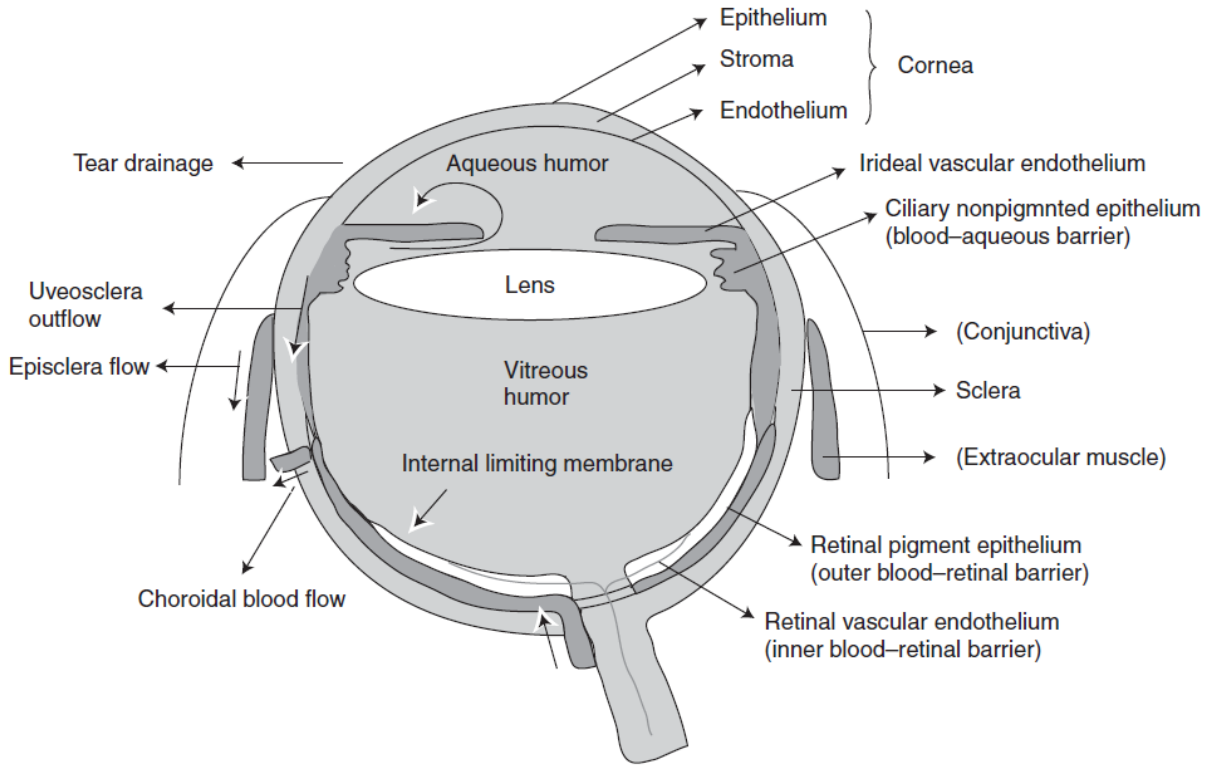

Figure 1.1: Schematic structure of the eye. From [9].

1.1.2 Dynamic and static ocular barriers

The eye is protected by various static (cornea, conjunctiva, sclera, blood-ocular barriers) and dynamic (tear turnover, nasolacrimal drainage, reflexive blinking, choroidal blood flow) barriers. They effectively protect the eye from external influences and limits the access of drugs into the eye (Figure 1.2) [10].

The first defense mechanism of the eye is the *tear-film barrier*. The tear fluid consists of three layers: a lipid, an aqueous and a mucin layer. The lipid layer protects the aqueous layer from evaporation. The aqueous layer makes for 90% of the tear film volume and keeps the ocular surface moist and lubricated. Through tear drainage and fluid turnover, it dilutes and washes away foreign particles and any substances administered topically. It also protects the eye against infection due to antibacterial lysozymes contained in the aqueous layer. The mucin layer provides the cornea with nutrients and also promotes adherence of the aqueous layer to the ocular surface [11–13].

The avascular *cornea* acts as a mechanical barrier which protects the ocular tissue and prevents exogenous substances from entering the eye due to its different layers and polarities. The outermost layer, the corneal epithelium, is comprised of 5-6 layers of cells with tight junctions. It is hydrophobic and, thus, the major barrier for hydrophilic compounds. Depending on the molecular weight and polarity, the drug can pass via two different routes: paracellular for ions and hydrophilic drugs with a molecular weight under 350 Da, or intracellular for lipophilic drugs. The stroma, which accounts for 90% of the corneal thickness, persists of collagen, proteoglycans, keratocytes and 70-80% of water. With its hydrophilicity, it prevents very lipophilic compounds from entering the eye. The endothelium is a thin cellular layer with limited permeability for hydrophilic molecules. Small lipophilic molecules may pass this layer. With its combination of different layers with different polarities, the cornea is the main barrier for topically applied substances. Only small molecules with an optimal lipophilicity may diffuse through the cornea [2,3,14,15]. Estimates indicate that only 5% of a topically administered drug actually passes the cornea and reaches the anterior chamber [16].

The *conjunctiva* is a thin transparent mucous epithelial barrier that covers the exposed part of the eyeball and the inner lining of the eye lids. It is comprised of two layers: the conjunctival epithelium and the stroma. The epithelium contains mucus-producing Goblet cells. The space between the epithelial cells are wider compared to the cornea and, thus, the permeability of the conjunctiva is higher. Additionally, its surface is around 17 times bigger than the cornea which increases the area for drug absorption. However, due to the blood capillaries in the stroma, a big amount of the absorbed drug gets lost into the systemic circulation [17–19].

The *sclera* mainly consists of glycoproteins and collagen fibrils and the permeability is higher than for the cornea and conjunctiva. The permeability is more dependent on the molecular radius than the molecular weight, as it has been shown that spherical molecules can permeate better than linear ones. Additionally, the negatively charged proteoglycan matrix hinders positively charged molecules from diffusing through the sclera [19–22].

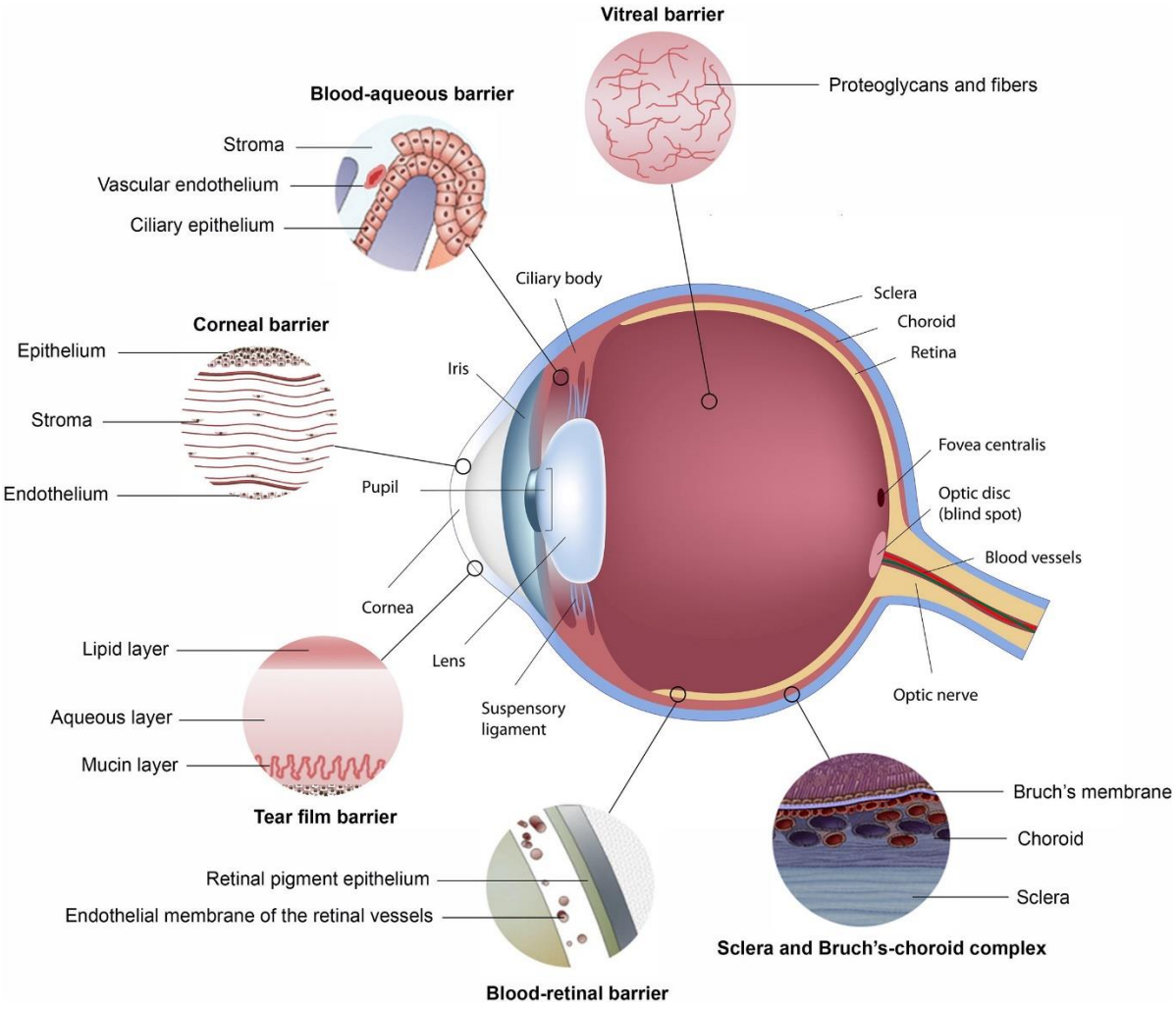

Figure 1.2: Physiological barriers in ocular drug delivery. From [19].

1.1.3 Blood-ocular barriers

The blood-ocular barrier consists of the blood-aqueous barrier (BAB) and the blood-retinal barrier (BRB) (Figure 1.2).

The **blood-aqueous barrier** (BAB) is located in the anterior segment of the eye. It is formed by the endothelium of the blood vessels of the iris, ciliary blood vessels and the nonpigmented epithelium of the ciliary body. Both cell layers contain tight junctions that control the non-specific drug-entry between the blood and aqueous humor. Additionally, they maintain the chemical composition of the humor and the transparency because they hinder blood proteins from entering. Even when intact, the BAB is incomplete and bigger molecules like horseradish peroxidase with a molecular weight of 40 kDa can access the aqueous humor through the fenestrated ciliary capillaries. Nevertheless, the BAB is efficient to prevent bigger proteins and

hydrophilic drugs from entering the aqueous humor under normal conditions. The integrity of the BAB might be disrupted during an inflammation [23–26].

The **blood-retinal barrier** (BRB) is formed by the retinal pigment epithelium (RPE) and retinal vascular endothelium (also called outer and inner blood-retinal barrier). It regulates the homeostasis of the retina and visual cells and restricts access of molecules from the blood into the posterior segment. The RPE is a monolayer with tight junctions and their function is supported by astrocytes and Müller cells. The RPE selectively transports nutrients between the choroid and retina and prevents intercellular diffusion of hydrophilic molecules. As a result, the passive diffusion of molecules from the choroid to the retina is restricted and the passage of nutrients regulated. The inner BRB (the endothelial cells of the retinal vessels) also has narrow tight junctions and prevents larger or hydrophilic compounds from entering the vitreous. Facilitated diffusion across the BRB is only possible for small molecules (e.g. glucose, sodium, potassium, phosphate), whereas active transport occurs with amino acids, prostaglandins and others [2,5,25,27–29].

1.1.4 Ocular clearance

Nearly every compound can be cleared from the vitreous via the anterior pathway (also called aqueous clearance), independently of their size or lipophilicity. The molecules diffuse from the vitreous through the vitreous membrane into the aqueous humor of the posterior chamber (between the iris, ciliary body and lens). From there they are eliminated through the canal of Schlemm via the trabecular pathway or the uveoscleral pathway (Figure 1.3). The aqueous humor is secreted at a rate of 2.0-2.5 µL/min and is estimated to be entirely replaced after approximately 100 min [4,30,31].

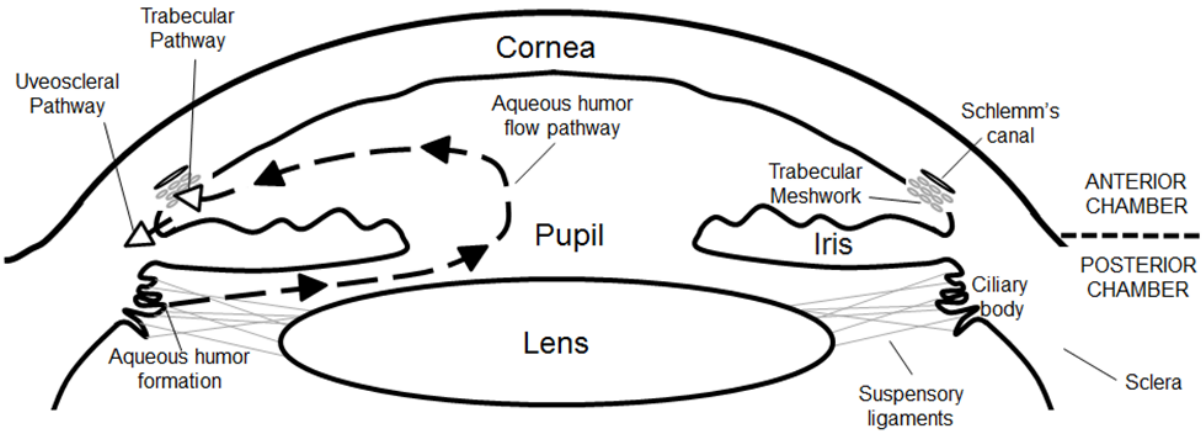

Figure 1.3: Schematic diagram of aqueous humor flow pathway. From [32].

Small, lipophilic drugs can be eliminated via the anterior and posterior pathway. Molecules with a molecular weight of <350 Da can passively diffuse through the retina and the blood-ocular barriers from where the choroidal blood flow transport them away. Due to the large surface of the retina compared to the anterior membrane and the fact that they can be eliminated via two pathways, small molecules have a drastically lower intravitreal half-life of several hours than bigger molecules such as proteins [28,33–35].

1.2 Diseases of the eye

Three of the most common diseases that can significantly impact the vision and lead to legal blindness in the western world are diabetic retinopathy, age-related macular degeneration and uveitis.

1.2.1 Diabetic retinopathy

In working-aged people diabetic retinopathy (DR) is the leading cause of preventable blindness [36,37]. The main risk factors for this disease are diabetes duration, level of HbA1c, blood pressure and hypertension [36,38]. With a growing incidence of diabetes mellitus, the number of people suffering from DR is expected to rise from 126.6 million people in 2010 to 191.0 million by 2030 with an increase from 37.3 to 56.3 million for vision-threatening DR [39].

DR can be divided into non-proliferative and proliferative DR [40]. The initial stages are asymptomatic. In non-proliferative DR, a sustained hyperglycemia can increase the permeability of retinal capillaries which in turn leads to a loss of elasticity of the endothelial capillary

wall. The number of pericytes, a layer of smooth muscle cells protecting the capillaries, decreases [41,42] and microaneurysm, small bulges filled with blood, form in the retina. Hemorrhages develop in the retina when those microaneurysms rupture. Eventually, the endothelial tight junctions that form the blood retinal barrier break down and fluids containing proteins leak into the retina. This subretinal fluid build-up leads to a swelling of the macula which is the typical characteristic of the diabetic macular edema (DME) [43,44]. In DME, the thickening of the macular area causes blurred vision and occurs in 10% of diabetics [45]. If DME is not treated it can lead to a proliferative DR. [41,42]

As the disease progresses, retinal capillary vascular lumen can get clogged by white blood cells or platelets causing a hypoxia. In low oxygen conditions, more vascular endothelial growth factor (VEGF) is excreted and new retinal vessels are formed. This process is called neovascularization and is a main characteristic of the proliferative DR. The newly formed vessels are fragile and can bleed easily, causing hemorrhage and retinal detachment ultimately leading to vision loss [46].

There are three main treatment options in DR, laser photocoagulation, vitrectomy, and pharmacotherapy. Only the latter is used in early stages. In proliferative DR, laser photocoagulation is used to prevent sever vision loss [47]. Vitrectomy is a surgical treatment that involves the removal of the vitreous humor (partly or completely). It reduces retinal neovascularization and macular edema [36]. Several drugs can be administered to treat the disease: Inflammatory cytokines have been shown to be elevated in aqueous and vitreous samples in DME and proliferative DR. The concentration of those cytokines correlate with the severity of the disease. [43,48–50] Ozurdex® (Allergan Inc.) and Iluvien® (Alimera Sciences) both contain glucocorticoids which inhibit the formation of certain inflammatory cytokines. They are approved for the use in DME and increase the efficacy of the treatment of persistent DME.

1.2.2 Age-related macular degeneration

Age- related macular degeneration (AMD) is the most common cause of irreversible blindness in people over 65 years [27]. In the United States over 1.75 million people suffer from this disease. Due to rapid aging, this number is expected to increase to almost 3 million by 2020 [51]. It can lead to vision impairment and vision loss. Common risk factors are smoking, hypertension, advanced age and race [52,53].

AMD can be divided into the "dry" or atrophic AMD and "wet" or neovascular AMD. The most prevalent form is the atrophic AMD and causes only mild vision impairment. In the beginning it is often asymptomatic. A typical characteristic of the atrophic AMD is the appearance of soft drusen (yellow aggregates containing extracellular material) between the Bruch's membrane and the retinal pigment epithelium (RPE). Drusen formation is a normal process in aging people but the presence of more than five small drusen or a few intermediate drusen is categorized as mild AMD (Table 1.1).

Table 1.1: Classification of AMD, according to AREDS. From [54].

Classification	Category	Clinical signs
No AMD	1	0-5 small drusen (<63 µm in diameter)
Early AMD	2	Multiple small drusen or a few intermediate-sized drusen (63-124 µm in diameter), or macular pigmentary changes
Intermediate AMD	3	Extensive intermediate drusen or at least one large drusen (≥125 µm), or GA not involving the foveal center
Advanced AMD	4	GA involving the foveal center or any evidence of choroidal neovascularization

Abbreviations: AMD, age-related macular degeneration; AREDS, Age-related disease study; GA, geographic atrophy

The RPE can be damaged by excess drusen. A retinal atrophy (also geographic atrophy, GA) can result from an inflammatory response and a hypoxic state can cause an over-expression of VEGF. The latter is associated with neovascular AMD and appears in about 15% of the patients. A high amount of VEGF causes an erratic growth of blood vessels from the choroid in the retina, also called choroidal neovascularization (CNV). Eventually, those newly formed blood vessels break through the Bruch's membrane, damaging the RPE and photoreceptors. In consequence, blood and proteins leak into the vitreous, leading to a blurry vision and even sudden vision loss [55].

Until today, no treatment for atrophic AMD is approved by the FDA. To reduce oxidative stress, a supplement of antioxidants, a reduced intake of fat and no smoking might be indicated. The first-line therapy for neovascular AMD is the intravitreal injection of anti-VEGF such as ranibizumab (Lucentis, Genentech), bevacizumab (Avastin, Genentech), and aflibercept (Eylea, Bayer). They inhibit the VEGF and, thus, decrease the choroidal neovascularization. Another

line of therapy is photodynamic therapy in combination with verteporfin. Verteporfin is injected intravenously and then activated with a laser in the eye, leading to a selective damage of ocular tissue. Steroids are a possible adjunctive to the standard therapy since inflammatory cells were found in CNV tissue. They are not suitable as a monotherapy but in combination with anti-VEGF therapy they may reduce injection frequency and improve long-term efficacy [56–59].

1.2.3 Uveitis

Uveitis, an ocular inflammation, is another very common cause of visual impairment in the developed world. The incidence is highest in the working age population [60,61]. It can be categorized anatomically based on the location of the inflammation into anterior (iris), intermediate (ciliary body, pars plana) and posterior (choroid) uveitis. It is classified in acute or chronic depending on if the inflammation lasts more than three months [62]. Both, the acute and chronic uveitis, are often associated with underlying systemic diseases such as tuberculosis, HIV, sarcoidosis and Behçet's syndrome, but also by exogenous factors like infections and trauma [63,64].

Different inflammatory mediators, for example T-cell cytokines, interleukins and tumor necrosis factor-α, are found to be involved in the disease. Probably caused by T-cells entering the eye, the BRB gets damaged and blood vessels start to leak into the retina [65]. This causes a cystoid macular edema (CME). In the beginning, this damage is reversible and the BRB can seal up again. However, a chronic or severe edema can permanently damage the retina and impair the vision [66].

Corticosteroids are a common treatment for uveitis. They inhibit certain inflammatory pathways, reduce retinal swelling (macular edema) and are also immunosuppressant [67]. Caused by the limited penetration of steroids into the posterior vitreous, a local administration of eye drops or ointments is only effective in anterior uveitis. For posterior uveitis a systemical/oral, periocular or intravitreal administration is necessary. When corticosteroids are administered to patients systemically over a prolonged period of time, they have to be monitored closely for side effects, such as diabetes, hypertension and osteoporosis [68]. After a periocular injection of triamcinolone acetonide high concentrations are found in the anterior and posterior part of the eye with low systemic concentrations. However, for long-term treatment, the injection has to be repeated every 2 to 4 months, thus, increasing the risks of side effects such as globe perforation, endophthalmitis, hemorrhage and ptosis (drooping lid) [6,69]. Nowadays, intravitreal

implants containing corticosteroids are approved by the FDA for the treatment of Uveitis, such as Retisert® (Bausch + Lomb) and Ozurdex® (Allergan Inc.) [64,70]. In some cases, the patient's treatment with corticosteroids is not sufficient and other immunosuppressive drugs are being administered systemically, including T-cell inhibitors, alkylating agents, and antimetabolites [71].

1.3 Therapy of the Eye

1.3.1 Laser Treatment

To prevent further vision loss, patients with DR and AMD can be treated with a focused laser beam (**L**ight **A**mplification by the **S**timulated **E**mission of **R**adiation).

Since the 1980s, laser photocoagulation is used as a standard treatment for DME. The Early Treatment of Diabetic Retinopathy Study (ETDRS) has shown that a focal laser photocoagulation of microaneurysms can decrease the probability of ongoing vision loss. In this process, a laser with a discrete wavelength is trained on affected parts of the retina. The light gets absorbed by the pigmented retinal layers, leading to a localized temperature increase. The elevated temperature denatures tissue proteins and induces necrosis; the hypoxia of the retina decreases. The exact mechanism of action is unknown. One hypothesis is that an improved oxygenation of the retina reduces the VEGF production and, thus, the neovascularization and edema. Possible side effects of the laser coagulation include, for example, retinal damage, inflammation, reduced night vision, decreased color vision and retinal hemorrhages. In contrast to the pharmacological treatment, the laser photocoagulation only prevents further vision loss and does not decrease vision impairment [47,72–77].

In neovascular AMD photodynamic therapy can be used. Before the approval of anti-VEGF factors, it was first line therapy. It involves a photosensitive compound called photosensitizer, a light with a wavelength absorbed by the photosensitizer and oxygen radicals. The photosensitizer approved for the use in AMD is verteporfin (Visudyne®, Bausch + Lomb). Approximately 10 min before the light treatment, an intravenously infusion is given to the patient. Verteporfin is a lipophilic compound with a high affinity to neovascular tissue that accumulates in the mitochondria. Without light-activation the drug is inactive, limiting systemic side effects. When a light with a specific wavelength is then directed on the retina, the verteporfin in the abnormal blood vessels absorbs the light and the ground state elevates into an excited triplet state. The energy, that gets released when the molecule falls back into its initial ground state,

gets transferred to other molecules in the surrounding area. During this energy transfer, oxygen radicals are generated which can damage proteins and lipid membranes in the surrounding tissue. The cytotoxicity caused by the oxygen only has a restricted area due to a reactive distance of only 0.1 µm which in turn limits the damage to other tissues. As with the laser photocoagulation, the vision is not improved, only the progress of vision loss is decreased [73,78–80].

1.3.2 Anti-VEGF Factors

Vascular endothelial growth-factors (VEGF) play an important role in the pathophysiology of AMD and DR. In mammals, the VEGF family is comprised of five different kinds: VEGF-A, -B, -C, -D and placental growth factor (PGF). The main mediator in the angiogenesis of the retina and choroid is the VEGF-A that interacts with various growth factor receptors. It activates the intracellular kinase domains via autophosphorylation and promotes a proliferative signal and angiogenesis [81–83].

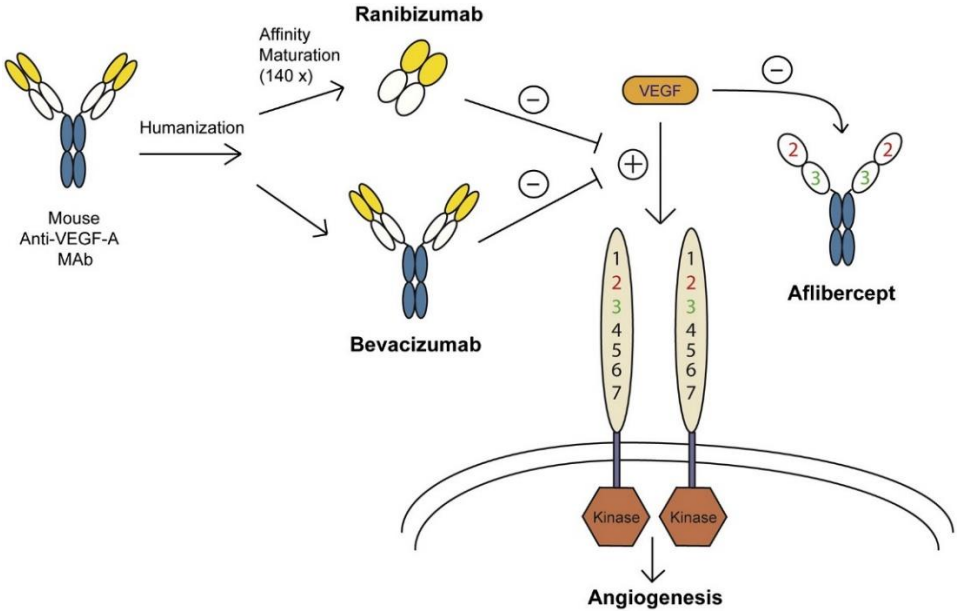

Figure 1.4: A representation of the three various types of anti-VEGF therapy and how they differ in development and mechanism of action. While ranibizumab and bevacizumab are both humanized monoclonal antibodies, ranibizumab has further affinity purification and decreased size. In contrast, aflibercept replicates two portions of the VEGF receptor (VEGFR) attached to an antibody Fc region, effectively working as a “trap receptor”. From [52].

To inhibit or reduce the effect of VEGF-A in the retina and choroid, different anti-VEGF therapies have been developed. Most commonly used are bevacizumab (Avastin®, Roche), ranibizumab (Lucentis®, Novartis), aflibercept (Eylea®, Bayer) and pegaptanib (Macugen®, Bausch+Lomb) (Figure 1.4). They inhibit the pathological neovascularization, prevent visual impairment and optimally reverse the on-set of vision loss [81,84].

Bevacizumab was developed and approved by the FDA for the systemic use in metastatic cancers in 2004. It inhibits all VEGF-A isoforms and is used off-label intravitreally to treat neovascular AMD and DME. It is a humanized monoclonal IgG antibody with a molecular weight of 149 kDa. Due to its large size the retinal penetration is limited. In order to increase the efficacy, ranibizumab was developed. It is a recombinant humanized Fab fragment with a molecular weight of only 48 kDa. Since 2006, it is FDA approved for the treatment of neovascular AMD, DME and macular edema secondary to retinal vein occlusion (RVO). Due to its reduced size compared to bevacizumab the ability to penetrate the retina should be increased. Also, after diffusion from the ocular tissue into the blood stream, the elimination half-live is lower, limiting systemic side effects [81,85,86].

Aflibercept is a recombinant fusion protein where the binding domains of VEGFR-1 and -2 are fused to an IgG Fc fragment. The 115 kDa big molecule has stronger affinity to bind VEGF-A isoforms than the receptors ("trap receptor"). In contrast to bevacizumab and ranibizumab it also inhibits VEGF-B and PLGF. It gained FDA approval for neovascular AMD in 2011 and for RVO in 2015. It is also approved and available as a systemic formulation to treat metastatic colorectal cancer [84,87–89].

In contrast, pegaptanib is an RNA aptamer that has a high selectivity for the isoform of VEGF-A165. With a molecular weight of approximately 50 kDa, it is the smallest of the compounds mentioned here. Compared to the other antibodies, the aptamer can be easily manufactured in a large scale and is cost-effective. It was approved for neovascular AMD in 2004 and is also used off-label in Branch RVO (occlusion of one of the branches of the retinal vein) and DME [90–92].

Due to the permeability of the anti-VEGF agents through the BRB, part of the injected drugs can reach the systemic circulation and decrease VEGF plasma levels. One of the functions of systemic VEGF is the up-regulation of NOS and protection of the vascular patency and integrity. When the plasma levels are reduced, the risk of hypertension and thromboembolic events increases. Due to the increase in prevalence of AMD and DR in age, many patients are elderly

and already an increased risk for hypertension and other cardiovascular diseases, which are the most common comorbidities with wet AMD [84,93–95].

Even though anti-VEGF therapy has shown a high efficacy in various studies, when injected over a long term, the efficacy can be reduced. Also, some patients seem to not respond to the treatment with no benefit to the intravitreal injection [96]. Additionally, every intravitreal injection bears risks such as hemorrhage, retinal detachment and endophthalmitis. Therefore, administration frequency should be limited.

1.3.3 Corticosteroids

Since the 1950s, corticosteroids are used to treat ocular inflammation such as uveitis. They can also reduce diabetic and cystoid macular edema and exudative AMD. They target different inflammatory pathways and angiogenic cascades. Their main mechanism of action is the binding to cystolic glucocorticoid receptors. When activated, these receptors decrease the production of pro-inflammatory proteins and increase the expression of anti-inflammatory proteins such as cytokines [97–100]. They also inhibit macrophages (and thus inhibiting the release of angiogenic growth factors) and leukocytes, which are pro-inflammatory, and suppress the VEGF expression. The latter might make them suitable as an adjunctive to treat CNV and could reduce the administration frequency of anti-VEGF injections. They also have been shown reduce the paracellular permeability and enhance the integrity of tight junctions, explaining their use in macular edema [97,99,101–103].

Corticosteroids are able to penetrate the eye through the BRB and are found in the choroid, retina and sclera after systemic administration in an even higher concentration than topical application [104–106]. However, a continuously high systemic concentration may lead to many side effects such as Cushing's syndrome, osteoporosis and diabetes [68]. These side effects can be limited with an intravitreal injection, where the corticosteroid is delivered directly to the side of action. In the eyes they can cause cataract and an elevated intraocular pressure leading to glaucoma [97,107]. Commonly used corticoids are triamcinolone acetonide, dexamethasone and fluocinolone acetonide (Figure 1.5).

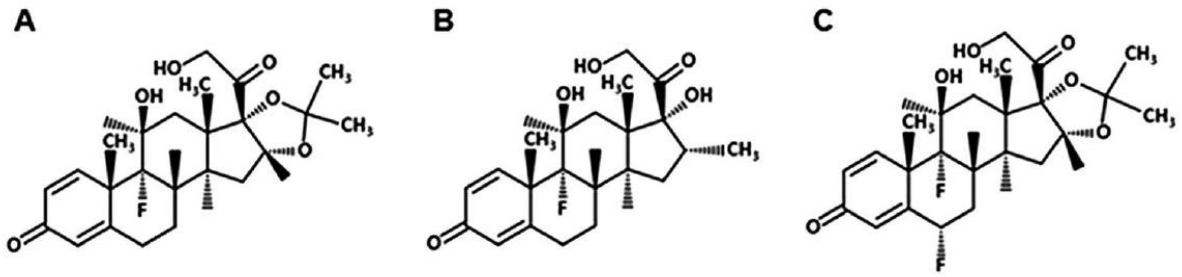

Figure 1.5: Chemical structure of triamcinolone acetonide (**A**), dexamethasone (**B**) and fluocinolone acetonide (**C**). From [108].

Triamcinolone acetonide (TA) is highly insoluble in water. When injected intravitreally, the drug crystals can act as a depot. It has an intravitreal half-life of approximately 18 days and can be detected for up to three months in the vitreous. It is commonly used as an intravitreal injection containing 4 mg TA in 0.1 mL [98,99].

Dexamethasone is one of the most prescribed corticosteroids for the treatment of ocular diseases and is five times more potent than triamcinolone acetonide. Due to its higher solubility, it has no depot formulation and only a very short intravitreal half-life of three hours. However, the lower lipophilicity could lead to a lesser accumulation in the trabecular meshwork and lens, resulting in lower risk of steroid-related side-effects, such as increased intraocular pressure and cataract. The biodegradable intravitreal implant Ozurdex® (Allergan Inc.) contains 0.7 mg dexamethasone that is released over a period of six months [34,97,109–111].

The potency of fluocinolone acetonide (FA) is comparable with that of dexamethasone and only has 1/24 of the solubility of dexamethasone in water. It is incorporated in the non-biodegradable implant Iluvien® (Alimera Sciences) which releases FA over a period of up to three years. The most common side effect of FA is increased intraocular pressure [97,112,113].

1.4 Ocular drug delivery

Due to its unique anatomy and physiology, ocular drug delivery remains challenging. The various ocular barriers significantly impede the drug delivery to the ocular tissues. In order to reach the retina in the back of the eye, several different methods are being investigated (Figure 1.6).

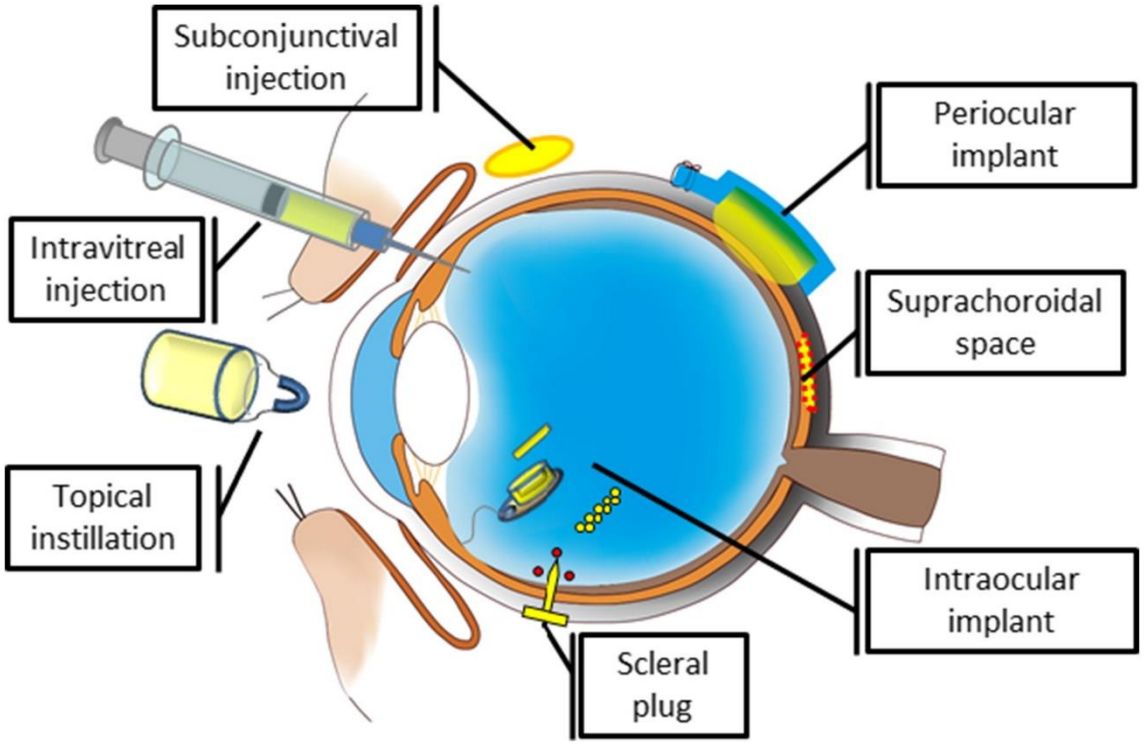

Figure 1.6: Examples of drug delivery systems and devices for the posterior segment of the eye. From [114].

1.4.1 Topical

A topical treatment (e.g. eye drops and ointments) is usually indicated for diseases affecting the front of the eye, such as conjunctivitis, keratitis, dry eye, elevated intraocular pressure and anterior uveitis. Eye drops are noninvasive and self-administrable which leads do a high patient compliance short-term. The challenge here is the small volume that can be administered (approximately 30 µL) and a tear volume of around 7 µL. Due to reflexive blinking, tear dilution and tear turnover, the residence time in the eye is limited and after 15-30 s most of the administered solution is washed away via the naso-lachrymal duct [3,115]. The part of the drug that gets absorbed can enter the eye via the corneal or non-corneal route. In the corneal route the molecules diffuse through the cornea into the aqueous humor and then in the intraocular tissue. Molecules that only have a poor corneal permeability (mostly hydrophilic and larger molecules) can get absorbed from the conjunctiva, passing the sclera, into the choroid or RPE of the posterior segment [24,27,116]. It is generally estimated that only about 5% of the applied dosage reaches the anterior segment and an even smaller amount (0.001%) passes through the aqueous humor and lens into the posterior segment [5,117–119]. To achieve therapeutic concentrations

eye drops have to be instilled frequently or in high doses [9]. Studies have shown that a frequent administration over a long period of time leads to poor patient adherence to the therapy. For example, 50% of patients suffering with glaucoma stopped their topical treatment within six months [120].

1.4.2 Periocular

In periocular administration, the drug gets injected into the surrounding area of the eye and includes sub-Tenon's, peribulbar, retrobulbar and subconjunctival injections. Small amounts of the drug could reach the vitreous through the choroid via systemic circulation or the anterior route (cornea → aqueous → vitreous) [1]. However, due to the high choroidal blood flow and the limited permeability of the cornea, these routes are secondary. The main route by which the drug can reach the vitreous is transscleral. The sclera covers approximately 95% of the ocular surface and, thus, offers a large region for absorption [121]. It is permeable for molecules up to 70 kDa (compared to < 1 kDa of the cornea) which makes it a more suitable administration technique especially for hydrophilic drugs compared to a topical application [122]. Interestingly, the scleral permeability mainly depends on size and not the lipophilicity of the drug [35,123]. In order to reach the aqueous and vitreous humor, the drugs have to permeate different layers of ocular tissue (sclera, choroid, Bruch's membrane, RPE). Additionally, the high choroidal blood flow limits the bioavailability. After a subconjunctival injection roughly 80-95% of the drug gets absorbed into the systemic circulation and only a small amount is able to penetrate the sclera. This leads to a short duration of action and a bioavailability of up to 10% in the aqueous and 0.1% in the vitreous [124,125]. However, the relatively high administration volume of up to 0.5 mL compensates for the low bioavailability. Studies have shown that the concentration of dexamethasone in the subretinal fluid is higher after subconjunctival injection than after peribulbar or oral administration [126]. Nevertheless, same as with a topical application, a frequent administration is necessary in order to maintain therapeutic concentrations in the ocular tissue, and every injection bears the risk of side effects such as subconjunctival hemorrhage, hyperemia and irritation of the conjunctiva [127,128].

1.4.3 Suprachoroidal

A relatively new method is the suprachoroidal injection and was first introduced by Einmahl et al. in 2002 [129]. The drug is administered into the suprachoroidal space between the sclera

and the choroid using a microneedle and an administration volume of up to 50 µL. Due to the circumvention of the sclera and the injection site being closer to the retina, the bioavailability is with 0.2-4% higher than after subconjunctival injections, especially for lipophilic drugs and macromolecules that do not have to pass the scleral barrier. The bioavailability mainly depends on the drug elimination by choroidal blood flow and the permeability across the RPE. Suprachoroidal injections do not penetrate the inner eye or influence visual acuity as opposed to intravitreal injections. They already have been tested for administration of bevacizumab for AMD and triamcinolone acetonide with high concentrations measured in the vitreous and retina [130–132]. However, each injection poses a small risk for subconjunctival and suprachoroidal hemorrhage [128,132–134].

1.4.4 Systemic/oral

A systemic or oral administration can be used for front- and back-of-the eye diseases. It is the most noninvasive route of administration and, thus, has a high patient compliance. However, the bioavailability is very low due to the BAB and BRB. Only about 2% of the administered drug can be found in the vitreous cavity. To reach efficient drug concentrations in the eye, high doses have to be given, which increases the risk of unwanted side effects. [5,115,135]

There are two possible pathways for a drug to reach the eye. The drug can penetrate through the leaky vessels of the ciliary body and the iris into the aqueous humor, passing the BAB, or through penetration of the RPE passing the BRB. The tight junctions limit this process considerably. For small hydrophilic compounds the permeability through the tight junctions is inversely correlated with the molecular weight, hindering big molecules from entering. For lipophilic drugs it is easier to penetrate the ocular barriers even through transcellular diffusion. Due to the limited permeability through the blood-ocular barriers only small or extremely lipophilic drugs can be administered systemically to treat ophthalmic conditions, e.g. steroids or antibiotics are given systemically to treat inflammatory conditions [2,135,136].

1.4.5 Intravitreal

The highest concentrations in the vitreous can be achieved with intravitreal injections. They directly bypass the BRB and have the highest bioavailability, but it is also the most invasive

method. The duration of action after an intravitreal injection strongly depends on the characteristics of the drug. The anterior elimination is available for all compounds, independent of size and hydrophilicity, and includes drug diffusion from the vitreous into the aqueous humor via the trabecular or uveoscleral pathway. The posterior way is mostly used by small, lipophilic drugs and includes a passive diffusion or active transport across the BRB. Since the retina has a rather big surface, drugs that get eliminated via both pathways (e.g. corticosteroids) have a drastically lower intravitreal half-life than larger compounds (e.g. anti-VEGF) [3,24]. The half-life of low-molecular weight drugs can be as small as 2 h to 6 h. In order to maintain a therapeutically effective concentration in the vitreous, frequent injections would be necessary which decreases patient compliance and increases the probability of serious side-effects. Those serious side effects have a low incidence rate but can be potentially sight-threatening and include retinal detachment, endophthalmitis, vitreous hemorrhage and cataract formation [1,2,5,9,115]. To reduce the incidence of these side effects, the drug release in the vitreous should be prolonged.

Table 1.2. Summary of the different administration techniques. Adapted from [13,128].

Administration technique	Advantages	Disadvantages	BA in the vitreous	Side effects
Topical	Easy self-administration, non-invasive	Frequent application necessary, poor compliance	0.001%	Conjunctival redness, irritation
Periocular	High administration volume	Frequent application necessary	0.1%	Hemorrhage, hyperemia, irritation of conjunctiva
Suprachoroidal	Minimal injection risk	Drug elimination via choroidal blood flow	0.2-4%	Subconjunctival and suprachoroidal hemorrhage
Systemic/oral	High compliance, non-invasive	Systemic toxicity	2%	Systemic side effects depending on the mechanism of action of the administered drug
Intravitreal	Targeted delivery, most direct	Invasive, poor compliance	100%	Retinal detachment, hemorrhage, cataract, endophthalmitis

Abbreviation: BA, bioavailability

1.5 Ocular implants for sustained drug release

Due to the limited ocular bioavailability of the different drug administrations and the increased side effects connected with multiple intraocular injections, implants for a prolonged drug release are an interesting possibility. Therapeutic agents are encapsulated in a biocompatible matrix that is then implanted in the eye. Depending on the system, the implants can release constant drug amounts over a period of days up to multiple years. The implants can be divided into non-biodegradable and biodegradable [115,137,138].

1.5.1 Non-biodegradable implants

Non-biodegradable implants are often made from polyvinyl alcohol (PVA) and ethylene vinyl acetate (EVA). The PVA is permeable for water which after implantation diffuses into the implant where it partially dissolves the drug contained inside, whereas EVA is impermeable and limits water penetration and drug diffusion. The dissolved drug can then diffuse into the surrounding tissue. Often, these implants are inserted via invasive surgery and usually require surgical removal upon completion of the drug release [9,97,115].

Retisert® (Bausch + Lomb) contains 0.59 mg fluocinolone acetonide in a PVA/EVA-matrix. It is disc-shaped with a size of 3x2 mm (see Figure. 7). To insert the implant, a 3-4 mm long incision through the pars plana is made during a surgical procedure. Initially it releases 0.6 µg/day and 0.3-0.4 µg/day in a steady state for about 30 months. It is FDA approved for chronic noninfectious uveitis affecting the posterior segment. It has been shown to reduce the recurrence rate of sever posterior uveitis, improve the visual acuity and decrease the need for adjunctive immunosuppressive therapy [9,97].

Figure 1.7: The size of Iluvien® (left) and Retisert® (right) in comparison. Adapted from [139].

Iluvien® (Alimera sciences) is a rod-shaped device with a size of 3.5x0.37 mm containing 0.19 mg fluocinolone acetonide (Figure 1.7). A polyimide tube with fluocinolone acetonide is embedded in a PVA matrix and injected with a 25-gauge inserter in a surgical procedure. It releases a low dose of fluocinolone acetonide over 13-36 months and was approved by the FDA in 2014 for diabetic macular edema [97,140].

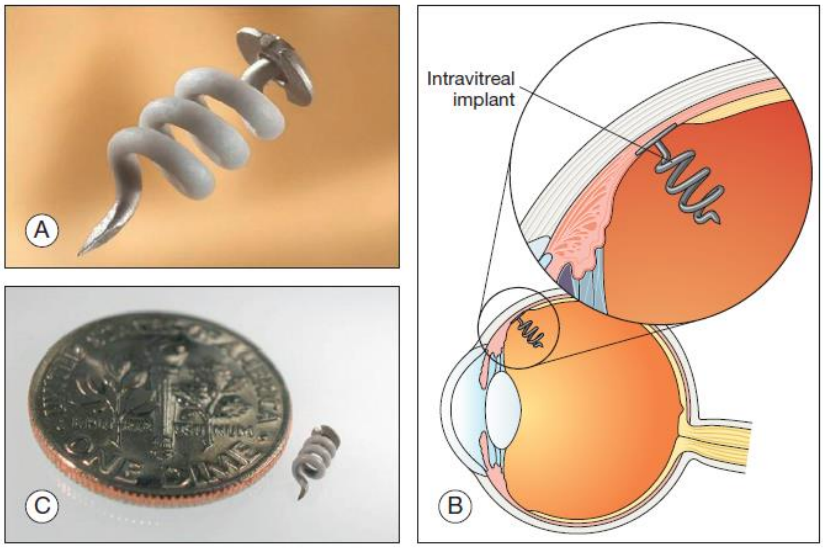

Figure 1.8: I-vation implant. A: structure, B: size, C: implantation. From [141].

A different approach is I-vation containing 0.925 mg triamcinolone acetonide. Its titanium, helical coil measures 0.5-0.21 mm and gets anchored in the sclera (Figure 1.8). Due to its shape, the surface area is maximized. It has no FDA approval yet. It was tested in a phase I clinical trial for the treatment of diabetic macular edema. A phase II trial was terminated leaving the current status of the implant unclear [97,142,143].

1.5.2 Biodegradable implants

Biodegradable implants consist of a biocompatible polymer that produces nontoxic degradation products. They can be eliminated safely and do not cause chronic-foreign body reactions. They often contain synthetic aliphatic polyesters of the poly-α-hydroxy family, such as PGA, PLA and PLGA [97,115].

Surodex® (Oculex Pharmaceuticals, Inc.) is a rod-shaped device with a size of 1.0x0.5 mm. It contains 0.060 mg dexamethasone in a PLGA matrix with HPMC. It gets inserted into the anterior chamber after cataract surgery and controls the postoperative inflammation. In a randomized controlled study for the control of postcataract surgery inflammation, Surodex® was found

to be more effective as 0.1% dexamethasone eyedrops. However, due to its limited release over 7-10 days, the application of the implant is limited. It is only approved in China and Singapore [135,144–146].

Figure 1.9: Ozurdex® intravitreal injection device. From [64].

Ozurdex® (Allergan Inc.) contains 0.7 mg dexamethasone within a PLGA copolymer (Novadur™, Allergan Inc.). The implant is rod shaped and releases the drug over a period of up to six months. The release is biphasic: the initial release within the first two months is higher than the release in the following (up to six) months. It gets injected with a specially designed applicator through the pars plana in an office-based procedure without the need for sutures (Figure 1.9). Upon injection in the eye, water diffuses into the implant and dexamethasone gets released. Over time the PLGA degrades into lactic acid and glycolic acid which are metabolized in the Krebs cycle to water and carbon dioxide. It got FDA approval for macular edema following central and branch retinal vein occlusion in 2009, followed by approval for the treatment of noninfectious uveitis involving the posterior segment in 2010 and for the treatment of diabetic macular edema in 2014 [64,97,147].

1.6 Poly(D, L-lactic-co-glycolic)acid

1.6.1 Physico-chemical properties

Poly(lactic-co-glycolic)acid (PLGA) is a biodegradable and biocompatible polymer that is syn0thesized via ring opening polymerization of the cyclic diesters lactide and glycolide. The dimers are linked together by ester linkages (Figure 1.10). PLGA is one of the most common biodegradable polymers and was first used in the 1960s as bioresorbable sutures. It is also possible to fabricate various forms such as membranes, rods and disc using molding, extrusion and

other techniques. They are commercially available in many FDA-approved products for parenteral controlled release and other administration techniques. PLGA is soluble in a wide range of solvents such as tetrahydrofuran, acetone, chlorinated solvents and ethyl acetate, which makes it suitable for a wide range of preparation techniques [115,148–151].

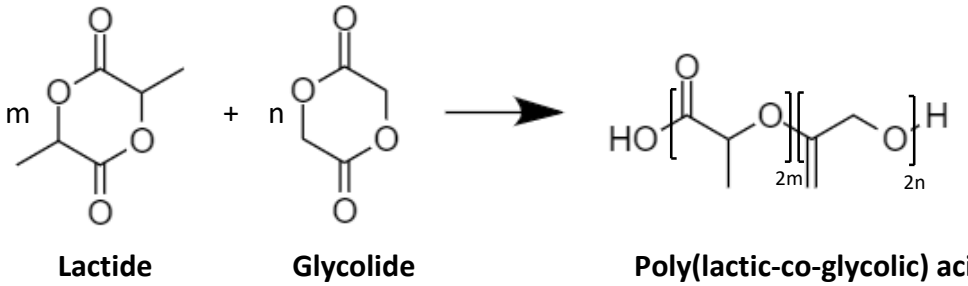

Figure 1.10: Principle of PLGA synthesis through ring-opening copolymerization of lactide and glycolide. Adapted from [152].

Due to the additional methyl group of lactic acid, the molecule is chiral. It exists in two enantiomers: D- and L-lactic acid. Normally, a racemic mixture is used for the polymerization, leading to equal amounts of D- and L-lactic acid in the polymer chain. The polymer structure of L-polylactic-acid (L-PLA) is highly regular and, thus, it is semi crystalline, whereas D,L-PLA is amorphous due to various irregularities of the polymer chain. Poly-glycolic acid (PGA) is highly crystalline. PLGAs containing less than 70% glycolide are amorphous [153,154]. Also, the additional methyl group of the lactic acid makes the molecule more hydrophobic compared to glycolic acid. Thus, by varying the composition of the PLGA (different ratios of lactide : glycolide used during polymerization, e.g. 50:50, 75:25, 85:15,…) the hydrophobicity of the polymer can be adjusted. More hydrophobic polymers take up less water and degrade slower. Figure 1.11 shows the relation between the lactide/glycolide ratio and its resulting degradation time. The fastest degrading PLGA contains a ratio of 50:50. The molecular weight of the PLGA can also influence the mechanical strength of the polymer and might influence the biodegradation rate and hydrolysis [154–157].

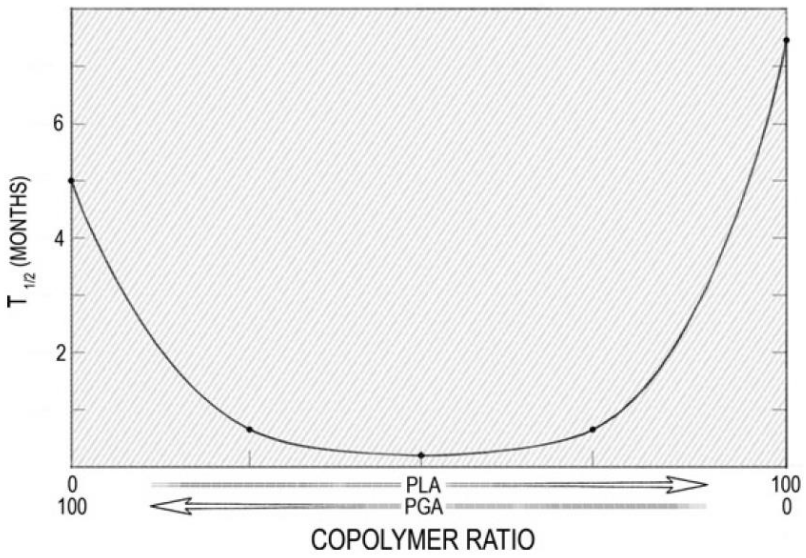

Figure 1.11: Relationship between lactide/glycolide content and degradation half-life of PLGA, Graph illustrates how PLA and PGA polymer ratios can be adjusted to result in a specific biodegradation half-life and drug release from the implant. From [158].

Due to the amorphous structure of the PLGA, it can also be characterized by a glass transition temperature (Tg). It describes the temperature at which the polymer changes from a glassy to a rubbery state. For most types of PLGA it is higher than 37° C. This means that the polymer is in a glassy state at a physiological temperature and the PLGA is practically immobile. The Tg increases with an increase of lactic acid and a higher molecular weight. Plasticizers can reduce the Tg of amorphous polymers and increase the flexibility of the polymer chain. Water is a known plasticizer for PLGA. If the Tg gets reduced to under 37° C, the PLGA turns into a rubbery state at physiological temperatures [159–162].

1.6.2 Biodegradation and biocompatibility

The polymer degrades due to a nonenzymatic hydrolysis of the ester linkages and undergoes bulk erosion. That means that the rate of medium penetration is faster than the polymer solubilization. The degradation takes place in different steps as seen in Figure 1.12. Drug molecules are shown in red, water molecules in blue. Before administration, the PLGA implant is dry (**A**). When the implant is administered, the drug molecules located on the surface of the implant immediately get released into the surrounding medium. This early drug release is called burst (**B**). Water slowly starts to penetrate the implant through various pores, leading to a swelling of the implant, and dissolves the drug inside. The drug slowly diffuses out of the implant. The

PLGA undergoes random chain scission caused by the water and slowly starts to degrade, increasing the porosity of the implant, facilitating the drug release (**C**). When the polymer chains are short enough to be soluble in the medium, they leave the implant causing a mass loss and a structural break down. Eventually, the shape of the implant alters further until there are only fragments left (**D-F**).

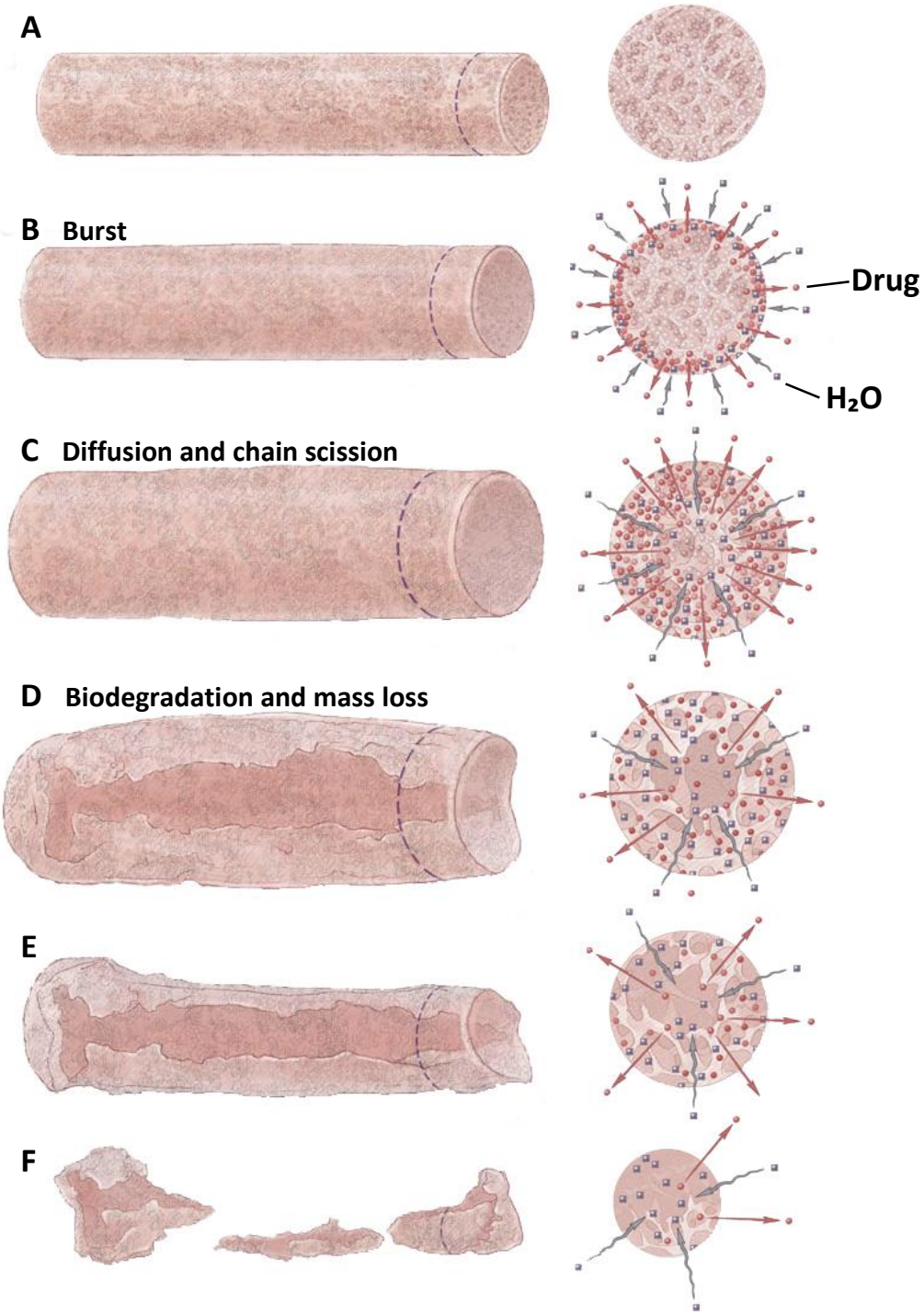

Figure 1.12: Drug-release mechanisms and biodegradation of matrix implant. Adapted from [115].

During degradation, carboxylic acids are formed. On the outside of the implant the acids only have a short diffusion pathway and can easily leave the implant. Further on the inside, the acids can accumulate and accelerate the degradation process by decreasing the pH. This leads to a faster degradation inside, often leaving a hollow implant. This process is called autocatalysis and a well-known phenomenon for PLGA-based drug delivery systems. This internal drop in pH can affect acid labile drugs such as proteins or accelerate the drug release [115,149,163–165].

The drug release rate from PLGA-based drug delivery systems depends on various factors, such as the total surface area, drug loading, solubility of the drug, polymer degradation, polymer swelling and others. The mechanisms behind the drug release are very complex and are not fully understood [9,166].

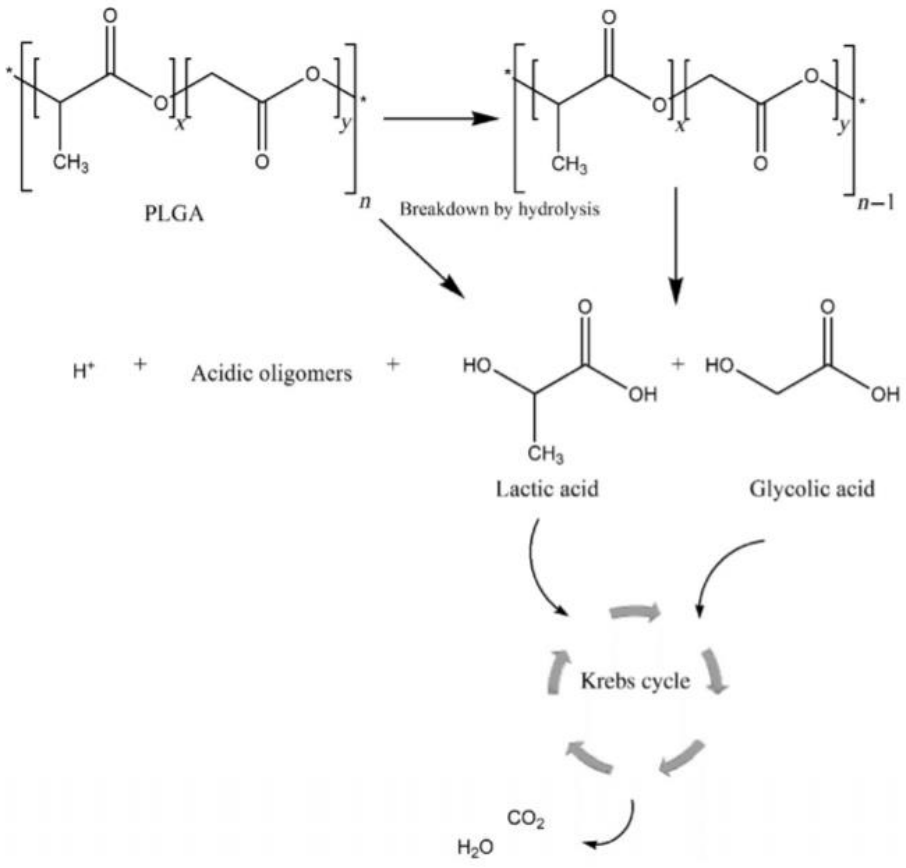

Figure 1.13: PLGA degradation and metabolism. Adapted from [167].

During the degradation, eventually the water-soluble monomers lactic acid and glycolic acid are formed. Glycolic acid either gets eliminated by the kidney or, like lactic acid, converted to

carbon dioxide and water in the Krebs cycle (Figure 1.13) [168]. Due to the slow rate of degradation and the metabolism of the monomers, PLGA was shown to be well tolerated and biocompatible in ocular and non-ocular tissues. It is widely used as suture material, fracture fixation devices and even intraocular implants that underwent clinical trials and are approved by the FDA. Studies have shown that intraocular injection of PLGA microspheres caused a mild inflammation of the vitreous, retina and sometimes choroid in the first stage after injection. After four days no clinical signs of inflammation were visible in the anterior and posterior segments of the eye [169]. After a few weeks, only localized foreign body reactions around the microspheres were found [170]. The volume, shape and surface of the implant/microspheres can influence the response and depends on the tissue, organ and species [171].

Studies suggest that the biocompatibility and tolerance of PLGA is better in ocular tissue compared to non-ocular tissue. The eye displays immune privilege (a lower inflammatory immune response to antigens) to protect it from inflammation that may cause vision impairment. A lack of lymphatic drainage pathways, the blood-ocular barrier, soluble immunosuppressive factors in the eye and others effectively limit the immune response and reduce inflammatory reactions [115,172–174].

1.6.3 Sterilization

For an intravitreal application of PLGA/PLA devices, the implant or implant formulation needs to be sterilized. Common methods for sterilization include dry or moist heat sterilization, ethylene oxide gas and ionizing radiation. High temperatures and humidity can induce degradation and hydrolysis of the polymer, thus is an inappropriate sterilization approach. When using ethylene oxid, remaining amounts of the gas in the product could cause toxicological problems. Therefore the use of γ-irradiation seems to be the best choice for sterilization of PLGA and PLA [175,176].

The γ-irradiation causes the ionization of atoms. The free electrons that are being formed can then interact with DNA and other cell structures and cause the death of the microorganisms. To sterilize pharmaceutical products a radiation dose of at least 25kGy is being used. Depending on the size and quantity of the products to be sterilized, a several hours or a few days are needed [177].

Even though γ-irradiation is the preferred sterilization method, it does influence the physical and chemical properties of PLGA and PLA. It has been shown that the biodegradable polyesters

undergo a dose dependent chain scission and cross-linking. This chain scission leads to a reduced molecular weight of the polymer and in consequence an accelerated polymer degradation [178–180]. Interestingly, the polydispersity indices do not change significantly after the irradiation which indicates that the chain scission is random and not predominantly at the end-groups [181,182].

Despite the reduction in molecular weight, studies have shown no consistent influence of γ-radiation on the drug release. Depending on the drug, the drug release can be increased, decreased or unaffected [183–185]. Studies on the PLGA-implant Ozurdex® (containing dexamethasone) showed, that the drug release was similar before and after sterilization [186].

1.7 Techniques prolonging drug release using PLGA

Due to the high biocompatibility and its possibility to vary degradation time via molecular weight and lactide/glycolide ratio, PLGA is a widely used polymer also for ophthalmic formulations.

1.7.1 Microparticles

Microparticles are small solid particles with a size between 1-1000 µm in diameter. They can be categorized into microcapsules in which the drug is encapsulated in a polymer shell and microspheres where the drug is dissolved or dispersed in a polymer matrix (Figure 1.14). They can be prepared for example via coacervation (phase separation), spray drying or solvent evaporation/extraction method. The latter includes dissolving the polymer in a volatile solvent that is immiscible with water, such as dichloromethane. The drug gets dissolved or dispersed in the polymer solution (inner phase). Under stirring, the polymer solution is then added to an aqueous phase containing an emulsifier like poly(vinyl alcohol) (external phase). The solvent gets extracted via evaporation at atmospheric pressure or under vacuum [154,187,188]. If the solubility of the inner phase in the external phase is sufficient enough to dissolve the whole amount of solvent, this process is called extraction. If part of the solvent needs to evaporate from the external phase in order to sufficiently harden the particles, it is called evaporation [188]. After solidification, the microparticles are filtered, washed and freeze dried to remove any remaining solvent. Depending on the rate of the solvent removal, stirring and temperature, the porosity of the microparticles can vary.

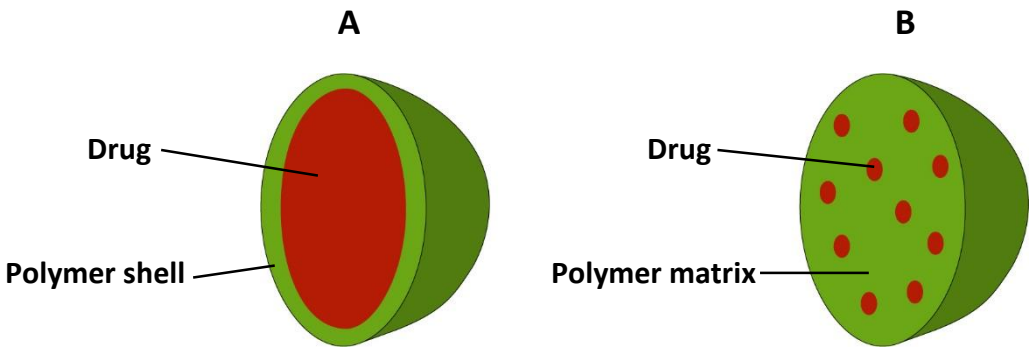

Figure 1.14: Schematic representation of a microcapsule (**A**) and a microsphere (**B**).

The drug release of microparticles depends on many factors such as drug diffusion, polymer degradation and polymer erosion. Often the release is bi- or triphasic [166,189]. Depending on the porosity of the microparticles, the drug that is located on the surface of the polymer matrix gets released fast upon exposure to the release medium ("burst effect"). Afterwards the release slows down and is mainly controlled by drug diffusion in the water-filled pores or in the polymer matrix. Finally, the drug release increases rapidly towards the end when the polymer degrades. This last step has been shown to coincide with polymer swelling [190–194].

Microparticles can be injected into the vitreous as a suspension through a small needle (30-32G). The administered amount of drug can easily be varied depending on the amount of microparticles [195]. Microspheres containing triamcinolone acetonide (RETAAC system) were already tested in humans. They showed good tolerance after intravitreal injection. Also, a phase I/II study with 21 patients with DME was conducted. After three months, a reduction from baseline exceeding 59% was shown. However, there was no significant improvement of visual acuity [142,196].

1.7.2 *In-situ* forming implants

In-situ forming implants (ISFIs) can be categorized by different formation processes such as ionic or chemical cross-linking, temperature and pH changes or solvent exchange [197,198]. One of the most commonly used technique for ISFIs is based on solvent exchange [199,200]. Compared to solid implants, ISFI systems are initially liquid, can be injected with a smaller needle size and are therefore less invasive and painful. They are also easy to manufacture at low costs. [198,200]. Dunn et al. first developed these implants in 1990 [201]. A water-insoluble polymer is dissolved in a water-miscible, biocompatible solvent together with the drug, which can be, depending on the solubility, either dissolved or dispersed in the formulation.

Immediately upon injection into an aqueous environment, the solvent diffuses out of the polymer and water penetrates into the polymer matrix leading to a solidification and implant-formation [197,199,202]. The polymer precipitation starts at the "liquid formulation – aqueous bulk fluid" interface forming a solid shell around the liquid/gel-like formulation inside. This shell creates a diffusion barrier for the solvent and nonsolvent. The remaining polymer inside fills out the interior system and, depending on the polymer concentration, creates a cavity or macrovoid. During this implant formation (from a liquid into a solid state), often a high initial drug release called burst is observed [203,204].

Possible polymers for solvent-induced ISFI are for example PLA, PGA, PLGA, poly-caprolactones, chitosan derivates, poly-vinyl alcohol, poly-vinyl derivates [197,205,206].

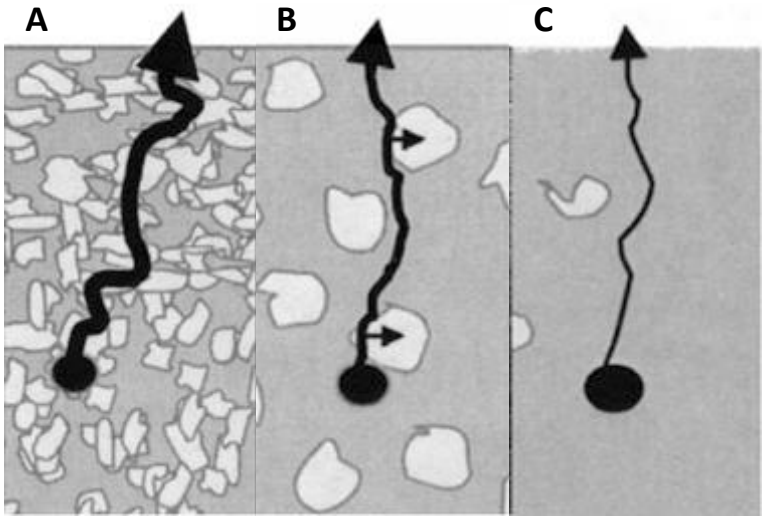

Figure 1.15: Scheme of matrix structure and postulated preferred pathway of protein release for NMP (**A**), triacetin (**B**) and ethyl benzoate (**C**) as solvents. Grey regions indicate the polymer-rich phase, bright areas represent water filled pores, and arrow thickness indicates release rates. Adapted from [207].

The water-miscibility of the solvents strongly influences the phase inversion rate. Based on the solvent, the system can be divided into fast- and slow-inverting systems. Highly water miscible solvents such as 2-N-methyl pyrrolidone (NMP) and dimethyl sulfoxide (DMSO) rapidly diffuse out of the implant solution, hence are part of a fast-inverting system. They are also strong solvents for PLGA which facilitates the preparation of high polymer concentrations that are still injectable [208]. However, due to their rapid phase inversion, they form thin surface membranes and promote finger-like porous cavities in the inner implant [197,200,209–211]. Contrary to fast inverting systems, slow inverting systems cause thicker films and a more homogenous

spongy layer of the implant. Slow inverting systems are usually based on solvents with a lower water miscibility such as ethyl benzoate and triacetin, or can be achieved with the addition of different excipients [209,210,212–215]. Figure 1.15 shows the influence of porosity on the drug release. Fast inverting ISFIs prepared with a highly water-miscible solvent, such as NMP, have a higher drug release due to the resulting porosity of the system. The water-filled pores increase the amount of dissolved drug inside the implants and facilitates the diffusion out of the implant.

A higher polymer concentration increases the viscosity of the formulation and thereby slows down the liquid-liquid phase separation and the water influx rate [209]. After the shell-formation due to the initial solvent exchange, more polymer is available to fill the void inside the implant which results in a thicker wall, a longer diffusional pathway for the drug and also a slower drug release. Another factor influencing the implant structure and drug release is the molecular weight of the polymer. It has been shown that polymers with a lower molecular weight have a higher phase inversion and higher initial drug release. This could be explained by a higher hydrophilicity and degradation rate of these polymers [216–218].

Apart from varying the solvent, the polymer molecular weight and polymer concentration it is possible to add different substances to vary the implant characteristics, formation and drug release. The addition of hydrophilic polymers, such as hydroxy methylcellulose (HPMC), could increase the bioadhesion of ISFI in the periodontal pocket [219–222]. Studies have shown, that additives with a low water-miscibility can reduce the formation of macrovoids and pore size in the implants and hence the drug release [203,204,223–225].

Despite their advantages, for example being less invasive, ISFIs also have various disadvantages. If the polymer concentration in the formulation is too high, the injectability is limited due to the high viscosity. The formation of the implants *in-situ* also results in a high variability of the implant shape which could influence the conformity of the drug release and a high burst release could cause initially toxic levels of the incorporated drug [198,212,226]. Additionally, the use of organic solvents, such as NMP, is controversially discussed. It can cause mild irritation to the eyes, mucous membranes and the skin and is myotoxic [227–229] Despite the controversial discussion, various products include NMP as a solvent, such as Atridox (for injection into periodontal pockets) [230] and Eligard (a leuprolide acetate suspension for subcutaneous injection) [231]. The toxicity of NMP upon intraocular injection is not yet sufficiently investigated.

1.7.3 Pre-formed implants

Pre-formed implants can be produced by different preparation techniques including solvents, heat, pressure or a combination of the different methods (Figure 1.16) to obtain different shapes such as rods, discs or membranes [168,232]. Depending on manufacturing processes and parameters the brittleness, flexibility and porosity of the implants may vary [233,234].

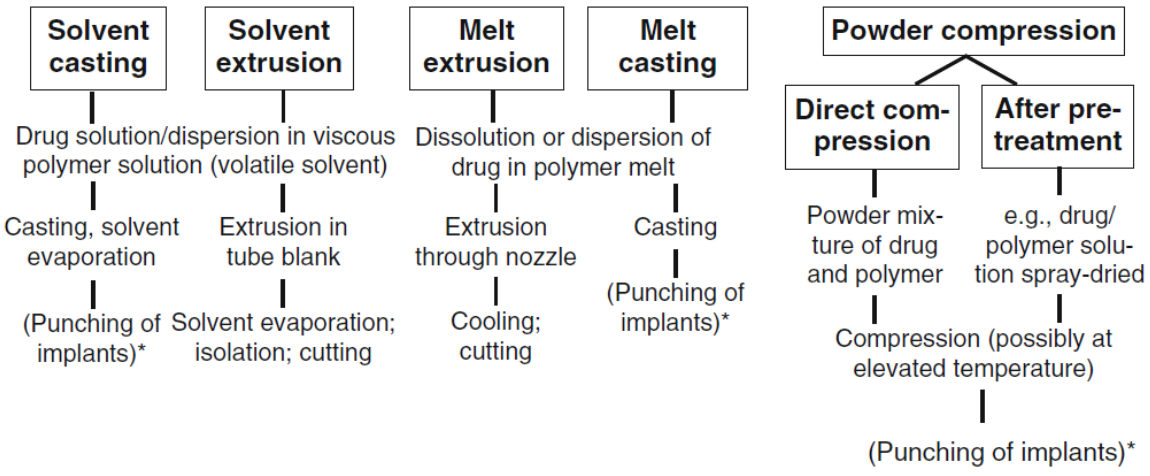

Figure 1.16: Summary of the principles of some common preparation techniques for implants. From [207].

Solvent casting and solvent extrusion are suitable for implants containing thermolabile compounds, due to the fact that no elevated temperatures are needed for the preparation. The polymer is dissolved in a suitable solvent, the drug dissolved or suspended and then spread on a plate or extruded into a silicone tube. During the solvent evaporation, the polymer-drug mixture precipitates and forms solid membranes or implants. Depending on the solvent, this evaporation can take long which increases the risks of demixing (if the drug is suspended) and Ostwald ripening (the dissolution of small drug crystals and formation of larger ones) [207,235]. If the solvent removal is incomplete, the residue could cause toxic reactions in-vivo. In order to decrease evaporation time and a complete solvent removal, solvents with a high vapor pressure such as acetone are usually preferred.

To avoid the use of solvents, implants can be formed via powder compression. A mixture of the polymer and drug can be either directly compressed or after a pre-treatment such as spray-

drying to improve homogeneity of the mixture. However, when it is pre-treated, residual solvent could still be contained in the implants [207].

Another possible preparation technique is melt extrusion or melt casting. The process of hot melt extrusion has been known to the food and plastic industry since the 1930s and is used for drug delivery systems since the 1970s [236,237]. The polymer-drug mixture is melted and extruded through a die which can vary in size (melt extrusion) or the molten mixture is transferred into a mold under high pressure to obtain various complex shapes (injection molding/melt casting). Big advantages of these processing methods are the lack of solvents and the possibility to control many process parameters and also use it for continuous manufacturing [238,239]. In a laboratory scale plastic syringes and syringe pumps can be used at elevated temperatures in order to reduce the amount of polymer [240,241]. However, the use of high temperature can influence the stability of the incorporated drug, especially for proteins [240,242], and decrease the molecular weight of the polymer [243]. An example for an implant prepared via hot melt extrusion is Ozurdex® (see Chapter 1.7.2).

References

[1] D. Ghate, H.F. Edelhauser, Ocular drug delivery, Expert Opin. Drug Deliv. 3 (2006) 275–287. doi:10.1517/17425247.3.2.275.

[2] B.R. Conway, Recent patents on ocular drug delivery systems, Recent Pat. Drug Deliv. Formul. 2 (2008) 1–8.

[3] R. Gaudana, H.K. Ananthula, A. Parenky, A.K. Mitra, Ocular Drug Delivery, AAPS J. 12 (2010) 348–360. doi:10.1208/s12248-010-9183-3.

[4] T.F. Freddo, Shifting the Paradigm of the Blood–Aqueous Barrier, Exp. Eye Res. 73 (2001) 581–592. doi:10.1006/exer.2001.1056.

[5] S. Duvvuri, S. Majumdar, A.K. Mitra, Drug delivery to the retina: challenges and opportunities, Expert Opin. Biol. Ther. 3 (2003) 45–56. doi:10.1517/14712598.3.1.45.

[6] R.D. Jager, L.P. Aiello, S.C. Patel, E.T. Cunningham, Risks of intravitreous injection: a comprehensive review, Retina Phila. Pa. 24 (2004) 676–698.

[7] M.S. Stay, J. Xu, T.W. Randolph, V.H. Barocas, Computer simulation of convective and diffusive transport of controlled-release drugs in the vitreous humor, Pharm. Res. 20 (2003) 96–102.

[8] D.W. Drolet, J. Nelson, C.E. Tucker, P.M. Zack, K. Nixon, R. Bolin, M.B. Judkins, J.A. Farmer, J.L. Wolf, S.C. Gill, R.A. Bendele, Pharmacokinetics and safety of an anti-vascular endothelial growth factor aptamer (NX1838) following injection into the vitreous humor of rhesus monkeys, Pharm. Res. 17 (2000) 1503–1510.

[9] T. Yasukawa, Y. Ogura, H. Kimura, E. Sakurai, Y. Tabata, Drug delivery from ocular implants, Expert Opin. Drug Deliv. 3 (2006) 261–273. doi:10.1517/17425247.3.2.261.

[10] V. Agrahari, A. Mandal, V. Agrahari, H.M. Trinh, M. Joseph, A. Ray, H. Hadji, R. Mitra, D. Pal, A.K. Mitra, A comprehensive insight on ocular pharmacokinetics, Drug Deliv. Transl. Res. 6 (2016) 735–754. doi:10.1007/s13346-016-0339-2.

[11] T.J. Millar, B.S. Schuett, The real reason for having a meibomian lipid layer covering the outer surface of the tear film – A review, Exp. Eye Res. 137 (2015) 125–138. doi:10.1016/j.exer.2015.05.002.

[12] J. Wang, D. Fonn, T.L. Simpson, L. Jones, Precorneal and pre- and postlens tear film thickness measured indirectly with optical coherence tomography, Invest. Ophthalmol. Vis. Sci. 44 (2003) 2524–2528.

[13] K. Nayak, M. Misra, A review on recent drug delivery systems for posterior segment of eye, Biomed. Pharmacother. 107 (2018) 1564–1582. doi:10.1016/j.biopha.2018.08.138.

[14] H.S. Huang, R.D. Schoenwald, J.L. Lach, Corneal penetration behavior of beta-blocking agents II: Assessment of barrier contributions, J. Pharm. Sci. 72 (1983) 1272–1279.

[15] M.J. Doughty, M.L. Zaman, Human Corneal Thickness and Its Impact on Intraocular Pressure Measures: A Review and Meta-analysis Approach, Surv. Ophthalmol. 44 (2000) 367–408. doi:10.1016/S0039-6257(00)00110-7.

[16] D.H. Geroski, H.F. Edelhauser, Drug Delivery for Posterior Segment Eye Disease, Invest. Ophthalmol. Vis. Sci. 41 (2000) 961–964.

[17] K. Hosoya, V.H.L. Lee, K.-J. Kim, Roles of the conjunctiva in ocular drug delivery: a review of conjunctival transport mechanisms and their regulation, Eur. J. Pharm. Biopharm. 60 (2005) 227–240. doi:10.1016/j.ejpb.2004.12.007.

[18] M. Ruponen, A. Urtti, Undefined role of mucus as a barrier in ocular drug delivery, Eur. J. Pharm. Biopharm. 96 (2015) 442–446. doi:10.1016/j.ejpb.2015.02.032.

[19] D. Huang, Y.-S. Chen, I.D. Rupenthal, Overcoming ocular drug delivery barriers through the use of physical forces, Adv. Drug Deliv. Rev. 126 (2018) 96–112. doi:10.1016/j.addr.2017.09.008.

[20] J. Ambati, C.S. Canakis, J.W. Miller, E.S. Gragoudas, A. Edwards, D.J. Weissgold, I. Kim, F.C. Delori, A.P. Adamis, Diffusion of high molecular weight compounds through sclera, Invest. Ophthalmol. Vis. Sci. 41 (2000) 1181–1185.

[21] T.W. Olsen, S.Y. Aaberg, D.H. Geroski, H.F. Edelhauser, Human sclera: Thickness and surface area, Am. J. Ophthalmol. 125 (1998) 237–241. doi:10.1016/S0002-9394(99)80096-8.

[22] O.A. Boubriak, J.P.G. Urban, S. Akhtar, K.M. Meek, A.J. Bron, The Effect of Hydration and Matrix Composition on Solute Diffusion in Rabbit Sclera, Exp. Eye Res. 71 (2000) 503–514. doi:10.1006/exer.2000.0909.

[23] J. Cunha-Vaz, The blood-ocular barriers, Surv. Ophthalmol. 23 (1979) 279–296.

[24] A. Urtti, Challenges and obstacles of ocular pharmacokinetics and drug delivery, Adv. Drug Deliv. Rev. 58 (2006) 1131–1135. doi:10.1016/j.addr.2006.07.027.

[25] J. Barar, A.R. Javadzadeh, Y. Omidi, Ocular novel drug delivery: impacts of membranes and barriers, Expert Opin. Drug Deliv. 5 (2008) 567–581. doi:10.1517/17425247.5.5.567.

[26] K. Cholkar, S.R. Dasari, D. Pal, A.K. Mitra, 1 - Eye: anatomy, physiology and barriers to drug delivery, in: A.K. Mitra (Ed.), Ocul. Transp. Recept., Woodhead Publishing, 2013: pp. 1–36. http://www.sciencedirect.com/science/article/pii/B9781907568862500010 (accessed August 25, 2015).

[27] P.M. Hughes, O. Olejnik, J.-E. Chang-Lin, C.G. Wilson, Topical and systemic drug delivery to the posterior segments, Adv. Drug Deliv. Rev. 57 (2005) 2010–2032. doi:10.1016/j.addr.2005.09.004.

[28] J.G. Cunha-Vaz, The blood-ocular barriers: past, present, and future, Doc. Ophthalmol. Adv. Ophthalmol. 93 (1997) 149–157.

[29] M.-S. Chen, P.-K. Hou, T.-Y. Tai, B.J. Lin, Blood-Ocular Barriers, Tzu Chi Med. J. 20 (2008) 25–34. doi:10.1016/S1016-3190(08)60004-X.

[30] S. Awwad, A. Lockwood, S. Brocchini, P.T. Khaw, The PK-Eye: A Novel In Vitro Ocular Flow Model for Use in Preclinical Drug Development, J. Pharm. Sci. (2015) n/a-n/a. doi:10.1002/jps.24480.

[31] R.F. Brubaker, The flow of aqueous humor in the human eye, Trans. Am. Ophthalmol. Soc. 80 (1982) 391–474.

[32] Y.A. Ito, M.A. Walter, Genetics and Environmental Stress Factor Contributions to Anterior Segment Malformations and Glaucoma, Glaucoma - Basic Clin. Asp. (2013). doi:10.5772/54653.

[33] N. Haghjou, M.J. Abdekhodaie, Y.-L. Cheng, Retina-Choroid-Sclera Permeability for Ophthalmic Drugs in the Vitreous to Blood Direction: Quantitative Assessment, Pharm. Res. 30 (2013) 41–59. doi:10.1007/s11095-012-0847-9.

[34] H.W. Kwak, D.J. D'Amico, Evaluation of the retinal toxicity and pharmacokinetics of dexamethasone after intravitreal injection, Arch. Ophthalmol. Chic. Ill 1960. 110 (1992) 259–266.

[35] L. Pitkänen, V.-P. Ranta, H. Moilanen, A. Urtti, Permeability of retinal pigment epithelium: effects of permeant molecular weight and lipophilicity, Invest. Ophthalmol. Vis. Sci. 46 (2005) 641–646. doi:10.1167/iovs.04-1051.

[36] N. Cheung, P. Mitchell, T.Y. Wong, Diabetic retinopathy, The Lancet. 376 (2010) 124–136. doi:10.1016/S0140-6736(09)62124-3.

[37] T.-T. Wan, X.-F. Li, Y.-M. Sun, Y.-B. Li, Y. Su, Recent advances in understanding the biochemical and molecular mechanism of diabetic retinopathy, Biomed. Pharmacother. 74 (2015) 145–147. doi:10.1016/j.biopha.2015.08.002.

[38] J.W.Y. Yau, S.L. Rogers, R. Kawasaki, E.L. Lamoureux, J.W. Kowalski, T. Bek, S.-J. Chen, J.M. Dekker, A. Fletcher, J. Grauslund, S. Haffner, R.F. Hamman, M.K. Ikram, T. Kayama, B.E.K. Klein, R. Klein, S. Krishnaiah, K. Mayurasakorn, J.P. O'Hare, T.J. Orchard, M. Porta, M. Rema, M.S. Roy, T. Sharma, J. Shaw, H. Taylor, J.M. Tielsch, R. Varma, J.J. Wang, N. Wang, S. West, L. Xu, M. Yasuda, X. Zhang, P. Mitchell, T.Y. Wong, Global Prevalence and Major Risk Factors of Diabetic Retinopathy, Diabetes Care. 35 (2012) 556–564. doi:10.2337/dc11-1909.

[39] Y. Zheng, M. He, N. Congdon, The worldwide epidemic of diabetic retinopathy, Indian J. Ophthalmol. 60 (2012) 428–431. doi:10.4103/0301-4738.100542.

[40] J.A. Davidson, T.A. Ciulla, J.B. McGill, K.A. Kles, P.W. Anderson, How the diabetic eye loses vision, Endocrine. 32 (2007) 107–116. doi:10.1007/s12020-007-0040-9.

[41] R.N. Frank, Diabetic retinopathy, N. Engl. J. Med. 350 (2004) 48–58. doi:10.1056/NEJMra021678.

[42] R.A. Kowluru, M. Mishra, Oxidative stress, mitochondrial damage and diabetic retinopathy, Biochim. Biophys. Acta BBA - Mol. Basis Dis. 1852 (2015) 2474–2483. doi:10.1016/j.bbadis.2015.08.001.

[43] K. Miller, J.A. Fortun, Diabetic Macular Edema: Current Understanding, Pharmacologic Treatment Options, and Developing Therapies, Asia-Pac. J. Ophthalmol. Phila. Pa. 7 (2018) 28–35. doi:10.22608/APO.2017529.

[44] J.F. Fangueiro, A.M. Silva, M.L. Garcia, E.B. Souto, Current nanotechnology approaches for the treatment and management of diabetic retinopathy, Eur. J. Pharm. Biopharm. 95, Part B (2015) 307–322. doi:10.1016/j.ejpb.2014.12.023.

[45] R. Klein, B.E.K. Klein, S.E. Moss, M.D. Davis, D.L. DeMets, The Wisconsin Epidemiologic Study of Diabetic Retinopathy: IV. Diabetic Macular Edema, Ophthalmology. 91 (1984) 1464–1474. doi:10.1016/S0161-6420(84)34102-1.

[46] L. Lu, Y. Jiang, R. Jaganathan, Y. Hao, Current Advances in Pharmacotherapy and Technology for Diabetic Retinopathy: A Systematic Review, J. Ophthalmol. (2018). doi:10.1155/2018/1694187.

[47] T.Y. Wong, C.M.G. Cheung, M. Larsen, S. Sharma, R. Simó, Diabetic retinopathy, Nat. Rev. Dis. Primer. 2 (2016) 16012. doi:10.1038/nrdp.2016.12.

[48] N. Dong, B. Xu, B. Wang, L. Chu, Study of 27 aqueous humor cytokines in patients with type 2 diabetes with or without retinopathy, Mol. Vis. 19 (2013) 1734–1746.

[49] S. Kaštelan, M. Tomić, A. Gverović Antunica, J. Salopek Rabatić, S. Ljubić, Inflammation and Pharmacological Treatment in Diabetic Retinopathy, Mediators Inflamm. (2013). doi:10.1155/2013/213130.

[50] J. Tang, T.S. Kern, Inflammation in Diabetic Retinopathy, Prog. Retin. Eye Res. 30 (2011) 343–358. doi:10.1016/j.preteyeres.2011.05.002.

[51] D.S. Friedman, B.J. O'Colmain, B. Muñoz, S.C. Tomany, C. McCarty, P.T.V.M. de Jong, B. Nemesure, P. Mitchell, J. Kempen, Eye Diseases Prevalence Research Group, Prevalence of age-related macular degeneration in the United States, Arch. Ophthalmol. Chic. Ill 1960. 122 (2004) 564–572. doi:10.1001/archopht.122.4.564.

[52] S.C. Tomany, J.J. Wang, R. Van Leeuwen, R. Klein, P. Mitchell, J.R. Vingerling, B.E.K. Klein, W. Smith, P.T.V.M. De Jong, Risk factors for incident age-related macular degeneration: pooled findings from 3 continents, Ophthalmology. 111 (2004) 1280–1287. doi:10.1016/j.ophtha.2003.11.010.

[53] X. Ding, M. Patel, C.-C. Chan, Molecular pathology of age-related macular degeneration, Prog. Retin. Eye Res. 28 (2009) 1–18. doi:10.1016/j.preteyeres.2008.10.001.

[54] W.M. Al-Zamil, S.A. Yassin, Recent developments in age-related macular degeneration: a review, Clin. Interv. Aging. 12 (2017) 1313–1330. doi:10.2147/CIA.S143508.

[55] R.D. Jager, W.F. Mieler, J.W. Miller, Age-Related Macular Degeneration, N. Engl. J. Med. 358 (2008) 2606–2617. doi:10.1056/NEJMra0801537.

[56] V. Bonfiglio, M. Reibaldi, M. Fallico, A. Russo, A. Pizzo, S. Fichera, C. Rapisarda, I. Macchi, T. Avitabile, A. Longo, Widening use of dexamethasone implant for the treatment of macular edema, Drug Des. Devel. Ther. 11 (2017) 2359–2372. doi:10.2147/DDDT.S138922.

[57] S.M. Couch, S.J. Bakri, Review of combination therapies for neovascular age-related macular degeneration, Semin. Ophthalmol. 26 (2011) 114–120. doi:10.3109/08820538.2011.577130.

[58] J. Ambati, B.J. Fowler, Mechanisms of Age-Related Macular Degeneration, Neuron. 75 (2012) 26–39. doi:10.1016/j.neuron.2012.06.018.

[59] N.J.S. London, A. Chiang, J.A. Haller, The dexamethasone drug delivery system: Indications and evidence, Adv. Ther. 28 (2011) 351–366. doi:10.1007/s12325-011-0019-z.

[60] O.M. Durrani, C.A. Meads, P.I. Murray, Uveitis: a potentially blinding disease, Ophthalmol. J. Int. Ophtalmol. Int. J. Ophthalmol. Z. Augenheilkd. 218 (2004) 223–236. doi:10.1159/000078612.

[61] M.S. Suttorp-Schulten, A. Rothova, The possible impact of uveitis in blindness: a literature survey., Br. J. Ophthalmol. 80 (1996) 844–848.

[62] J. Deschenes, P.I. Murray, N.A. Rao, R.B. Nussenblatt, International Uveitis Study Group, International Uveitis Study Group (IUSG): clinical classification of uveitis, Ocul. Immunol. Inflamm. 16 (2008) 1–2. doi:10.1080/09273940801899822.

[63] G.J. Jaffe, D. Martin, D. Callanan, P.A. Pearson, B. Levy, T. Comstock, Fluocinolone Acetonide Implant (Retisert) for Noninfectious Posterior Uveitis: Thirty-Four–Week Results of a Multicenter Randomized Clinical Study, Ophthalmology. 113 (2006) 1020–1027. doi:10.1016/j.ophtha.2006.02.021.

[64] S.R.J. Taylor, H. Isa, L. Joshi, S. Lightman, New Developments in Corticosteroid Therapy for Uveitis, Ophthalmologica. 224 (2010) 46–53. doi:10.1159/000318021.

[65] T.G. Rotsos, M.M. Moschos, Cystoid macular edema, Clin. Ophthalmol. Auckl. NZ. 2 (2008) 919–930.

[66] Y. Guex-Crosier, The pathogenesis and clinical presentation of macular edema in inflammatory diseases, Doc. Ophthalmol. Adv. Ophthalmol. 97 (1999) 297–309.

[67] C.J. Brady, A.C. Villanti, H.A. Law, E. Rahimy, R. Reddy, P.C. Sieving, S.J. Garg, J. Tang, Corticosteroid implants for chronic non-infectious uveitis, Cochrane Database Syst. Rev. 2 (2016) CD010469. doi:10.1002/14651858.CD010469.pub2.

[68] S. Moghadam-Kia, V.P. Werth, Prevention and treatment of systemic glucocorticoid side effects, Int. J. Dermatol. 49 (2010) 239–248. doi:10.1111/j.1365-4632.2009.04322.x.

[69] C.L. Haupert, G.J. Jaffe, New and emerging treatments for patients with uveitis, Int. Ophthalmol. Clin. 40 (2000) 205–220.

[70] J.A. Haller, F. Bandello, R. Belfort, M.S. Blumenkranz, M. Gillies, J. Heier, A. Loewenstein, Y.-H. Yoon, M.-L. Jacques, J. Jiao, X.-Y. Li, S.M. Whitcup, Randomized, Sham-Controlled Trial of Dexamethasone Intravitreal Implant in Patients with Macular Edema Due to Retinal Vein Occlusion, Ophthalmology. 117 (2010) 1134-1146.e3. doi:10.1016/j.ophtha.2010.03.032.

[71] P.J. McCluskey, H.M. Towler, S. Lightman, Management of chronic uveitis, BMJ. 320 (2000) 555–558.

[72] Y. Wu, P. Ai, Z. Ai, G. Xu, Subthreshold diode micropulse laser versus conventional laser photocoagulation monotherapy or combined with anti-VEGF therapy for diabetic macular edema: A Bayesian network meta-analysis, Biomed. Pharmacother. 97 (2018) 293–299. doi:10.1016/j.biopha.2017.10.078.

[73] I. Kozak, J.K. Luttrull, Modern retinal laser therapy, Saudi J. Ophthalmol. 29 (2015) 137–146. doi:10.1016/j.sjopt.2014.09.001.

[74] D.R. Lally, C.P. Shah, J.S. Heier, Vascular endothelial growth factor and diabetic macular edema, Surv. Ophthalmol. 61 (2016) 759–768. doi:10.1016/j.survophthal.2016.03.010.

[75] N. Bhagat, R.A. Grigorian, A. Tutela, M.A. Zarbin, Diabetic Macular Edema: Pathogenesis and Treatment, Surv. Ophthalmol. 54 (2009) 1–32. doi:10.1016/j.survophthal.2008.10.001.

[76] D.F. Rosberger, Diabetic Retinopathy: Current Concepts and Emerging Therapy, Endocrinol. Metab. Clin. North Am. 42 (2013) 721–745. doi:10.1016/j.ecl.2013.08.001.

[77] A.A. Alghadyan, Diabetic retinopathy – An update, Saudi J. Ophthalmol. 25 (2011) 99–111. doi:10.1016/j.sjopt.2011.01.009.

[78] Y. Su, J. Wu, Y. Gu, Photodynamic therapy in combination with ranibizumab versus ranibizumab monotherapy for wet age-related macular degeneration: A systematic review and meta-analysis, Photodiagnosis Photodyn. Ther. 22 (2018) 263–273. doi:10.1016/j.pdpdt.2018.05.002.

[79] P. Nowak-Sliwinska, H. van den Bergh, M. Sickenberg, A.H.C. Koh, Photodynamic therapy for polypoidal choroidal vasculopathy, Prog. Retin. Eye Res. 37 (2013) 182–199. doi:10.1016/j.preteyeres.2013.09.003.

[80] R.Z. Renno, J.W. Miller, Photosensitizer delivery for photodynamic therapy of choroidal neovascularization, Adv. Drug Deliv. Rev. 52 (2001) 63–78. doi:10.1016/S0169-409X(01)00195-8.

[81] T. Al-Debasi, A. Al-Bekairy, A. Al-Katheri, S. Al Harbi, M. Mansour, Topical versus subconjunctival anti-vascular endothelial growth factor therapy (Bevacizumab, Ranibizumab and Aflibercept) for treatment of corneal neovascularization, Saudi J. Ophthalmol. 31 (2017) 99–105. doi:10.1016/j.sjopt.2017.02.008.

[82] N. Cheung, I.Y. Wong, T.Y. Wong, Ocular anti-VEGF therapy for diabetic retinopathy: overview of clinical efficacy and evolving applications, Diabetes Care. 37 (2014) 900–905. doi:10.2337/dc13-1990.

[83] W. Philipp, L. Speicher, C. Humpel, Expression of vascular endothelial growth factor and its receptors in inflamed and vascularized human corneas, Invest. Ophthalmol. Vis. Sci. 41 (2000) 2514–2522.

[84] M. Amadio, S. Govoni, A. Pascale, Targeting VEGF in eye neovascularization: What's new?: A comprehensive review on current therapies and oligonucleotide-based interventions under development, Pharmacol. Res. 103 (2016) 253–269. doi:10.1016/j.phrs.2015.11.027.

[85] L. Xu, T. Lu, L. Tuomi, N. Jumbe, J. Lu, S. Eppler, P. Kuebler, L.A. Damico-Beyer, A. Joshi, Pharmacokinetics of ranibizumab in patients with neovascular age-related macular degeneration: a population approach, Invest. Ophthalmol. Vis. Sci. 54 (2013) 1616–1624. doi:10.1167/iovs.12-10260.

[86] N. Ferrara, L. Damico, N. Shams, H. Lowman, R. Kim, Development of ranibizumab, an anti-vascular endothelial growth factor antigen binding fragment, as therapy for neovascular age-related macular degeneration, Retina Phila. Pa. 26 (2006) 859–870. doi:10.1097/01.iae.0000242842.14624.e7.

[87] J.A. Dixon, S.C.N. Oliver, J.L. Olson, N. Mandava, VEGF Trap-Eye for the treatment of neovascular age-related macular degeneration, Expert Opin. Investig. Drugs. 18 (2009) 1573–1580. doi:10.1517/13543780903201684.

[88] M.W. Stewart, Aflibercept (VEGF-TRAP): the next anti-VEGF drug, Inflamm. Allergy Drug Targets. 10 (2011) 497–508.

[89] F.R. Stefanini, E. Badaró, P. Falabella, M. Koss, M.E. Farah, M. Maia, Anti-VEGF for the Management of Diabetic Macular Edema, J. Immunol. Res. (2014). doi:10.1155/2014/632307.

[90] E.W.M. Ng, D.T. Shima, P. Calias, E.T. Cunningham, D.R. Guyer, A.P. Adamis, Pegaptanib, a targeted anti-VEGF aptamer for ocular vascular disease, Nat. Rev. Drug Discov. 5 (2006) 123–132. doi:10.1038/nrd1955.

[91] E.S. Caplan, A.S. Kesselheim, Anti-VEGF therapy in ophthalmology: a qualitative analysis of transformative drug development, Drug Discov. Today. 21 (2016) 1019–1026. doi:10.1016/j.drudis.2016.05.001.

[92] S. Fogli, S. Mogavero, C.G. Egan, M. Del Re, R. Danesi, Pathophysiology and pharmacological targets of VEGF in diabetic macular edema, Pharmacol. Res. 103 (2016) 149–157. doi:10.1016/j.phrs.2015.11.003.

[93] Y. Duan, J. Mo, R. Klein, I.U. Scott, H.-M. Lin, J. Caulfield, M. Patel, D. Liao, Age-related macular degeneration is associated with incident myocardial infarction among elderly Americans, Ophthalmology. 114 (2007) 732–737. doi:10.1016/j.ophtha.2006.07.045.

[94] S.R. Hayman, N. Leung, J.P. Grande, V.D. Garovic, VEGF Inhibition, Hypertension, and Renal Toxicity, Curr. Oncol. Rep. 14 (2012) 285–294. doi:10.1007/s11912-012-0242-z.

[95] L.H. Curtis, B.G. Hammill, K.A. Schulman, S.W. Cousins, Risks of mortality, myocardial infarction, bleeding, and stroke associated with therapies for age-related macular degeneration, Arch. Ophthalmol. Chic. Ill 1960. 128 (2010) 1273–1279. doi:10.1001/archophthalmol.2010.223.

[96] C. Ehlken, S. Jungmann, D. Böhringer, H.T. Agostini, B. Junker, A. Pielen, Switch of anti-VEGF agents is an option for nonresponders in the treatment of AMD, Eye. 28 (2014) 538–545. doi:10.1038/eye.2014.64.

[97] D.F. Kiernan, W.F. Mieler, The use of intraocular corticosteroids, Expert Opin. Pharmacother. 10 (2009) 2511–2525. doi:10.1517/14656560903160671.

[98] P.M. Beer, S.J. Bakri, R.J. Singh, W. Liu, G.B. Peters III, M. Miller, Intraocular concentration and pharmacokinetics of triamcinolone acetonide after a single intravitreal injection, Ophthalmology. 110 (2003) 681–686. doi:10.1016/S0161-6420(02)01969-3.

[99] J. Cáceres-del-Carpio, R.D. Costa, A. Haider, R. Narayanan, B.D. Kuppermann, Corticosteroids: Triamcinolone, Dexamethasone and Fluocinolone, Retin. Pharmacother. 55 (2016) 221–231. doi:10.1159/000431198.

[100] P.J. Barnes, Glucocorticosteroids: current and future directions, Br. J. Pharmacol. 163 (2011) 29–43. doi:10.1111/j.1476-5381.2010.01199.x.

[101] D.A. Antonetti, E.B. Wolpert, L. DeMaio, N.S. Harhaj, R.C. Scaduto, Hydrocortisone decreases retinal endothelial cell water and solute flux coincident with increased content and decreased phosphorylation of occludin, J. Neurochem. 80 (2002) 667–677. doi:10.1046/j.0022-3042.2001.00740.x.

[102] E.A. Felinski, D.A. Antonetti, Glucocorticoid Regulation of Endothelial Cell Tight Junction Gene Expression: Novel Treatments for Diabetic Retinopathy, Curr. Eye Res. 30 (2005) 949–957. doi:10.1080/02713680500263598.

[103] T.A. Ciulla, A. Harris, N. McIntyre, C. Jonescu-Cuypers, Treatment of diabetic macular edema with sustained-release glucocorticoids: intravitreal triamcinolone acetonide, dexamethasone implant, and fluocinolone acetonide implant, Expert Opin. Pharmacother. 15 (2014) 953–959. doi:10.1517/14656566.2014.896899.

[104] F.F. Behar-Cohen, S. Gauthier, A. El Aouni, P. Chapon, J.M. Parel, G. Renard, D. Chauvaud, Methylprednisolone concentrations in the vitreous and the serum after pulse therapy, Retina Phila. Pa. 21 (2001) 48–53.

[105] O. Weijtens, R.C. Schoemaker, A.F. Cohen, F.P. Romijn, E.G. Lentjes, J. van Rooij, J.C. van Meurs, Dexamethasone concentration in vitreous and serum after oral administration, Am. J. Ophthalmol. 125 (1998) 673–679.

[106] Z. Sherif, U. Pleyer, Corticosteroids in Ophthalmology: Past – Present – Future, Ophthalmologica. 216 (2002) 305–315. doi:10.1159/000066189.

[107] R. Herrero-Vanrell, J.A. Cardillo, B.D. Kuppermann, Clinical applications of the sustained-release dexamethasone implant for treatment of macular edema, Clin. Ophthalmol. Auckl. NZ. 5 (2011) 139–146. doi:10.2147/OPTH.S15783.

[108] Y. Yang, C. Bailey, A. Loewenstein, P. Massin, INTRAVITREAL CORTICOSTEROIDS IN DIABETIC MACULAR EDEMA, Retina Phila. Pa. 35 (2015) 2440–2449. doi:10.1097/IAE.0000000000000726.

[109] J. Rodríguez Villanueva, L. Rodríguez Villanueva, M. Guzmán Navarro, Pharmaceutical technology can turn a traditional drug, dexamethasone into a first-line ocular medicine. A global perspective and future trends, Int. J. Pharm. 516 (2017) 342–351. doi:10.1016/j.ijpharm.2016.11.053.

[110] A. Thakur, R. Kadam, U.B. Kompella, Trabecular meshwork and lens partitioning of corticosteroids: Implications for elevated intraocular pressure and cataracts, Arch. Ophthalmol. 129 (2011) 914–920. doi:10.1001/archophthalmol.2011.39.

[111] J. Rodríguez Villanueva, I. Bravo-Osuna, R. Herrero-Vanrell, I.T. Molina Martínez, M. Guzmán Navarro, Optimising the controlled release of dexamethasone from a new generation of PLGA-based microspheres intended for intravitreal administration, Eur. J. Pharm. Sci. 92 (2016) 287–297. doi:10.1016/j.ejps.2016.03.012.

[112] M.A. Cunningham, J.L. Edelman, S. Kaushal, Intravitreal Steroids for Macular Edema: The Past, the Present, and the Future, Surv. Ophthalmol. 53 (2008) 139–149. doi:10.1016/j.survophthal.2007.12.005.

[113] V. Sarao, D. Veritti, F. Boscia, P. Lanzetta, Intravitreal Steroids for the Treatment of Retinal Diseases, Sci. World J. 2014 (2014) e989501. doi:10.1155/2014/989501.

[114] H. Kaji, N. Nagai, M. Nishizawa, T. Abe, Drug delivery devices for retinal diseases, Adv. Drug Deliv. Rev. 128 (2018) 148–157. doi:10.1016/j.addr.2017.07.002.

[115] S.S. Lee, P. Hughes, A.D. Ross, M.R. Robinson, Biodegradable Implants for Sustained Drug Release in the Eye, Pharm. Res. 27 (2010) 2043–2053. doi:10.1007/s11095-010-0159-x.

[116] I. Ahmed, T.F. Patton, Importance of the noncorneal absorption route in topical ophthalmic drug delivery., Invest. Ophthalmol. Vis. Sci. 26 (1985) 584–587.

[117] L. Xinming, C. Yingde, A.W. Lloyd, S.V. Mikhalovsky, S.R. Sandeman, C.A. Howel, L. Liewen, Polymeric hydrogels for novel contact lens-based ophthalmic drug delivery systems: A review, Contact Lens Anterior Eye. 31 (2008) 57–64. doi:10.1016/j.clae.2007.09.002.

[118] I.P. Kaur, S. Kakkar, Nanotherapy for posterior eye diseases, J. Controlled Release. 193 (2014) 100–112. doi:10.1016/j.jconrel.2014.05.031.

[119] H.H. Sigurdsson, F. Konráðsdóttir, T. Loftsson, E. Stefánsson, Topical and systemic absorption in delivery of dexamethasone to the anterior and posterior segments of the eye, Acta Ophthalmol. Scand. 85 (2007) 598–602. doi:10.1111/j.1600-0420.2007.00885.x.

[120] B.L. Nordstrom, D.S. Friedman, E. Mozaffari, H.A. Quigley, A.M. Walker, Persistence and Adherence With Topical Glaucoma Therapy, Am. J. Ophthalmol. 140 (2005) 598.e1-598.e11. doi:10.1016/j.ajo.2005.04.051.

[121] C. Yang, G.S. Tirucherai, A.K. Mitra, Prodrug based optimal drug delivery via membrane transporter/receptor, Expert Opin. Biol. Ther. 1 (2001) 159–175. doi:10.1517/14712598.1.2.159.

[122] S. Raghava, M. Hammond, U.B. Kompella, Periocular routes for retinal drug delivery, Expert Opin. Drug Deliv. 1 (2004) 99–114. doi:10.1517/17425247.1.1.99.

[123] M.R. Prausnitz, J.S. Noonan, Permeability of cornea, sclera, and conjunctiva: A literature analysis for drug delivery to the eye, J. Pharm. Sci. 87 (1998) 1479–1488. doi:10.1021/js9802594.

[124] D.M. Maurice, S. Mishima, Ocular Pharmacokinetics, in: M.L. Sears (Ed.), Pharmacol. Eye, Springer Berlin Heidelberg, Berlin, Heidelberg, 1984: pp. 19–116. doi:10.1007/978-3-642-69222-2_2.

[125] H. Kim, M.R. Robinson, M.J. Lizak, G. Tansey, R.J. Lutz, P. Yuan, N.S. Wang, K.G. Csaky, Controlled drug release from an ocular implant: an evaluation using dynamic three-dimensional magnetic resonance imaging, Invest. Ophthalmol. Vis. Sci. 45 (2004) 2722–2731. doi:10.1167/iovs.04-0091.

[126] O. Weijtens, R.C. Schoemaker, E.G.W.M. Lentjes, F.P.H.T.M. Romijn, A.F. Cohen, J.C. van Meurs, Dexamethasone concentration in the subretinal fluid after a subconjunctival injection, a peribulbar injection, or an oral dose, Ophthalmology. 107 (2000) 1932–1938. doi:10.1016/S0161-6420(00)00344-4.

[127] A. Thakur, R.S. Kadam, U.B. Kompella, Influence of Drug Solubility and Lipophilicity on Transscleral Retinal Delivery of Six Corticosteroids, Drug Metab. Dispos. 39 (2011) 771–781. doi:10.1124/dmd.110.037408.

[128] H.F. Edelhauser, C.L. Rowe-Rendleman, M.R. Robinson, D.G. Dawson, G.J. Chader, H.E. Grossniklaus, K.D. Rittenhouse, C.G. Wilson, D.A. Weber, B.D. Kuppermann, K.G. Csaky, T.W. Olsen, U.B. Kompella, V.M. Holers, G.S. Hageman, B.C. Gilger, P.A. Campochiaro, S.M. Whitcup, W.T. Wong, Ophthalmic Drug Delivery Systems for the Treatment of Retinal Diseases: Basic Research to Clinical Applications, Investig. Opthalmology Vis. Sci. 51 (2010) 5403. doi:10.1167/iovs.10-5392.

[129] S. Einmahl, M. Savoldelli, F. D'Hermies, C. Tabatabay, R. Gurny, F. Behar-Cohen, Evaluation of a novel biomaterial in the suprachoroidal space of the rabbit eye, Invest. Ophthalmol. Vis. Sci. 43 (2002) 1533–1539.

[130] M. Chen, X. Li, J. Liu, Y. Han, L. Cheng, Safety and pharmacodynamics of suprachoroidal injection of triamcinolone acetonide as a controlled ocular drug release model, J. Controlled Release. 203 (2015) 109–117. doi:10.1016/j.jconrel.2015.02.021.

[131] M. Tetz, S. Rizzo, A.J. Augustin, Safety of submacular suprachoroidal drug administration via a microcatheter: retrospective analysis of European treatment results, Ophthalmol. J. Int. Ophtalmol. Int. J. Ophthalmol. Z. Augenheilkd. 227 (2012) 183–189. doi:10.1159/000336045.

[132] V.-P. Ranta, E. Mannermaa, K. Lummepuro, A. Subrizi, A. Laukkanen, M. Antopolsky, L. Murtomäki, M. Hornof, A. Urtti, Barrier analysis of periocular drug delivery to the posterior segment, J. Controlled Release. 148 (2010) 42–48. doi:10.1016/j.jconrel.2010.08.028.

[133] S.R. Patel, D.E. Berezovsky, B.E. McCarey, V. Zarnitsyn, H.F. Edelhauser, M.R. Prausnitz, Targeted Administration into the Suprachoroidal Space Using a Microneedle for Drug Delivery to the Posterior Segment of the Eye, Invest. Ophthalmol. Vis. Sci. 53 (2012) 4433–4441. doi:10.1167/iovs.12-9872.

[134] E.M. del Amo, A.-K. Rimpelä, E. Heikkinen, O.K. Kari, E. Ramsay, T. Lajunen, M. Schmitt, L. Pelkonen, M. Bhattacharya, D. Richardson, A. Subrizi, T. Turunen, M. Reinisalo, J. Itkonen, E. Toropainen, M. Casteleijn, H. Kidron, M. Antopolsky, K.-S. Vellonen, M. Ruponen, A. Urtti, Pharmacokinetic aspects of retinal drug delivery, Prog. Retin. Eye Res. 57 (2017) 134–185. doi:10.1016/j.preteyeres.2016.12.001.

[135] V.R. Kearns, R.L. Williams, Drug delivery systems for the eye, Expert Rev. Med. Devices. 6 (2009) 277–290. doi:10.1586/erd.09.4.

[136] V. Agrahari, V. Agrahari, A. Mandal, D. Pal, A.K. Mitra, How are we improving the delivery to back of the eye? Advances and challenges of novel therapeutic approaches, Expert Opin. Drug Deliv. 0 (2016) 1–17. doi:10.1080/17425247.2017.1272569.

[137] L. Solorio, A.M. Olear, J.I. Hamilton, R.B. Patel, A.C. Beiswenger, J.E. Wallace, H. Zhou, A.A. Exner, Noninvasive Characterization of the Effect of Varying PLGA Molecular Weight Blends on In Situ Forming Implant Behavior Using Ultrasound Imaging, Theranostics. 2 (2012) 1064–1077. doi:10.7150/thno.4181.

[138] Q. Liu, H. Zhang, G. Zhou, S. Xie, H. Zou, Y. Yu, G. Li, D. Sun, G. Zhang, Y. Lu, Y. Zhong, In vitro and in vivo study of thymosin alpha1 biodegradable in situ forming poly(lactide-co-glycolide) implants, Int. J. Pharm. 397 (2010) 122–129. doi:10.1016/j.ijpharm.2010.07.015.

[139] P. Belin, A. Khalili, R. Ginsburg, R.M. Lieberman, Recent Innovations in Drug Delivery for Retinal Diseases, Adv. Ophthalmol. Optom. 3 (2018) 155–183. doi:10.1016/j.yaoo.2018.04.009.

[140] M.N. Yasin, D. Svirskis, A. Seyfoddin, I.D. Rupenthal, Implants for drug delivery to the posterior segment of the eye: A focus on stimuli-responsive and tunable release systems, J. Controlled Release. 196 (2014) 208–221. doi:10.1016/j.jconrel.2014.09.030.

[141] E.B. Lavik, B.D. Kuppermann, M.S. Humayun, Chapter 38 - Drug Delivery, in: S.J. Ryan, S.R. Sadda, D.R. Hinton, A.P. Schachat, S.R. Sadda, C.P. Wilkinson, P. Wiedemann, A.P. Schachat (Eds.), Retina Fifth Ed., W.B. Saunders, London, 2013: pp. 734–745. doi:10.1016/B978-1-4557-0737-9.00038-2.

[142] N. Kuno, S. Fujii, Biodegradable Intraocular Therapies for Retinal Disorders, Drugs Aging. 27 (2010) 117–134. doi:10.2165/11530970-000000000-00000.

[143] A Study of MK0140 in Diabetic Patients With Macular Edema (0140-001), (n.d.). https://clinicaltrials.gov/ct2/show/NCT00692614 (accessed January 16, 2019).

[144] D.T. Tan, S.P. Chee, L. Lim, A.S. Lim, Randomized clinical trial of a new dexamethasone delivery system (Surodex) for treatment of post-cataract surgery inflammation, Ophthalmology. 106 (1999) 223–231. doi:10.1016/S0161-6420(99)90060-X.

[145] D.F. Chang, I.H. Garcia, J.D. Hunkeler, T. Minas, Phase II results of an intraocular steroid delivery system for cataract surgery, Ophthalmology. 106 (1999) 1172–1177. doi:10.1016/S0161-6420(99)90262-2.

[146] D.J. Lee, Intraocular Implants for the Treatment of Autoimmune Uveitis, J. Funct. Biomater. 6 (2015) 650–666. doi:10.3390/jfb6030650.

[147] S.M. Whitcup, M.R. Robinson, Development of a dexamethasone intravitreal implant for the treatment of noninfectious posterior segment uveitis, Ann. N. Y. Acad. Sci. (2015) n/a-n/a. doi:10.1111/nyas.12824.

[148] D.K. Gilding, A.M. Reed, Biodegradable polymers for use in surgery—polyglycolic/poly(actic acid) homo- and copolymers: 1, Polymer. 20 (1979) 1459–1464. doi:10.1016/0032-3861(79)90009-0.

[149] S.M. Li, H. Garreau, M. Vert, Structure-property relationships in the case of the degradation of massive aliphatic poly-(α-hydroxy acids) in aqueous media, J. Mater. Sci. Mater. Med. 1 (1990) 123–130. doi:10.1007/BF00700871.

[150] Z. Ghalanbor, M. Körber, R. Bodmeier, Protein release from poly(lactide-co-glycolide) implants prepared by hot-melt extrusion: Thioester formation as a reason for incomplete release, Int. J. Pharm. 438 (2012) 302–306. doi:10.1016/j.ijpharm.2012.09.015.

[151] A.A. Zaghloul, beta-Estradiol biodegradable microspheres: effect of formulation parameters on encapsulation efficiency and in vitro release, Pharm. 61 (2006) 775–779.

[152] M. Parent, C. Nouvel, M. Koerber, A. Sapin, P. Maincent, A. Boudier, PLGA in situ implants formed by phase inversion: Critical physicochemical parameters to modulate drug release, J. Controlled Release. 172 (2013) 292–304. doi:10.1016/j.jconrel.2013.08.024.

[153] S. Cohen, M.J. Alonso, R. Langer, Novel Approaches to Controlled-Release Antigen Delivery, Int. J. Technol. Assess. Health Care. 10 (1994) 121–130. doi:10.1017/S0266462300014045.

[154] R.A. Jain, The manufacturing techniques of various drug loaded biodegradable poly(lactide-co-glycolide) (PLGA) devices, Biomaterials. 21 (2000) 2475–2490. doi:10.1016/S0142-9612(00)00115-0.

[155] H.K. Makadia, S.J. Siegel, Poly Lactic-co-Glycolic Acid (PLGA) as Biodegradable Controlled Drug Delivery Carrier, Polymers. 3 (2011) 1377–1397. doi:10.3390/polym3031377.

[156] A.M. Reed, D.K. Gilding, Biodegradable polymers for use in surgery — poly(glycolic)/poly(Iactic acid) homo and copolymers: 2. In vitro degradation, Polymer. 22 (1981) 494–498. doi:10.1016/0032-3861(81)90168-3.

[157] J.P. Kitchell, D.L. Wise, [32] Poly(lactic/glycolic acid) biodegradable drug—polymer matrix systems, in: Methods Enzymol., Academic Press, 1985: pp. 436–448. doi:10.1016/S0076-6879(85)12034-3.

[158] S.S. Lee, P. Hughes, A.D. Ross, M.R. Robinson, Advances in Biodegradable Ocular Drug Delivery Systems, in: U.B. Kompella, H.F. Edelhauser (Eds.), Drug Prod. Dev. Back Eye, Springer US, 2011: pp. 185–230. http://link.springer.com/chapter/10.1007/978-1-4419-9920-7_9 (accessed August 20, 2015).

[159] S. D'Souza, R. Dorati, P.P. DeLuca, Effect of Hydration on Physicochemical Properties of End-Capped PLGA, Adv. Biomater. 2014 (2014). doi:10.1155/2014/834942.

[160] P. Blasi, S.S. D'Souza, F. Selmin, P.P. DeLuca, Plasticizing effect of water on poly(lactide-co-glycolide), J. Controlled Release. 108 (2005) 1–9. doi:10.1016/j.jconrel.2005.07.009.

[161] B.C. Hancock, G. Zografi, The Relationship Between the Glass Transition Temperature and the Water Content of Amorphous Pharmaceutical Solids, Pharm. Res. 11 (1994) 471–477. doi:10.1023/A:1018941810744.

[162] N. Passerini, D.Q.M. Craig, An investigation into the effects of residual water on the glass transition temperature of polylactide microspheres using modulated temperature DSC, J. Controlled Release. 73 (2001) 111–115. doi:10.1016/S0168-3659(01)00245-0.

[163] S.M. Li, H. Garreau, M. Vert, Structure-property relationships in the case of the degradation of massive poly(α-hydroxy acids) in aqueous media, J. Mater. Sci. Mater. Med. 1 (1990) 131–139. doi:10.1007/BF00700872.

[164] J. Siepmann, K. Elkharraz, F. Siepmann, D. Klose, How Autocatalysis Accelerates Drug Release from PLGA-Based Microparticles: A Quantitative Treatment, Biomacromolecules. 6 (2005) 2312–2319. doi:10.1021/bm050228k.

[165] L. Li, S.P. Schwendeman, Mapping neutral microclimate pH in PLGA microspheres, J. Controlled Release. 101 (2005) 163–173. doi:10.1016/j.jconrel.2004.07.029.

[166] S. Fredenberg, M. Wahlgren, M. Reslow, A. Axelsson, The mechanisms of drug release in poly(lactic-co-glycolic acid)-based drug delivery systems—A review, Int. J. Pharm. 415 (2011) 34–52. doi:10.1016/j.ijpharm.2011.05.049.

[167] J.A.D. Sequeira, A.C. Santos, J. Serra, F. Veiga, A.J. Ribeiro, Chapter 10 - Poly(lactic-co-glycolic acid) (PLGA) matrix implants, in: A.M. Grumezescu (Ed.), Nanostructures Eng. Cells Tissues Organs, William Andrew Publishing, 2018: pp. 375–402. doi:10.1016/B978-0-12-813665-2.00010-7.

[168] H. Kimura, Y. Ogura, Biodegradable polymers for ocular drug delivery, Ophthalmol. J. Int. Ophtalmol. Int. J. Ophthalmol. Z. Augenheilkd. 215 (2001) 143–155. doi:10.1159/000050849.

[169] G.G. Giordano, P. Chevez-Barrios, M.F. Refojo, C.A. Garcia, Biodegradation and tissue reaction to intravitreous biodegradable poly(D,L-lactic-co-glycolic)acid microspheres, Curr. Eye Res. 14 (1995) 761–768. doi:10.3109/02713689508995797.

[170] A.A. Veloso, Q. Zhu, R. Herrero-Vanrell, M.F. Refojo, Ganciclovir-loaded polymer microspheres in rabbit eyes inoculated with human cytomegalovirus, Invest. Ophthalmol. Vis. Sci. 38 (1997) 665–675.

[171] J.M. Anderson, M.S. Shive, Biodegradation and biocompatibility of PLA and PLGA microspheres, Adv. Drug Deliv. Rev. 28 (1997) 5–24. doi:10.1016/S0169-409X(97)00048-3.

[172] J.W. Streilein, Ocular immune privilege: the eye takes a dim but practical view of immunity and inflammation, J. Leukoc. Biol. 74 (2003) 179–185. doi:10.1189/jlb.1102574.

[173] E. Fournier, C. Passirani, C.N. Montero-Menei, J.P. Benoit, Biocompatibility of implantable synthetic polymeric drug carriers: focus on brain biocompatibility, Biomaterials. 24 (2003) 3311–3331. doi:10.1016/S0142-9612(03)00161-3.

[174] R. Zhou, R.R. Caspi, Ocular immune privilege, F1000 Biol. Rep. 2 (2010). doi:10.3410/B2-3.

[175] M.B. Sintzel, A. Merkli, C. Tabatabay, R. Gurny, Influence of Irradiation Sterilization on Polymers Used as Drug Carriers—A Review, Drug Dev. Ind. Pharm. 23 (1997) 857–878. doi:10.3109/03639049709148693.

[176] M. Igartua, R.M. Hernández, J.E. Rosas, M.E. Patarroyo, J.L. Pedraz, γ-Irradiation effects on biopharmaceutical properties of PLGA microspheres loaded with SPf66 synthetic vaccine, Eur. J. Pharm. Biopharm. 69 (2008) 519–526. doi:10.1016/j.ejpb.2007.12.014.

[177] W. Friess, M. Schlapp, Sterilization of gentamicin containing collagen/PLGA microparticle composites, Eur. J. Pharm. Biopharm. 63 (2006) 176–187. doi:10.1016/j.ejpb.2005.11.007.

[178] G. Spenlehauer, M. Vert, J.P. Benoit, A. Boddaert, In vitro and In vivo degradation of poly(D,L lactide/glycolide) type microspheres made by solvent evaporation method, Biomaterials. 10 (1989) 557–563. doi:10.1016/0142-9612(89)90063-X.

[179] L. Zhang, C.C. Chu, I.H. Loh, Effect of a combined gamma irradiation and Parylene plasma treatment on the hydrolytic degradation of synthetic biodegradable sutures, J. Biomed. Mater. Res. 27 (1993) 1425–1441. doi:10.1002/jbm.820271110.

[180] B. Bittner, K. Mäder, C. Kroll, H.-H. Borchert, T. Kissel, Tetracycline-HCl-loaded poly(dl-lactide-co-glycolide) microspheres prepared by a spray drying technique: influence of γ-irradiation on radical formation and polymer degradation, J. Controlled Release. 59 (1999) 23–32. doi:10.1016/S0168-3659(98)00170-9.

[181] D. Mohr, M. Wolff, T. Kissel, Gamma irradiation for terminal sterilization of 17β-estradiol loaded poly-(d,l-lactide-co-glycolide) microparticles, J. Controlled Release. 61 (1999) 203–217. doi:10.1016/S0168-3659(99)00118-2.

[182] C. Volland, M. Wolff, T. Kissel, The influence of terminal gamma-sterilization on captopril containing poly(d,l-lactide-co-glycolide) microspheres, J. Controlled Release. 31 (1994) 293–305. doi:10.1016/0168-3659(94)90012-4.

[183] R. Herrero-Vanrell, L. Ramirez, A. Fernandez-Carballido, M.F. Refojo, Biodegradable PLGA microspheres loaded with ganciclovir for intraocular administration. Encapsulation technique, in vitro release profiles, and sterilization process, Pharm. Res. 17 (2000) 1323–1328.

[184] J.K. Lalla, K. Sapna, Biodegradable microspheres of poly(DL-lactic acid) containing piroxicam as a model drug for controlled release via the parenteral route, J. Microencapsul. 10 (1993) 449–460. doi:10.3109/02652049309015322.

[185] N. Faisant, J. Siepmann, J. Richard, J.P. Benoit, Mathematical modeling of drug release from bioerodible microparticles: effect of gamma-irradiation, Eur. J. Pharm. Biopharm. 56 (2003) 271–279. doi:10.1016/S0939-6411(03)00104-8.

[186] Evaluation of Medicines for Human Use CHMP Assessment report Ozurdex International Nonproprietary Name: dexamethasone Procedure No: EMEA/H/C/001140., (n.d.). https://www.ema.europa.eu/documents/assessment-report/ozurdex-epar-public-assessment-report_en.pdf (accessed January 13, 2019).

[187] R. Herrero-Vanrell, I. Bravo-Osuna, V. Andrés-Guerrero, M. Vicario-de-la-Torre, I.T. Molina-Martínez, The potential of using biodegradable microspheres in retinal diseases and other intraocular pathologies, Prog. Retin. Eye Res. 42 (2014) 27–43. doi:10.1016/j.preteyeres.2014.04.002.

[188] S. Freitas, H.P. Merkle, B. Gander, Microencapsulation by solvent extraction/evaporation: reviewing the state of the art of microsphere preparation process technology, J. Controlled Release. 102 (2005) 313–332. doi:10.1016/j.jconrel.2004.10.015.

[189] C. Busatto, J. Pesoa, I. Helbling, J. Luna, D. Estenoz, Effect of particle size, polydispersity and polymer degradation on progesterone release from PLGA microparticles: Experimental and mathematical modeling, Int. J. Pharm. 536 (2018) 360–369. doi:10.1016/j.ijpharm.2017.12.006.

[190] H. Gasmi, F. Danede, J. Siepmann, F. Siepmann, Does PLGA microparticle swelling control drug release? New insight based on single particle swelling studies, J. Controlled Release. 213 (2015) 120–127. doi:10.1016/j.jconrel.2015.06.039.

[191] H. Gasmi, J.-F. Willart, F. Danede, M.C. Hamoudi, J. Siepmann, F. Siepmann, Importance of PLGA microparticle swelling for the control of prilocaine release, J. Drug Deliv. Sci. Technol. 30 (2015) 123–132. doi:10.1016/j.jddst.2015.10.009.

[192] H. Gasmi, F. Siepmann, M.C. Hamoudi, F. Danede, J. Verin, J.-F. Willart, J. Siepmann, Towards a better understanding of the different release phases from PLGA microparticles: Dexamethasone-loaded systems, Int. J. Pharm. 514 (2016) 189–199. doi:10.1016/j.ijpharm.2016.08.032.

[193] W. Friess, M. Schlapp, Release mechanisms from gentamicin loaded poly(lactic-co-glycolic acid) (PLGA) microparticles, J. Pharm. Sci. 91 (2002) 845–855. doi:10.1002/jps.10012.

[194] I. Mylonaki, E. Allémann, F. Delie, O. Jordan, Imaging the porous structure in the core of degrading PLGA microparticles: The effect of molecular weight, J. Controlled Release. 286 (2018) 231–239. doi:10.1016/j.jconrel.2018.07.044.

[195] J. Rodríguez Villanueva, L. Rodríguez Villanueva, Turning the screw even further to increase microparticle retention and ocular bioavailability of associated drugs: The bioadhesion goal, Int. J. Pharm. 531 (2017) 167–178. doi:10.1016/j.ijpharm.2017.08.067.

[196] J.A. Cardillo, A.A. Souza-Filho, A.G. Oliveira, Intravitreal Bioerudivel sustained-release triamcinolone microspheres system (RETAAC). Preliminary report of its potential usefulnes for the treatment of diabetic macular edema, Arch. Soc. Espanola Oftalmol. 81 (2006) 675–677, 679–681.

[197] A. Hatefi, B. Amsden, Biodegradable injectable in situ forming drug delivery systems, J. Controlled Release. 80 (2002) 9–28. doi:10.1016/S0168-3659(02)00008-1.

[198] S. Kempe, K. Mäder, In situ forming implants — an attractive formulation principle for parenteral depot formulations, J. Controlled Release. 161 (2012) 668–679. doi:10.1016/j.jconrel.2012.04.016.

[199] R. Astaneh, M. Erfan, J. Barzin, H. Mobedi, H. Moghimi, Effects of ethyl benzoate on performance, morphology, and erosion of PLGA implants formed in situ, Adv. Polym. Technol. 27 (2008) 17–26. doi:10.1002/adv.20114.

[200] C.B. Packhaeuser, J. Schnieders, C.G. Oster, T. Kissel, In situ forming parenteral drug delivery systems: an overview, Eur. J. Pharm. Biopharm. 58 (2004) 445–455. doi:10.1016/j.ejpb.2004.03.003.

[201] R.L. Dunn, J.P. English, D.R. Cowsar, D.P. Vanderbilt, Biodegradable in-situ forming implants and methods of producing the same, US4938763A, 1990. https://patents.google.com/patent/US4938763A/en?oq=4938763 (accessed October 11, 2018).

[202] H. Kranz, R. Bodmeier, A novel in situ forming drug delivery system for controlled parenteral drug delivery, Int. J. Pharm. 332 (2007) 107–114. doi:10.1016/j.ijpharm.2006.09.033.

[203] C.A. Smolders, A.J. Reuvers, R.M. Boom, I.M. Wienk, Microstructures in phase-inversion membranes. Part 1. Formation of macrovoids, J. Membr. Sci. 73 (1992) 259–275. doi:10.1016/0376-7388(92)80134-6.

[204] R. Bakhshi, E. Vasheghani-Farahani, H. Mobedi, A. Jamshidi, M. Khakpour, The effect of additives on naltrexone hydrochloride release and solvent removal rate from an injectable in situ forming PLGA implant, Polym. Adv. Technol. 17 (2006) 354–359. doi:10.1002/pat.717.

[205] T.A. Ahmed, H.M. Ibrahim, A.M. Samy, A. Kaseem, M.T.H. Nutan, M.D. Hussain, Biodegradable Injectable In Situ Implants and Microparticles for Sustained Release of Montelukast: In Vitro Release, Pharmacokinetics, and Stability, AAPS PharmSciTech. 15 (2014) 772–780. doi:10.1208/s12249-014-0101-3.

[206] R.L. Dunn, A.J. Tipton, Polymeric compositions useful as controlled release implants, US5702716A, 1997. https://patents.google.com/patent/US5702716/en (accessed October 8, 2018).

[207] C. Wischke, S.P. Schwendeman, Degradable Polymeric Carriers for Parenteral Controlled Drug Delivery, in: J. Siepmann, R.A. Siegel, M.J. Rathbone (Eds.), Fundam. Appl. Control. Release Drug Deliv., Springer US, Boston, MA, 2012: pp. 171–228. doi:10.1007/978-1-4614-0881-9_8.

[208] H. Kranz, E. Yilmaz, G.A. Brazeau, R. Bodmeier, In Vitro and In Vivo Drug Release from a Novel In Situ Forming Drug Delivery System, Pharm. Res. 25 (2008) 1347–1354. doi:10.1007/s11095-007-9478-y.

[209] P.D. Graham, K.J. Brodbeck, A.J. McHugh, Phase inversion dynamics of PLGA solutions related to drug delivery, J. Controlled Release. 58 (1999) 233–245. doi:10.1016/S0168-3659(98)00158-8.

[210] R.B. Patel, A. Carlson, L. Solorio, A.A. Exner, Characterization of formulation parameters affecting low molecular weight drug release from in situ forming drug delivery systems, J. Biomed. Mater. Res. A. 94 (2010) 476–484. doi:10.1002/jbm.a.32724.

[211] R.B. Patel, L. Solorio, H. Wu, T. Krupka, A.A. Exner, Effect of injection site on in situ implant formation and drug release in vivo, J. Controlled Release. 147 (2010) 350–358. doi:10.1016/j.jconrel.2010.08.020.

[212] J.R. DesNoyer, A.J. McHugh, The effect of Pluronic on the protein release kinetics of an injectable drug delivery system, J. Controlled Release. 86 (2003) 15–24. doi:10.1016/S0168-3659(02)00293-6.

[213] K.J. Brodbeck, A.T. Gaynor-Duarte, T.T.-I. Shen, Gel composition and methods, US6130200A, 2000. https://patents.google.com/patent/US6130200A/en?oq=6130200 (accessed October 8, 2018).

[214] K.J. Brodbeck, J.R. DesNoyer, A.J. McHugh, Phase inversion dynamics of PLGA solutions related to drug delivery: Part II. The role of solution thermodynamics and bath-side mass transfer, J. Controlled Release. 62 (1999) 333–344. doi:10.1016/S0168-3659(99)00159-5.

[215] A.J. McHugh, The role of polymer membrane formation in sustained release drug delivery systems, J. Controlled Release. 109 (2005) 211–221. doi:10.1016/j.jconrel.2005.09.038.

[216] R. Astaneh, M. Erfan, H. Moghimi, H. Mobedi, Changes in morphology of in situ forming PLGA implant prepared by different polymer molecular weight and its effect on release behavior, J. Pharm. Sci. 98 (2009) 135–145. doi:10.1002/jps.21415.

[217] X. Luan, R. Bodmeier, In situ forming microparticle system for controlled delivery of leuprolide acetate: Influence of the formulation and processing parameters, Eur. J. Pharm. Sci. 27 (2006) 143–149. doi:10.1016/j.ejps.2005.09.002.

[218] X. Luan, R. Bodmeier, Influence of the poly(lactide-co-glycolide) type on the leuprolide release from in situ forming microparticle systems, J. Controlled Release. 110 (2006) 266–272. doi:10.1016/j.jconrel.2005.10.005.

[219] K. Agossa, M. Lizambard, T. Rongthong, E. Delcourt-Debruyne, J. Siepmann, F. Siepmann, Physical key properties of antibiotic-free, PLGA/HPMC-based in-situ forming implants for local periodontitis treatment, Int. J. Pharm. 521 (2017) 282–293. doi:10.1016/j.ijpharm.2017.02.039.

[220] M.P. Do, C. Neut, E. Delcourt, T. Seixas Certo, J. Siepmann, F. Siepmann, In situ forming implants for periodontitis treatment with improved adhesive properties, Eur. J. Pharm. Biopharm. 88 (2014) 342–350. doi:10.1016/j.ejpb.2014.05.006.

[221] M.P. Do, C. Neut, H. Metz, E. Delcourt, K. Mäder, J. Siepmann, F. Siepmann, In-situ forming composite implants for periodontitis treatment: How the formulation determines system performance, Int. J. Pharm. 486 (2015) 38–51. doi:10.1016/j.ijpharm.2015.03.026.

[222] M.P. Do, C. Neut, H. Metz, E. Delcourt, J. Siepmann, K. Mäder, F. Siepmann, Mechanistic analysis of PLGA/HPMC-based in-situ forming implants for periodontitis treatment, Eur. J. Pharm. Biopharm. 94 (2015) 273–283. doi:10.1016/j.ejpb.2015.05.018.

[223] J.-Y. Lai, F.-C. Lin, C.-C. Wang, D.-M. Wang, Effect of nonsolvent additives on the porosity and morphology of asymmetric TPX membranes, J. Membr. Sci. 118 (1996) 49–61. doi:10.1016/0376-7388(96)00084-1.

[224] D.-M. Wang, F.-C. Lin, T.-T. Wu, J.-Y. Lai, Formation mechanism of the macrovoids induced by surfactant additives, J. Membr. Sci. 142 (1998) 191–204. doi:10.1016/S0376-7388(97)00322-0.

[225] H.A. Tsai, L.D. Li, K.R. Lee, Y.C. Wang, C.L. Li, J. Huang, J.Y. Lai, Effect of surfactant addition on the morphology and pervaporation performance of asymmetric polysulfone membranes, J. Membr. Sci. 176 (2000) 97–103. doi:10.1016/S0376-7388(00)00435-X.

[226] L. Wang, L. Kleiner, S. Venkatraman, Structure formation in injectable poly(lactide–co-glycolide) depots, J. Controlled Release. 90 (2003) 345–354. doi:10.1016/S0168-3659(03)00198-6.

[227] J.P. Moreau, P.J. Vachon, M.C. Huneau, Elevated glycemia and local inflammation after injecting N-methyl-2-pyrrolidone (NMP) into the marginal ear vein of rabbits, Contemp. Top. Lab. Anim. Sci. 40 (2001) 38–40.

[228] J.-P. Payan, D. Beydon, J.-P. Fabry, I. Boudry, B. Cossec, E. Ferrari, Toxicokinetics and Metabolism ofN-[14C]Methylpyrrolidone in Male Sprague-Dawley Rats. A Saturable NMP Elimination Process, Drug Metab. Dispos. 30 (2002) 1418–1424. doi:10.1124/dmd.30.12.1418.

[229] H. Kranz, G.A. Brazeau, J. Napaporn, R.L. Martin, W. Millard, R. Bodmeier, Myotoxicity studies of injectable biodegradable in-situ forming drug delivery systems, Int. J. Pharm. 212 (2001) 11–18. doi:10.1016/S0378-5173(00)00568-8.

[230] D. Steinberg, M. Friedman, Dental drug-delivery devices: local and sustained-release applications, Crit. Rev. Ther. Drug Carrier Syst. 16 (1999) 425–459.

[231] O. Sartor, Eligard: leuprolide acetate in a novel sustained-release delivery system, Urology. 61 (2003) 25–31. doi:10.1016/S0090-4295(02)02396-8.

[232] L.R. Asmus, J.P.A. Grimshaw, P. Richle, B. Eicher, D.M. Urech, R. Gurny, M. Möller, Injectable formulations for an intravitreal sustained-release application of a novel single-chain VEGF antibody fragment, Eur. J. Pharm. Biopharm. 95, Part B (2015) 250–260. doi:10.1016/j.ejpb.2015.02.007.

[233] J.-W. Rhim, A.K. Mohanty, S.P. Singh, P.K.W. Ng, Effect of the processing methods on the performance of polylactide films: Thermocompression versus solvent casting, J. Appl. Polym. Sci. 101 (2006) 3736–3742. doi:10.1002/app.23403.

[234] C.-K. Wang, W.-Y. Wang, R.F. Meyer, Y. Liang, K.I. Winey, S.J. Siegel, A Rapid Method for Creating Drug Implants: Translating Laboratory Based Methods into a Scalable Manufacturing Process, J. Biomed. Mater. Res. B Appl. Biomater. 93 (2010) 562–572. doi:10.1002/jbm.b.31617.

[235] C.T. Laurencin, S.E.M. Ibim, R.S. Langer, Poly (anhydrides), in: Biomed. Appl. Synth. Biodegrad. Polym., CRC Press, Boca Raton, FL, 1995: pp. 59–102.

[236] C. Rauwendaal, Polymer extrusion, Carl Hanser Verlag GmbH Co KG, 2014.

[237] M. Maniruzzaman, A. Nokhodchi, Continuous manufacturing via hot-melt extrusion and scale up: regulatory matters, Drug Discov. Today. 22 (2017) 340–351. doi:10.1016/j.drudis.2016.11.007.

[238] M.M. Crowley, B. Schroeder, A. Fredersdorf, S. Obara, M. Talarico, S. Kucera, J.W. McGinity, Physicochemical properties and mechanism of drug release from ethyl cellulose matrix tablets prepared by direct compression and hot-melt extrusion, Int. J. Pharm. 269 (2004) 509–522. doi:10.1016/j.ijpharm.2003.09.037.

[239] D. Li, G. Guo, R. Fan, J. Liang, X. Deng, F. Luo, Z. Qian, PLA/F68/Dexamethasone implants prepared by hot-melt extrusion for controlled release of anti-inflammatory drug to implantable medical devices: I. Preparation, characterization and hydrolytic degradation study, Int. J. Pharm. 441 (2013) 365–372. doi:10.1016/j.ijpharm.2012.11.019.

[240] Z. Ghalanbor, M. Körber, R. Bodmeier, Improved Lysozyme Stability and Release Properties of Poly(lactide-co-glycolide) Implants Prepared by Hot-Melt Extrusion, Pharm. Res. 27 (2010) 371–379. doi:10.1007/s11095-009-0033-x.

[241] L. Tamaddon, S.A. Mostafavi, R. Karkhane, M. Riazi-Esfahani, F.A. Dorkoosh, M. Rafiee-Tehrani, Design and development of intraocular polymeric implant systems for long-term controlled-release of clindamycin phosphate for toxoplasmic retinochoroiditis, Adv. Biomed. Res. 4 (2015). doi:10.4103/2277-9175.150426.

[242] A. Rothen-Weinhold, N. Oudry, K. Schwach-Abdellaoui, S. Frutiger-Hughes, G.J. Hughes, D. Jeannerat, U. Burger, K. Besseghir, R. Gurny, Formation of peptide impurities in polyester matrices during implant manufacturing, Eur. J. Pharm. Biopharm. 49 (2000) 253–257. doi:10.1016/S0939-6411(00)00066-7.

[243] S. Gogolewski, M. Jovanovic, S.M. Perren, J.G. Dillon, M.K. Hughes, The effect of melt-processing on the degradation of selected polyhydroxyacids: polylactides, polyhydroxybutyrate, and polyhydroxybutyrate-co-valerates, Polym. Degrad. Stab. 40 (1993) 313–322. doi:10.1016/0141-3910(93)90137-8.

CHAPTER 2:

MATERIALS AND METHODS

2.1 Materials

- Polymers:

  Poly(D,L-lactic-co-glycolic acid) (PLGA) (Resomer RG 502H and Resomer RG 504H: 50:50 lactic acid:glycolic acid, -COOH end groups; and Resomer RG 752H: 75:25 lactic acid:glycolic acid, -COOH end groups) and poly(D,L-lactic acid) (PLA) (Resomer R 202H: -COOH end groups) (Evonik, Darmstadt, Germany)

- Drugs and colored agents:

  dexamethasone (Discovery Fine Chemicals, Dorset, UK); riboflavin (DSM Nutritional Products, Basel, Switzerland); Sudan-III-red (Merck, Darmstadt, Germany); methylene blue (Sigma Aldrich, Steinheim, Germany)

- Organic solvents and acids:

  N-methyl-pyrrolidone (NMP), acetonitrile and tetrahydrofuran (Fisher Scientific, Illkirch, France); ethanol 96% (VWR, Fontenay-sous-Bois, France); formic acid (Riedel-de Haen, Seelze, Germany)

- Additives:

  Carbopol® 980 Polymer (Lubrizol, Wickliffe, Ohio, USA); Poly(ethylene glycol) (PEG 400) (Acros organics, Geel, Belgium); stearic acid (Fisher Scientific, Illkirch, France); acetyltributyl citrate (ATBC) (Morflex, Greensboro, NC, USA); hydroxypropyl methyl cellulose (HPMC, Methocel E15 and K100; Colorcon, Dartford, UK); polyoxyethylene glycol sorbitan monooleate (Tween 80; Cooper, Melun, France)

2.2 Methods

2.2.1 *In-situ* forming PLGA implants for intraocular dexamethasone delivery

2.2.1.1 Preparation of the liquid formulations

Appropriate amounts of PLGA and dexamethasone were dissolved in NMP in glass vials under stirring at 500 rpm (Multipoint Stirrer, Thermo Scientific, Loughborough, UK) at room temperature for 60 min. Afterwards, the vials were kept without stirring for 1 h at room temperature in order to remove air bubbles. The formulations were stored at 2-8 °C, and allowed to reach room temperature prior to use.

2.2.1.2 *In-situ* formation of implants

Eppendorf vials were filled with 2.25 or 4.5 mL phosphate buffer pH 7.4 (USP 40) and kept at 37 °C overnight. One hundred µl of the liquid PLGA/dexamethasone/NMP formulations (prepared as described in section 2.2.) were injected into the vials using a syringe pump (2 mL/min; PHD 2000; Harvard Apparatus, Holliston, USA). Solvent exchange initiated polymer precipitation and *in-situ* implant formation. The Eppendorf vials were placed into a horizontal shaker (80 rpm, 37 °C; GFL 3033, Gesellschaft fuer Labortechnik, Burgwedel, Germany).

2.2.1.3 Characterization of *in-situ* formed implants

In vitro drug release: At determined time points, the phosphate buffer pH 7.4 was completely renewed. The amount of dexamethasone in the withdrawn bulk fluid was determined by HPLC-UV analysis, using a Thermo Fisher Scientific Ultimate 3000 Series HPLC, equipped with a LPG 3400 SD/RS pump, an auto sampler (WPS-3000 SL) and a UV-Vis detector (VWD-3400RS) (Thermo Fisher Scientific, Waltham, USA). Samples were centrifuged for 2.5 min at 10,000 rpm (Centrifuge Universal 320; Hettich, Tuttlingen, Germany), and filtered with a 0.45 µm PVDF syringe filter (Millex-HV, Merck Millipore, Tullagreen, Ireland). Fifty µL samples were injected into an A C18 RP column (Gemini 3 µm C18 110 Å, 100 mm x 4.6 mm; Phenomenex, Le Pecq, France). The mobile phase consisted of acetonitrile and water (33:67 v/v), the flow rate was 1.5 mL/min. Dexamethasone had a retention time of approximately 3.8 min, the detection wavelength was $\lambda = 254$ nm. The calibration curve was linear ($R > 0.999$) within the range of 0.06 to 0.00003 mg/mL. To determine the amount of dexamethasone potentially remaining in the implants after 35 d exposure to phosphate buffer pH 7.4, the remnants were

freeze-dried for 3 d (Christ Epsilon 2–4 LSC; Martin Christ, Osterode, Germany) and the lyophilisates were dissolved in a mixture of acetonitrile and ethanol (2:1 v/v). The solutions were filtered using 0.45 µm PVDF filter syringes, and analyzed for their drug contents by HPLC-UV (as described above). In case of incomplete drug release at the end of the observation period, the "missing" amounts were experimentally recovered in the implant remnants. All experiments were conducted in triplicate. In addition, the pH of the release medium was measured at pre-determined time points using a pH meter (InoLab pH Level 1; WTW, Weilheim, Germany) (n = 3).

Implant swelling and erosion: At pre-determined time points, implant samples were withdrawn, excess water carefully removed using Kimtech precision wipes (Kimberly-Clark, Rouen, France) and weighed [wet mass (t)]. The samples were lyophilized for 3 d (Christ Epsilon 2–4 LSC) and weighed again [dry mass (t)]. The wet mass (%) (t), water/NMP content (%) (t), and dry mass loss (%) (t) were calculated as follows:

$$wet\ mass\ (\%)(t) = \frac{wet\ mass\ (t)}{formulation\ mass} \times 100\ \% \quad (1)$$

$$water/NMP\ content\ (\%)(t) = \frac{wet\ mass\ (t) - dry\ mass(t)}{wet\ mass\ (t)} \times 100\ \% \quad (2)$$

$$dry\ mass\ loss\ (\%)(t) = \frac{dry\ mass\ (0) - dry\ mass\ (t)}{dry\ mass\ (0)} \times 100\ \% \quad (3)$$

where formulation mass is the initial total mass of the liquid formulation (PLGA + dexamethasone + NMP), and dry mass (0) is the dry mass of the liquid formulation prior to exposure to the release medium (PLGA + dexamethasone). All experiments were conducted in triplicate.

Polymer degradation: At pre-determined time points, implants were withdrawn, freeze-dried and the lyophilisates were dissolved in tetrahydrofuran (at a concentration of 3 mg/mL). The average polymer molecular weight (Mw) of the PLGA was determined by Gel Permeation Chromatography (GPC, Separation Modules e2695 and e2695D, 2419 RI Detector, Empower GPC software; Waters, Guyancourt, France) using a PLGel 5 µm MIXED-D column, 7.5 x 300 mm (Agilent Technologies, Interchim, Montluçon, France). The injection volume was 50 µL.

Tetrahydrofuran was the mobile phase (flow rate: 1 mL/min). Polystyrene standards with molecular weights between 1,090 and 70,950 Da (Polymer Labaratories, Varian, Les Ulis, France) were used to prepare the calibration curve. All experiments were conducted in triplicate.

Implant morphology: At pre-determined time points, implants were withdrawn and optionally freeze-dried. Cross-sections were obtained by manual breaking. Pictures were taken with an optical image analysis system (Nikon SMZ-U; Nikon, Tokyo, Japan), equipped with a Zeiss camera (AxioCam ICc1; Zeiss, Jena, Germany).

2.2.1.4 Determination of the drug solubility

The solubility of dexamethasone (as received) in phosphate buffer pH 7.4 at 37 °C was determined in agitated glass flasks. An excess amount of dexamethasone powder (approximately 30 mg) was exposed to 80 mL bulk fluid, kept at 37 °C under horizontal shaking (80 rpm; GFL 3033). Samples were withdrawn, filtered (0.45 µm PVDF syringe filter), diluted and analyzed for their drug content by HPLC-UV (as described above, using an injection volume of 20 µL) until equilibrium was reached. Each experiment was conducted in triplicate.

2.2.2 Often neglected: PLGA/PLA swelling orchestrates drug release - HME implants

2.2.2.1 Implant preparation

Appropriate amounts of polymer (PLGA or PLA) and drug (dexamethasone) were mixed for 5 min at 98 rpm in a Turbula Shaker-Mixer (T2A, Willy A. Bachofen, Basel, Switzerland), followed by 5 min manual blending in a mortar with a pestle. The mixtures were filled into 5 mL syringes (Injekt Luer Lock Solo, B Braun, Melsungen, Germany), equipped with a shortened (1.5 cm) 16G needle. Figure 2.1 shows schematically the experimental set-up used to prepare the implants by hot melt extrusion. Briefly, a syringe was fixed in a holder. The water was kept at 95 °C. After 5 min, the content of the syringe was molten, and a texture analyzer (TAXT plus, Stable Micro Systems, Surrey, UK), equipped with a 50 kg load cell, was used to drive the syringe plunger downwards at a speed of 0.6 mm/min. The obtained extrudates were manually cut into cylinders (5 mm length), using a heated blade.

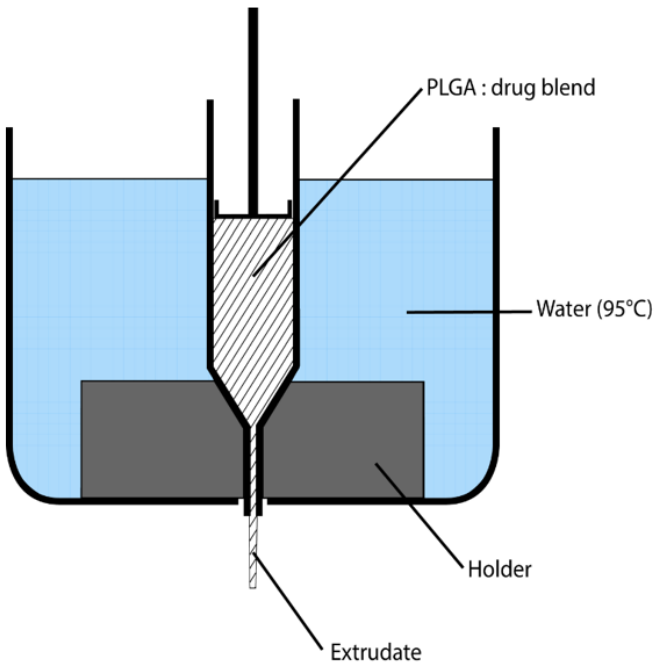

Figure 2.1: Schematic presentation of the experimental set-up used to prepare dexamethasone implants by hot melt extrusion.

2.2.2.2 Implant characterization

The diameter of the implants was measured with a SMZ-U microscope (Nikon, Tokyo, Japan), equipped with an AxioCam ICc1 camera and the Axiovision Zeiss Software (Carl Zeiss, Jena Germany).

The practical drug loading was determined as follows: Samples were dissolved in 5 mL of a 1:4 (v/v) ethanol:acetonitrile mixture. The drug content of the solutions was analyzed using a Thermo Fisher Scientific Ultimate 3000 Series HPLC, equipped with a LPG 3400 SD/RS pump, an auto sampler (WPS-3000 SL) and a UV-Vis detector (VWD-3400RS) (Thermo Fisher Scientific, Waltham, USA). Samples were centrifuged for 2.5 min at 10,000 rpm (Centrifuge Universal 320; Hettich, Tuttlingen, Germany) and filtered with a 0.45 µm PVDF syringe filter (Millex-HV, Merck Millipore, Tullagreen, Ireland). Ten µL samples were injected into an A C18 RP column (Gemini 3 µm C18 110 Å, 100 mm x 4.6 mm; Phenomenex, Le Pecq, France). The mobile phase consisted of a 33:67 (v/v) acetonitrile:water mixture, the flow rate was 1.5 mL/min. Dexamethasone had a retention time of approximately 3.8 min, the detection wavelength was $\lambda = 254$ nm. The calibration curve was linear ($R > 0.999$) within the range of 0.06 to 0.00003 mg/mL. All experiments were conducted in triplicate. Mean values +/- standard deviations are reported.

In vitro drug release: Implants were placed into Eppendorf vials (1 implant per vial), filled with 4 mL phosphate buffer pH 7.4 (USP 40, 37 °C) and horizontally shaken at 80 rpm and 37 °C (GFL 3033, Gesellschaft fuer Labortechnik, Burgwedel, Germany). At pre-determined time points, the release medium was completely replaced. The amount of dexamethasone in the withdrawn bulk fluid was determined by HPLC-UV analysis, as described above (injection volume: 100 µL). If implant remnants remained at the end of the observation period, the amount of potentially "not released" dexamethasone was determined as follows: The remnants were freeze-dried for 3 d (Christ Epsilon 2–4 LSC; Martin Christ, Osterode, Germany) and the lyophilisates were dissolved in a 4:1 (v/v) acetonitrile:ethanol mixture. The solutions were filtered (0.45 µm PVDF filter syringes) and analyzed for their drug contents by HPLC-UV (as described above). Note that these experiments showed that in case of incomplete drug release at the end of the observation period, the amounts that had not been released, were experimentally recovered in the implant remnants (100 % mass balance). All experiments were conducted in triplicate. Mean values +/- standard deviations are reported. In addition, the pH of the release medium was measured at pre-determined time points using a pH meter (InoLab pH Level 1; WTW, Weilheim, Germany) (n = 3, mean values +/- standard deviations are reported).

Implant swelling and erosion: Implants were treated as for drug release studies. At pre-determined time points, specimen were withdrawn, excess water carefully removed using Kimtech precision wipes (Kimberly-Clark, Rouen, France) and weighed [wet mass (t)]. The samples were lyophilized for 3 d (Christ Epsilon 2–4 LSC) and weighed again [dry mass (t)]. The wet mass (%) (t), water content (%) (t), and dry mass loss (%) (t) were calculated as follows:

$$wet\ mass\ (\%)(t) = \frac{wet\ mass\ (t)}{initial\ weight} \times 100\ \% \quad (4)$$

$$water\ content\ (\%)(t) = \frac{wet\ mass\ (t) - dry\ mass(t)}{wet\ mass\ (t)} \times 100\ \% \quad (5)$$

$$dry\ mass\ loss\ (\%)(t) = \frac{initial\ weight - dry\ mass\ (t)}{initial\ weight} \times 100\ \% \quad (6)$$

where initial weight is the weight of the implants before exposure to the release medium (t = 0). All experiments were conducted in triplicate. Mean values +/- standard deviations are reported.

Polymer degradation: Implants were treated as for drug release studies. At pre-determined time points, specimen were withdrawn, freeze-dried for 3 d (Christ Epsilon 2–4 LSC) and the lyophilisates were dissolved in tetrahydrofuran (at a concentration of 1.5 mg/mL). The average polymer molecular weight (Mw) of the PLGA and PLA in the samples was determined by Gel Permeation Chromatography (GPC, Separation Modules e2695 and e2695D, 2419 RI Detector, Empower GPC software; Waters, Guyancourt, France), using a PLGel 5 µm MIXED-D column, 7.5 x 300 mm (Agilent Technologies, Interchim, Montluçon, France). The injection volume was 50 µL. Tetrahydrofuran was the mobile phase (flow rate: 1 mL/min). Polystyrene standards with molecular weights between 1,090 and 70,950 Da (Polymer Labaratories, Varian, Les Ulis, France) were used to prepare the calibration curve. All experiments were conducted in triplicate. Mean values +/- standard deviations are reported.

Implant morphology: Implants were treated as for drug release studies. At pre-determined time points, specimen were withdrawn and freeze-dried as described above. Pictures were taken with an optical image analysis system (Nikon SMZ-U), equipped with a Zeiss camera (AxioCam ICc1).

2.2.2.3 Determination of drug solubility

The solubility of dexamethasone (as received) in phosphate buffer pH 7.4 at 37 °C was determined in agitated glass flasks. An excess amount of dexamethasone powder (approximately 30 mg) was exposed to 80 mL bulk fluid, and kept at 37 °C under horizontal shaking (80 rpm; GFL 3033). At pre-determined time points, samples were withdrawn, immediately filtered (0.45 µm PVDF syringe filter), diluted and analyzed for their drug content by HPLC-UV analysis (as described above, using an injection volume of 20 µL). Measurements were performed until equilibrium was reached. Each experiment was conducted in triplicate. Mean values +/- standard deviations are reported.

2.2.3 Coloring of PLGA implants to better understand drug release mechanisms

2.2.3.1 Implant preparation

Hot melt extrusion (HME): Poly(lactic-co-glycolic acid) (PLGA Resomer RG 502H) and 1% riboflavin or Sudan-III-red were mixed for 5 min at 98 rpm in a Turbula Shaker-Mixer (T2A; Willy A. Bachofen, Basel, Switzerland), followed by 5 min manual blending with a mortar and pestle to ensure a homogenous blend. The mixtures were filled into 5 mL syringes, equipped with a shortened 16G needle (1.5 cm). Figure 2.1 shows schematically the set-up used to prepare the implants by hot melt extrusion. The syringe was fixed in a holder. A water bath kept the temperature at 95 °C. After 5 min, the content of the syringe was molten, and a texture analyzer (TAXT plus, 50 kg loading cell; Stable Micro Systems, Surrey, UK) was used to drive the syringe plunger downwards at a speed of 0.6 mm/min. The obtained extrudates were manually cut into cylinders of approximately 5 mm length, using a heated blade.

In-situ forming implants: Appropriate amounts of PLGA (Resomer RG 502H) and riboflavin or Sudan-III-red were dissolved in NMP in glass vials under stirring at 500 rpm (Multipoint Stirrer, Thermo Scientific, Loughborough, UK) at room temperature for 60 min. Afterwards, the vials were kept without stirring for 1 h at room temperature to remove air bubbles. The formulations were stored at 2–8 °C, and allowed to reach room temperature prior to use. Eppendorf vials were filled with 4 mL: (i) phosphate buffer pH 7.4 (USP 40) in the case of riboflavin, (ii) phosphate buffer pH 7.4 (USP 40) containing 0.02% Tween 80 in the case of Sudan-III-red, or (iii) phosphate buffer pH 7.4 (USP 40) containing 0.01% methylene blue in the case of vitamin/dye-free implants. All vials were pre-heated overnight at 37 °C. One hundred µl of the liquid PLGA/vitamin/dye/NMP formulations were injected into the vials using a syringe pump (2 mL/min; PHD 2000; Harvard Apparatus, Holliston, USA). Solvent exchange initiated polymer precipitation and *in-situ* implant formation. The Eppendorf vials were placed into a horizontal shaker (80 rpm, 37 °C; GFL 3033, Gesellschaft fuer Labortechnik, Burgwedel, Germany).

2.2.3.2 Implant characterization

In vitro vitamin/dye release from HME implants: One implant was placed in 1 Eppendorf vial, filled with 4 mL pre-heated phosphate buffer pH 7.4 (USP 40) in the case of riboflavin, or 4 mL pre-heated phosphate buffer pH 7.4 (USP 40) containing 0.02 % Tween 80 in the case of Sudan-III-red. At determined time points, the release medium was completely renewed. The

amount of riboflavin in the withdrawn bulk fluid was determined by HPLC-UV analysis, using a Thermo Fisher Scientific Ultimate 3000 Series HPLC, equipped with a LPG 3400 SD/RS pump, an auto sampler (WPS-3000 SL) and a UV-Vis detector (VWD-3400RS) (Thermo Fisher Scientific, Waltham, USA). Samples were centrifuged for 2.5 min at 10,000 rpm (Centrifuge Universal 320; Hettich, Tuttlingen, Germany), and filtered with a 0.45 µm PVDF syringe filter (Millex-HV, Merck Millipore, Tullagreen, Ireland). Ten µL samples were injected into a polar C18 column (Luna Omega 3 µm Polar C18 100 Å, 150 mm x 4.6 mm; Phenomenex, Le Pecq, France). The mobile phase consisted of a 85:15 (v/v) mixture of a 0.1 % formic acid solution and acetonitrile, the flow rate was 0.8 mL/min. Riboflavin had a retention time of approximately 6.8 min, the detection wavelength was λ = 270 nm. The calibration curve was linear (R > 0.999) within the range of 0.06 to 0.00004 mg/mL. To determine the amount of riboflavin potentially remaining in the implants at the end of the observation period, the remnants were freeze-dried for 3 d (Christ Epsilon 2–4 LSC; Martin Christ, Osterode, Germany). The lyophilisates were dissolved in a 4:1 (v/v) mixture of acetonitrile and ethanol. The solutions were filtered using 0.45 µm PVDF filter syringes and analyzed for their riboflavin contents by HPLC-UV (as described above). In case of incomplete vitamin release at the end of the observation period, the "missing" amounts were experimentally recovered in the implant remnants in all cases. All experiments were conducted in triplicate. Mean values +/- standard deviations are reported. In the case of Sudan-III-red, dye release was followed visually: At pre-determined time points, implant samples were withdrawn, freeze-dried for 3 d (Christ Epsilon 2–4 LSC), and cross-sections observed with an optical image analysis system (Nikon SMZ-U; Nikon, Tokyo, Japan), equipped with a Zeiss camera (AxioCam ICc1; Zeiss, Jena, Germany). The cross-sections were obtained by cutting with a heated blade in the case of HME implants, and by manual breaking in the case of *in-situ* forming implants. In vitro vitamin/dye release from *in-situ* forming implants was measured in the same way (the implants were formed in the Eppendorf vials used for the in vitro release studies).

Implant swelling: Implants were treated as for the in vitro release studies. At pre-determined time points, implant samples were withdrawn, excess water carefully removed using Kimtech precision wipes (Kimberly-Clark, Rouen, France) and weighed [wet mass (t)]. The wet mass (%) (t) was calculated as follows:

$$wet\ mass\ (\%)(t) = \frac{wet\ mass\ (t)}{initial\ weight} \times 100\ \% \qquad (7)$$

where initial weight is the weight of the pre-formed implant in the case of HME implants, or the total mass of the liquid formulation (PLGA + vitamin/dye + NMP) in the case of *in-situ* forming implants. All experiments were conducted in triplicate. Mean values +/- standard deviations are reported.

Implant morphology: Implants were treated as for the in vitro release studies. At pre-determined time points, implants were withdrawn and freeze-dried for 3 d (Christ Epsilon 2–4 LSC). Pictures were taken with an optical image analysis system (Nikon SMZ-U), equipped with a Zeiss camera (AxioCam ICc1). Cross-sections were obtained by cutting (with a heated blade) in the case of HME implants, and by manual breaking in the case of *in-situ* formed implants.

2.2.3.3 Determination of the solubility of riboflavin

The solubility of riboflavin (as received) in phosphate buffer pH 7.4 at 37 °C was determined in agitated glass flasks. An excess amount of riboflavin powder (approximately 30 mg) was exposed to 80 mL bulk fluid, kept at 37 °C under horizontal shaking (80 rpm; GFL 3033). Samples were withdrawn, immediately filtered (0.45 µm PVDF syringe filter), diluted and analyzed for their riboflavin content by HPLC-UV (as described above, using an injection volume of 20 µL) until equilibrium was reached. Each experiment was conducted in triplicate. Mean values +/- standard deviations are reported.

2.2.4 *In-situ* forming PLGA implants: How additives affect swelling and drug release

2.2.4.1 Preparation of the liquid formulations

PLGA (40 %), dexamethasone (1 %) and varying amounts of different additives (Carbopol, PEG 400, HPMC K100, HPMC E15, stearic acid or ATBC were dissolved in NMP (in all cases clear solutions were obtained) in glass vials under stirring at 500 rpm (Multipoint Stirrer, Thermo Scientific, Loughborough, UK) at room temperature for 60 min. All percentages refer to the total liquid formulation mass (100 % = polymer + drug + additive + NMP). The NMP content was adjusted accordingly (as a function of the additive content). Afterwards, the vials were kept for 1 h at room temperature without stirring to remove air bubbles. The formulations were stored at 2-8 °C, and allowed to reach room temperature prior to use.

2.2.4.2 *In-situ* implant formation

Eppendorf vials were filled with 4 mL phosphate buffer pH 7.4 (USP 40) (37 °C). One hundred µl of the liquid PLGA/dexamethasone/additive/NMP formulations (prepared as described in *section 2.2.*) were injected using a syringe pump (2 mL/min; PHD 2000; Harvard Apparatus, Holliston, USA). Solvent exchange initiated polymer precipitation and *in-situ* implant formation. The Eppendorf vials were placed into a horizontal shaker (80 rpm, 37 °C; GFL 3033, Gesellschaft fuer Labortechnik, Burgwedel, Germany).

2.2.4.3 Characterization of *in-situ* formed implants

In vitro drug release: At determined time points, the phosphate buffer pH 7.4 in the vials in which the implants formed was completely renewed. The amount of dexamethasone in the withdrawn bulk fluid was determined by HPLC-UV analysis, using a Thermo Fisher Scientific Ultimate 3000 Series HPLC, equipped with a LPG 3400 SD/RS pump, an auto sampler (WPS-3000 SL) and a UV-Vis detector (VWD-3400RS) (Thermo Fisher Scientific, Waltham, USA). Samples were centrifuged for 2.5 min at 10,000 rpm (Centrifuge Universal 320; Hettich, Tuttlingen, Germany), and filtered with a 0.45 µm PVDF syringe filter (Millex-HV, Merck Millipore, Tullagreen, Ireland). One hundred µL samples were injected into an A C18 RP column (Gemini 3 µm C18 110 Å, 100 mm x 4.6 mm; Phenomenex, Le Pecq, France). The mobile phase consisted of acetonitrile and water (33:67 v/v), the flow rate was 1.5 mL/min. Dexamethasone had a retention time of approximately 3.8 min, the detection wavelength was λ = 254

nm. The calibration curve was linear (R > 0.999) within the range of 0.06 to 0.00003 mg/mL. To determine the amount of dexamethasone potentially remaining in the implants at the end of the observation period, the remnants were dissolved in a mixture of acetonitrile and ethanol (2:1 v/v). The solutions were filtered using 0.45 µm PVDF filter syringes, and analyzed for their drug contents by HPLC-UV (as described above). In all cases, no noteworthy drug amounts were detected in implant remnants. All experiments were conducted in triplicate. In addition, the pH of the release medium was measured at pre-determined time points using a pH meter (InoLab pH Level 1; WTW, Weilheim, Germany) (n = 3, +/- standard deviation).

Implant swelling: At pre-determined time points, implant samples were withdrawn, excess water carefully removed using Kimtech precision wipes (Kimberly-Clark, Rouen, France) and weighed [*wet mass (t)*]. The *wet mass (%) (t)* was calculated as follows:

$$wet\ mass\ (\%)(t) = \frac{wet\ mass\ (t)}{formulation\ mass} \times 100\ \% \qquad (8)$$

where *formulation mass* is the initial total mass of the liquid formulation (PLGA + dexamethasone + additive + NMP). All experiments were conducted in triplicate. Mean values +/- standard deviations are reported.

NMP release: At pre-determined time points, the phosphate buffer pH 7.4 in the vials in which the implants formed was completely renewed. The amount of NMP in the withdrawn bulk fluid was determined by HPLC-UV analysis, using a Thermo Fisher Scientific Ultimate 3000 Series HPLC, equipped with a LPG 3400 SD/RS pump, an auto sampler (WPS-3000 SL) and a UV-Vis detector (VWD-3400RS). Samples were centrifuged for 2.5 min at 10,000 rpm (Centrifuge Universal 320), and filtered with a 0.45 µm PVDF syringe filter (Millex-HV). Ten µL samples were injected into a polar column (Luna 3 µm HILIC 200 Å, 150 mm x 4.6 mm; Phenomenex). The mobile phase consisted of acetonitrile and water (50:50 v/v) containing 0.1% formic acid, the flow rate was 1.5 mL/min. NMP had a retention time of approximately 4.8 min, the detection wavelength was λ = 210 nm. The calibration curve was linear (R > 0.999) within the range of 0.55 to 0.025 mg/mL. After more than 7 d exposure time to the release medium, NMP was no more detected in the bulk fluid (= 100 % NMP release). All experiments were conducted in triplicate. Mean values +/- standard deviations are reported.

Implant morphology: At pre-determined time points, implants were withdrawn and freeze-dried for 3 d (Christ Epsilon 2–4 LSC; Martin Christ, Osterode, Germany). Cross-sections were obtained by manual breaking. *Macroscopic* pictures of freeze-dried implants were obtained with an optical image analysis system (Nikon SMZ-U; Nikon, Tokyo, Japan), equipped with a Zeiss camera (AxioCam ICc1; Zeiss, Jena, Germany). *SEM* pictures of freeze-dried implants were made with a JEOL Field Emission Scanning Electron Microscope JSM-7800F (Tokyo, Japan). Samples were fixed with a ribbon carbon double-sided adhesive on the sample holder and covered with a fine chrome layer using the Gatan Model 682 Precision Etching and Coating System (Pleasanton, CA, USA).

Glass transition temperature: The glass transition temperature (Tg) of freeze-dried implants was determined by differential scanning calorimetry (DSC 1 Star System; Mettler Toledo, Greifensee, Switzerland). After 3 d exposure to the release medium, samples were removed and freeze-dried for 3 d (Christ Epsilon 2–4 LSC). Approximately 3 mg samples were accurately weighed in sealed aluminum pans. The pans were heated to 120° C, cooled to -70° C, and reheated to 120° C (at a rate of 10 °C/min in nitrogen atmosphere). The Tg was determined during the second heating cycle. All experiments were conducted in triplicate. Mean values +/- standard deviations are reported.

CHAPTER 3:

RESULTS AND DISCUSSION

Part 1: *In-situ* forming PLGA implants for intraocular dexamethasone delivery

The aim of this study was to prepare different types of *in-situ* forming implants based on PLGA for intraocular dexamethasone delivery. The systems were thoroughly characterized physico-chemically, including for instance dynamic changes in the wet mass, dry mass, water/NMP content, morphology, polymer molecular weight, potential changes in the pH of the release medium, and drug release kinetics.

3.1.1 Importance of the volume of the release medium

Since the investigated implants are formed *in-situ* following solvent exchange, it was important to evaluate the impact of the volume of the release medium into which the PLGA/drug/NMP solutions were injected. Potentially, the volume of this aqueous phase can affect the diffusion rate of NMP into the surrounding aqueous phase and/or the diffusion rate of water into the (initially) liquid formulation. Such changes might affect the resulting implant size and inner structure and, hence, the drug release kinetics.

The volume of vitreous humor in humans has been reported to be about 4 to 5 mL [1]. To monitor potential effects of variations in the bulk fluid volume in this order of magnitude on the key properties of the *in-situ* formed implants, 2.25 and 4.5 mL have been investigated in this study. Furthermore, most drugs are eliminated via the anterior pathway [2,3]. To simulate drug elimination and fluid renewal, the release medium was completely exchanged every day during the first week (which is most decisive for implant formation) in this study.

Figure 3.1.1 shows macroscopic pictures of PLGA-based implants formed upon injection of 100 µL of a PLGA/dexamethasone/NMP solution into 2.25 or 4.5 mL phosphate buffer pH 7.4 (37 °C). The liquid formulations contained 30 % Resomer RG 502H and 0.75 % dexamethasone. The photos were taken after 3 d. At the top, implants in Eppendorf tubes (filled with the release medium) are shown. Below, higher magnifications of implants, which had been carefully withdrawn from the release medium are illustrated (surfaces). At the bottom, surfaces and cross-sections of implant samples after freeze-drying are shown. The cross-sections were obtained by manual breaking. The dashed regions highlight the hollow cores of the implants. As it can be seen, there was no remarkable impact of the volume of the aqueous bulk fluid (2.25 vs. 4.5 mL) on the resulting implant morphology: left- vs. right-hand side in Figure 3.1.1.

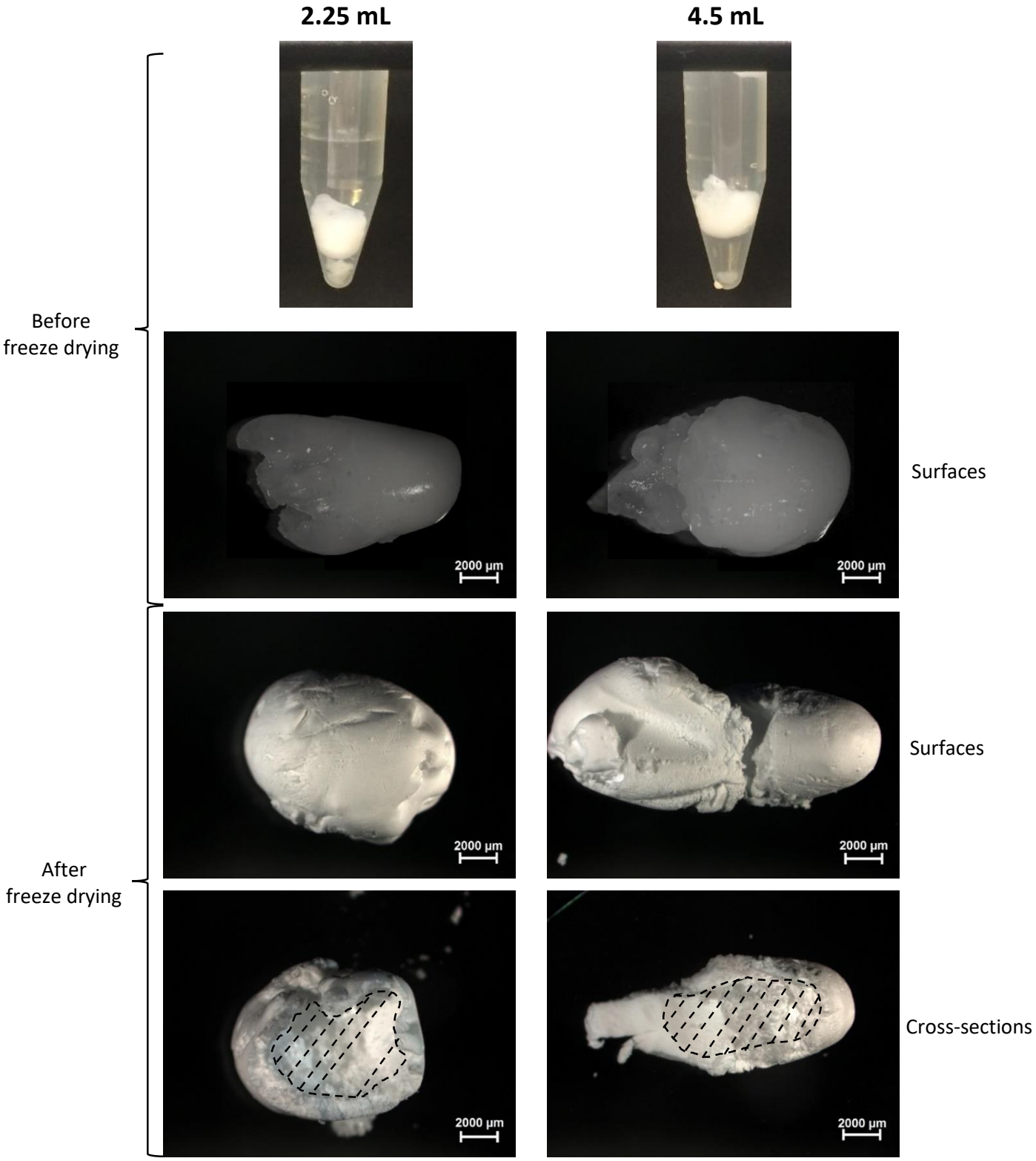

Figure 3.1.1: Macroscopic pictures of implants formed *in-situ* upon exposure to phosphate buffer pH 7.4 before and after freeze drying (surfaces and cross-sections). The formulations contained 0.75 % dexamethasone and 30 % PLGA 502H. The volume of the release medium was 2.25 mL (left column) or 4.5 mL (right column). The pictures were taken after 3 d. The dashed regions highlight the hollow cores of the implants.

Please note that caution must be paid when drawing conclusions from the pictures of lyophilized implants, because of artifact creation during freeze-drying. Importantly, the implants were hollow also in the wet state (data not shown). This can be explained as follows: Upon contact with water, NMP diffuses into the outer bulk fluid and water diffuses into the liquid NMP formulation. Since PLGA is soluble in NMP, but not in water, at a certain time point the polymer precipitates (once the solubility of the polymer in the water/NMP mixture is reached). This process likely starts at the "formulation – aqueous bulk fluid" interface, because the water concentration is highest and the NMP concentration lowest at this location. The continuous decrease in PLGA solubility in the NMP/water mixture (the NMP content decreases, whereas the water content increases) leads to continued polymer precipitation. Thus, the PLGA "shell" becomes thicker and thicker, growing "inwards". Once all PLGA has precipitated, potentially remaining inner volumes (here the centers of the implants) cannot be filled with polymer and become water-filled cavities. Please note that complete solvent exchange took up to several days in this study: Thus, the implant cores remained liquid for a significant period of time. Importantly, no noteworthy impact of the bulk fluid volume on this cavity formation was observed.

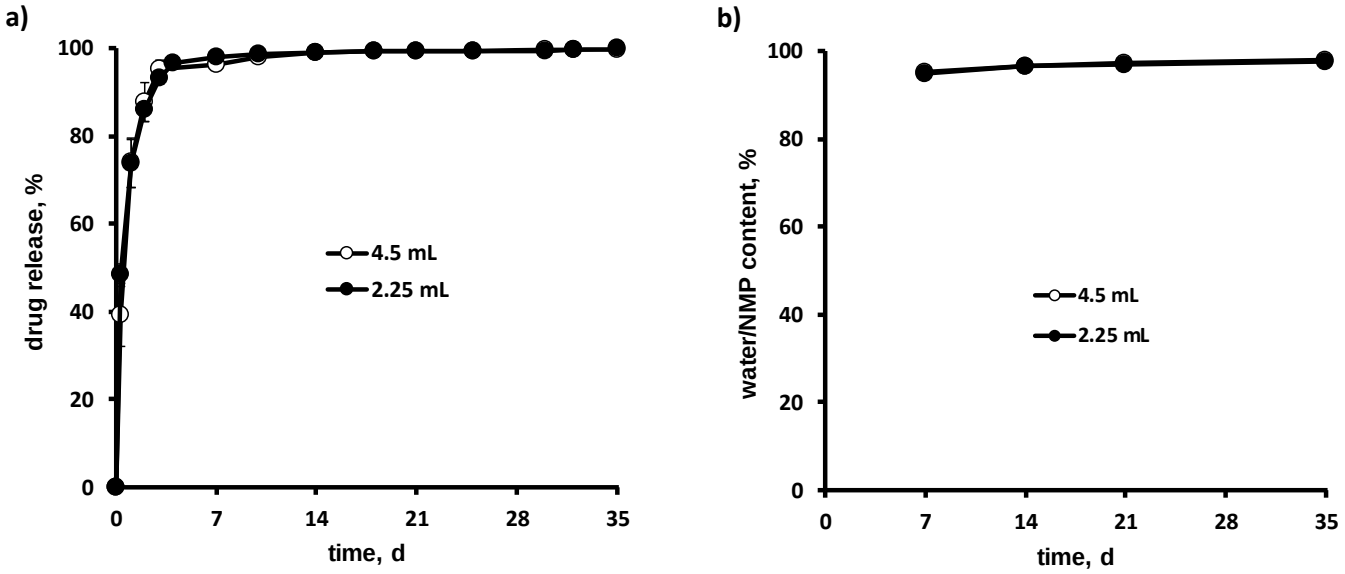

Figure 3.1.2: Impact of the volume of the release medium (phosphate buffer pH 7.4) on: a) drug release, and b) the dynamic changes in the water/NMP content of *in-situ* forming implants. The formulations contained 0.75 % dexamethasone and 30 % PLGA 502H. Mean values +/- standard deviation are indicated (n=3).

Figures 3.1.2a and b show the resulting dexamethasone release kinetics and the dynamic changes of the systems' water/NMP contents over time. The water/NMP contents of the implants were determined gravimetrically as the difference between the wet and dry mass of

the withdrawn samples (before and after freeze-drying). As it can be seen, the drug release curves were virtually overlapping for the investigated bulk fluid volumes (2.25 vs. 4.5 mL). Also, the resulting water/NMP contents were very similar. This can probably be attributed to the fact that NMP and water are freely miscible: So, there are no saturation effects, resulting in potentially reduced NMP diffusion rates into smaller (eventually more saturated) outer aqueous phases (and vice versa).

Importantly, limited drug solubility effects in the surrounding release medium are unlikely to affect dexamethasone release from the *in-situ* forming implants at an initial drug loading of 0.75 %: The solubility of dexamethasone in phosphate buffer pH 7.4 at 37 °C was determined to be 77 ± 4 µg/mL. In NMP, the drug is freely soluble. Thus, at early time points (when the surrounding bulk fluid contains considerable amounts of NMP) saturation effects in the surrounding bulk fluid are unlikely. Furthermore, even if assuming the absence of any NMP in the surrounding bulk fluid from day 3 on (this is a "worst case scenario" for the drug solubility), sink conditions were also provided for the remaining observation period (considering the drug solubility determined in pure phosphate buffer pH 7.4 at 37 °C).

These findings are important, since they demonstrate that variations in the volume of the bulk fluid into which the PLGA/drug/NMP solutions are injected, are not substantially affecting the key properties of the resulting implants. In other words: The proposed *in-situ* forming implant formulations can be expected to be rather robust with respect to variations in the vitreous humor volumes encountered in vivo.

3.1.2 Impact of the drug loading

Figure 3.1.3 shows the impact of the initial drug loading of the *in-situ* forming implant formulations on the resulting dexamethasone release kinetics and the dynamic changes in the implants' wet mass as well as water/NMP contents. The initial drug content was varied from 0.25 to 7.5 %, as indicated. Please note that 100 µL of the formulation with the intermediate drug loading (0.75 %) contain a similar drug dose as the commercially available drug product Ozurdex® (0.7 mg) [4]. The release medium was 2.25 mL phosphate buffer pH 7.4. Resomer RG 502H (30 %) was the polymer. Clearly, the relative drug release rates were similar for formulations loaded with 0.25 and 0.75 % dexamethasone (filled and open circles in Figure 3.1.2a), whereas the relative drug release rate was substantially lower at 7.5 % drug loading (filled triangles).

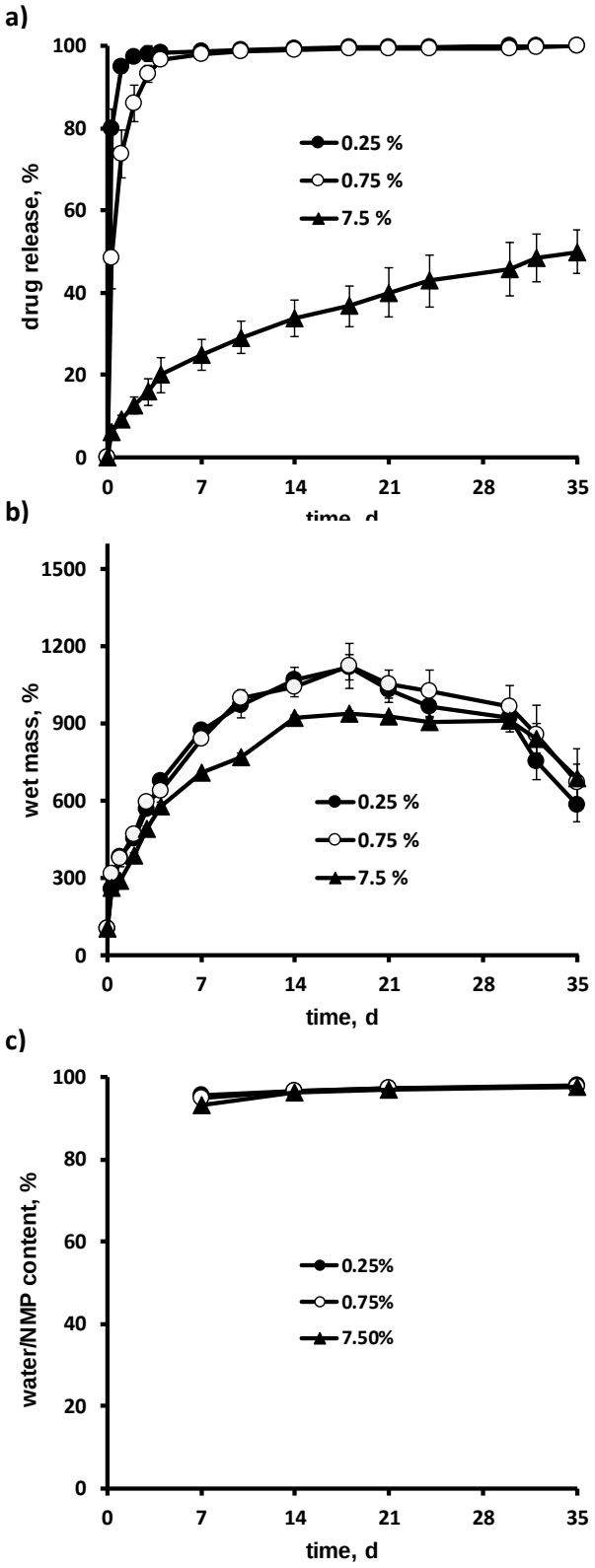

Figure 3.1.3: Impact of the initial drug loading (indicated in the diagrams) of *in-situ* forming implants on the resulting: a) drug release kinetics, b) dynamic changes in the wet mass and c) dynamic changes in the water/NMP content of the systems after exposure to phosphate buffer pH 7.4. The formulations contained 30 % PLGA 502H. The volume of the release medium was 2.25 mL. Mean values +/- standard deviation are indicated (n=3).

This cannot be attributed to differences in the dynamic changes in the systems' wet mass, as illustrated in Figure 3.1.3b (which were rather similar for all drug loadings). Given the limited solubility of dexamethasone in the release medium (77 ± 4 µg/mL in phosphate buffer pH 7.4 at 37 °C), one hypothesis can be that the substantially reduced drug release rate at 7.5 % initial dexamethasone loading is due to saturation effects. To evaluate the validity of this hypothesis, the renewal rate of the release medium was altered: Figures 3.1.4a and b show the resulting drug release kinetics and degrees of bulk fluid saturation (with respect to the drug) observed at a higher and lower sampling frequency (at each sampling time point, the release medium was completely renewed). The degrees of saturation of the release medium were calculated based on the solubility of dexamethasone in phosphate buffer pH 7.4 at 37 °C. Since the surrounding bulk fluid contained important amounts of NMP at early time points, and since dexamethasone is soluble in NMP, no values are indicated in the first week (Figure 3.1.4b). Clearly, the higher sampling frequency lead to faster drug release after about 1 week, corresponding to lower degrees of bulk fluid saturation with the drug. Furthermore, after about 3 weeks, the degree of bulk fluid saturation substantially decreased (to about 10 % = sink conditions) in the case of the higher sampling frequency, while the release rate *de*creased. These observations indicate that saturation effects likely refer to both: dexamethasone saturation in the *surrounding* bulk fluid as well as drug saturation effects *within* the implants: At an initial drug loading of 7.5 %, important parts of the dexamethasone can be expected to precipitate *within* the *in-situ* forming PLGA implants upon water penetration into and NMP leaching out of the system. Consequently, dissolved and non-dissolved dexamethasone co-exist within the implant. It has to be pointed out that only dissolved drug is available for diffusion and can be released into the surrounding bulk fluid [5,6]. Hence, drug release is also likely to be limited by saturation effects *within* the implants.

Please note that during the first week, the observed dexamethasone release rates were very similar for the lower and higher sampling frequency (filled and open circles in Figure 3.1.4a). This might be explained by the fact that during this time period noteworthy amounts of NMP were still present *within* the implants and the surrounding bulk fluid (limiting the importance of drug saturation effects).

Furthermore, the initial drug loading had no major impact on the resulting dynamic changes in the implants' wet mass over time (Figure 3.1.3b). The latter increased during the first 2.5 weeks, and then decreased again. The initial increase can be attributed to the progressing PLGA degradation and subsequent water penetration into the more and more hydrophilic

polymer matrices. The subsequent decrease is likely attributable to the dissolution/disappearance of the remnants (more hydrated regions dissolving faster than less hydrated regions). The water/NMP contents were very high during the observation period, irrespective of the initial drug loading (Figure 3.1.3c).

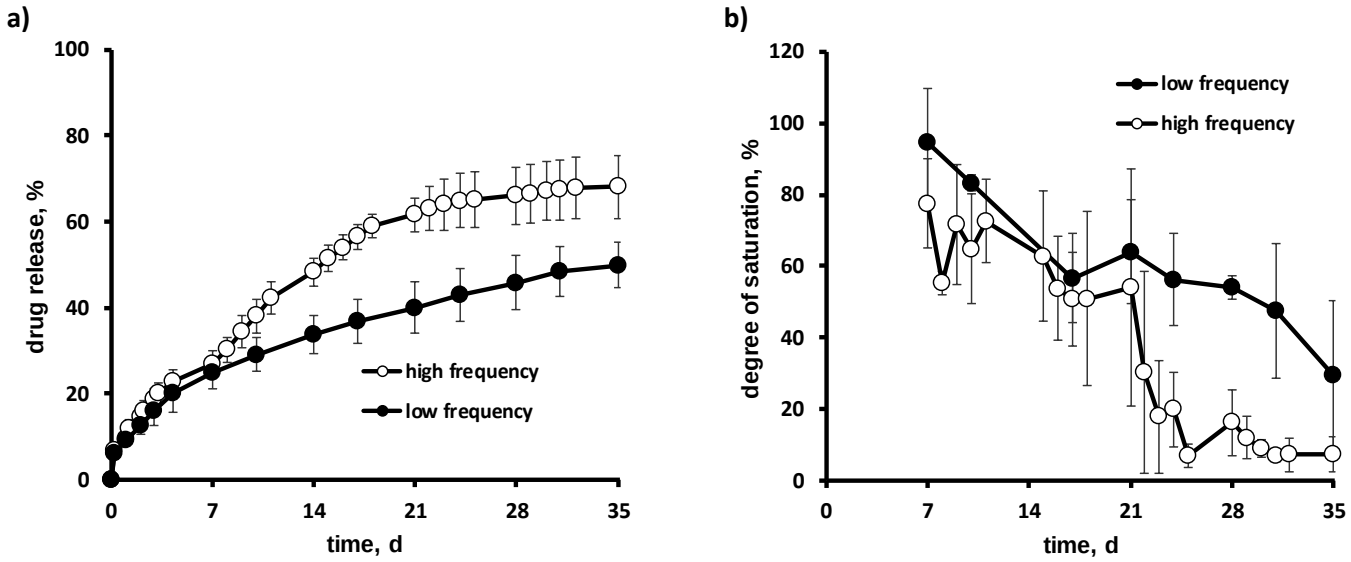

Figure 3.1.4: Impact of the sampling frequency during the drug release measurements on: a) the cumulative relative amount of drug released, and b) the degree of saturation of the withdrawn samples. The formulations contained 7.5 % dexamethasone and 30 % PLGA 502H. The volume of the release medium was 4.5 mL. Mean values +/- standard deviation are indicated (n=3).

3.1.3 Impact of the PLGA polymer molecular weight

The effects of the polymer molecular weight of the PLGA on drug release and the dynamic changes in the implants' wet mass as well as water/NMP contents upon exposure to phosphate buffer pH 7.4 are illustrated in Figure 3.1.5: Resomer RG 502H (Mw about 15 k Da) and Resomer RG 504H (Mw about 45 k Da) are compared. The initial dexamethasone loading was 0.25 %, the polymer concentration in the liquid formulation was 30 %, and the volume of the release medium was 2.25 mL. As it can be seen, the polymer molecular weight substantially impacted the dynamic changes in the systems' wet mass and water/NMP content: Implants based on longer chain PLGA took up fundamentally less water than systems based on shorter chain PLGA. This can be attributed to the facts that: (i) longer chain PLGA is more hydrophobic than shorter chain PLGA, and (ii) longer chain PLGA is likely to precipitate earlier than shorter chain PLGA upon water penetration into the system and NMP diffusion out of the formulation.

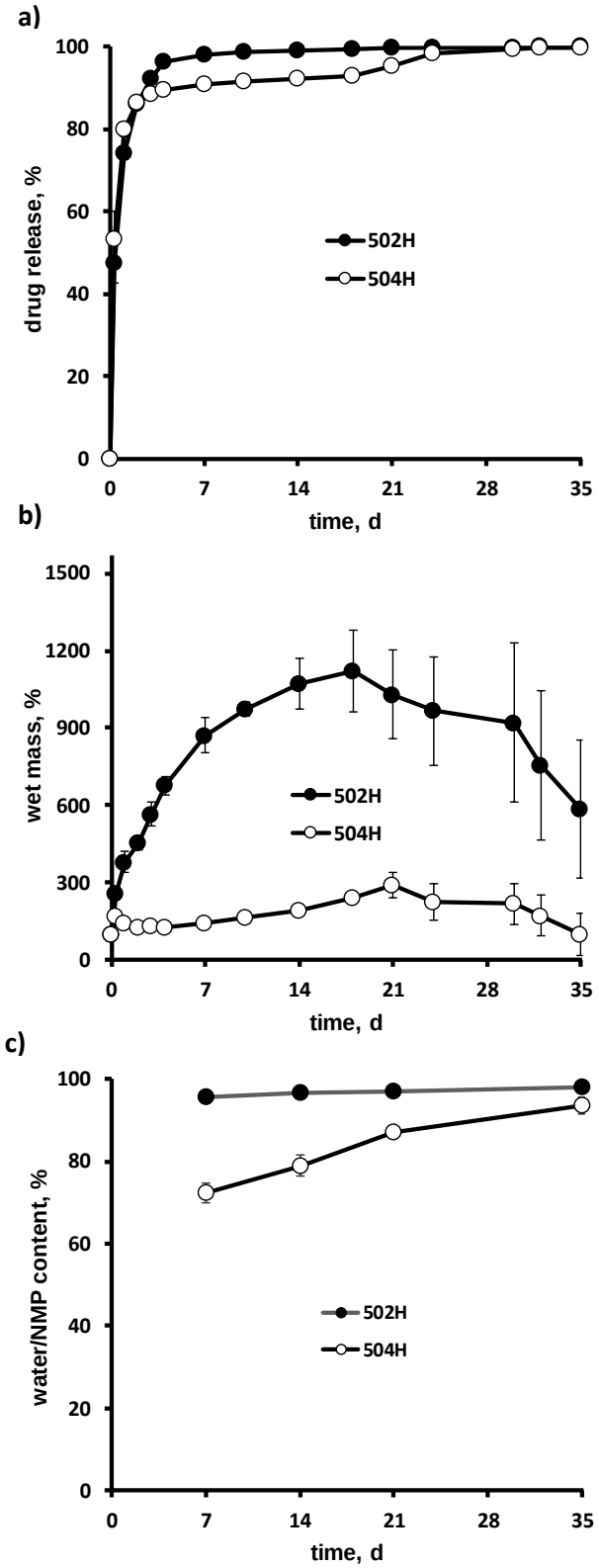

Figure 3.1.5: Importance of the polymer molecular weight of the PLGA (Resomer 502H vs. 504H) for: a) drug release, b) the dynamic changes in the wet mass, and c) the dynamic changes in the water/NMP content from/of implants formed *in-situ* upon exposure to phosphate buffer pH 7.4. The formulations contained 0.25 % dexamethasone and 30 % PLGA. The volume of the release medium was 2.25 mL. Mean values +/- standard deviation are indicated (n=3).

The observed differences in the wet mass of the implants based on shorter and longer chain PLGA (Figure 3.1.5b) are consistent with the different water/NMP contents of systems (Figure 3.1.5c). Whereas the implants based on the more hydrophilic Resomer RG 502H show high water contents right from the beginning, the water contents of Resomer RG 504H-based systems was initially substantially lower, but significantly increased during the observation period (due to the progressive polymer chain cleavage). From a practical point of view, substantial implant swelling should be avoided to minimize any related side effects in vivo. This might for instance be achieved via the selection of appropriate PLGA molecular weights or monomer (lactic acid: glycolic acid) ratios, or specific additives [7–9].

Interestingly, these substantial differences in the implants' compositions and water uptake behaviors are "not fully" reflected in the observed release kinetics (Figure 3.1.5a). This is because drug release was almost complete within the first few days: the time period of implant formation. For instance, after 4 d only 3.8 ± 0.8 and 10.5 ± 1.0 % dexamethasone remained trapped within the implants based on Resomer RG 502H and Resomer RG 504H, respectively. These amounts were slowly released during the subsequent 3 weeks. The observed slower drug release from Resomer RG 504H-based implants compared to Resomer RG 502H-based implants can at least partially be attributed to the lower water contents of the systems (and, thus, denser polymer networks). Please note that with other drugs, which are not almost completely released within the first few days during implant formation, substantial differences in the resulting release kinetics can be expected from Resomer RG 502H- and Resomer RG 504H-based implants, due to the fundamentally different conditions for drug release in these systems (Figures 3.1.5b and c).

3.1.4 Impact of the polymer concentration

Figure 3.1.6 shows the observed dexamethasone release kinetics from *in-situ* formed implants prepared with drug-polymer solutions in NMP containing 30 vs. 45% Resomer RG 502H, or 15 vs. 30 % Resomer RG 504H. Please note that in the latter case, higher polymer concentrations lead to considerable viscosities, rendering injection difficult. The volume of the release medium was 2.25 mL, the initial drug content 0.25 %. As it can be seen, the polymer concentration in the liquid formulations affected the resulting drug release kinetics, irrespective of the PLGA polymer molecular weight:

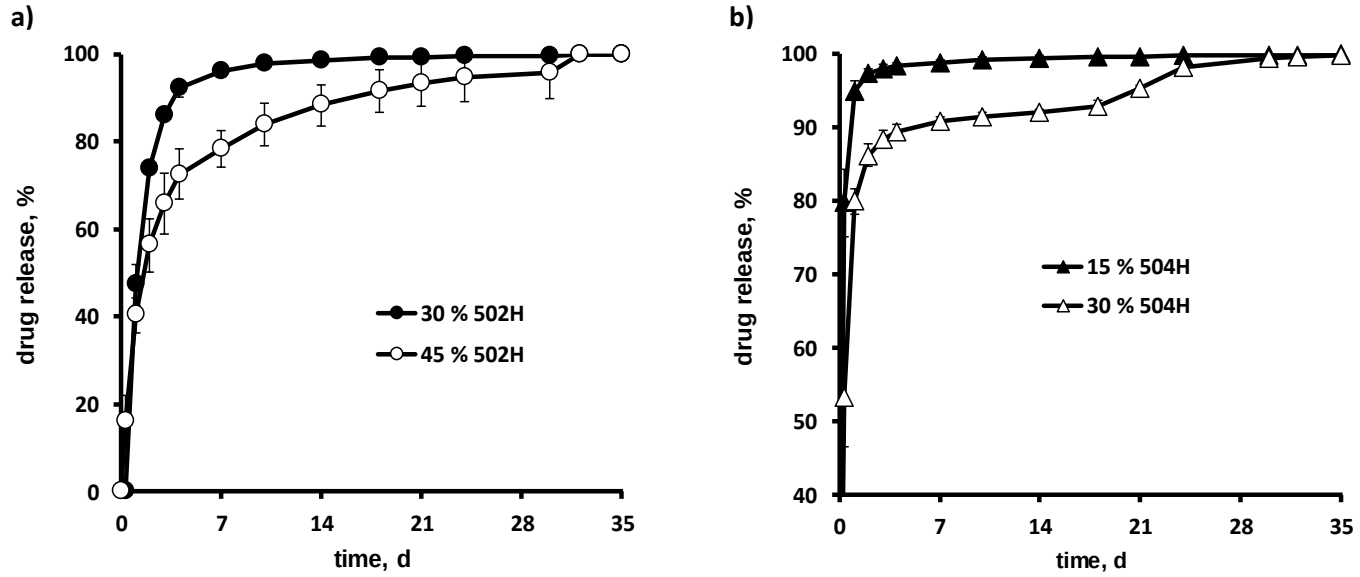

Figure 3.1.6: Impact of the PLGA concentration in the formulation on the resulting dexamethasone release kinetics from *in-situ* formed implants upon exposure to 2.25 mL phosphate buffer pH 7.4: a) PLGA 502H and b) PLGA 504H. The drug content was 0.25 %. Mean values +/- standard deviation are indicated (n=3).

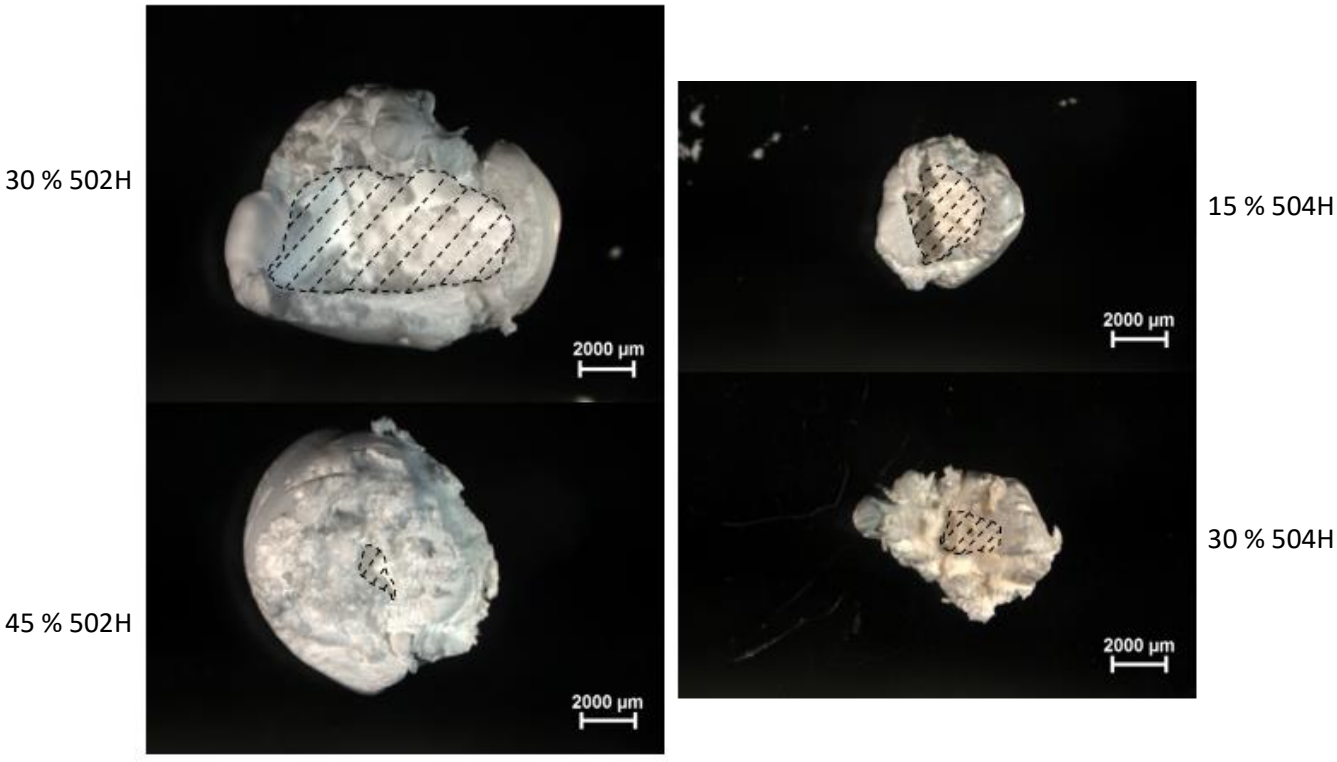

Figure 3.1.7: Macroscopic pictures of cross-sections of freeze-dried *in-situ* formed implants after 3 d exposure to 2.25 mL phosphate buffer 7.4. The formulations contained 0.25 % dexamethasone and 30 % or 45 % PLGA 502H or 15 % or 30 % PLGA 504H. The cross-sections were obtained by manual breaking. All implants were hollow, the cavities are highlighted by the dashed areas.

With increasing polymer concentration, the dexamethasone release rate decreased. This can at least partially be attributed to differences in the implants' inner structure, as shown in Figure 3.1.7: At the top, cross-sections of freeze-dried implants based on Resomer RG 502H are illustrated, at the bottom cross-sections of implants based on Resomer RG 504H. The implants were lyophilized after 3 d exposure to phosphate buffer pH 7.4. Again, please note that caution should be paid because of potential artifact creation during freeze-drying. The dashed regions indicate the hollow central implant cavities. Clearly, higher polymer concentrations in the liquid formulations lead to smaller cavities. This can be attributed to the fact that PLGA precipitation started at the "liquid formulation – aqueous bulk fluid" interface. Subsequent PLGA precipitation "filled" the *in-situ* forming implants. In the case of higher polymer concentrations, more polymer was available to fill the interior of the systems, resulting in smaller cavities. The thicker the polymer shells, the longer are the diffusion pathways through the PLGA matrices to be overcome by the trapped drug. Thus, higher polymer concentrations in the formulations lead to thicker polymer shells/barriers and, hence, slower drug release (irrespective of the polymer molecular weight).

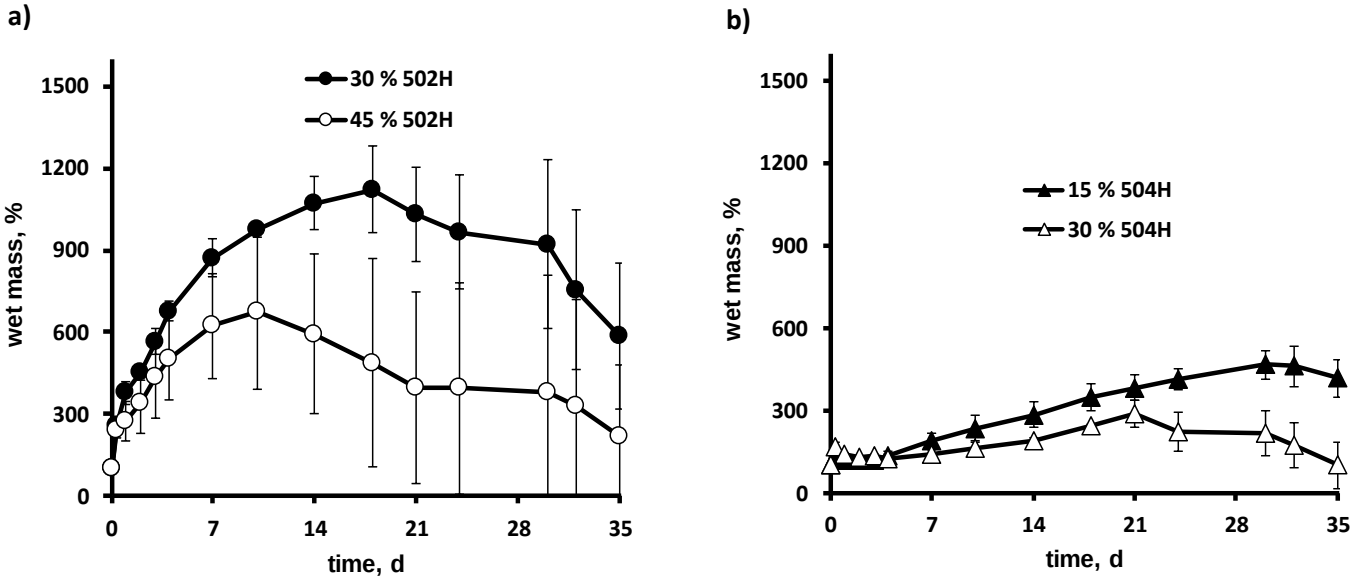

Figure 3.1.8: Impact of the PLGA concentration in the formulation on the dynamic changes in the wet mass of implants formed *in-situ* upon exposure to 2.25 mL phosphate buffer pH 7.4: a) PLGA 502H and b) PLGA 504H. The formulations contained 0.25 % dexamethasone. Mean values +/- standard deviation are indicated (n=3).

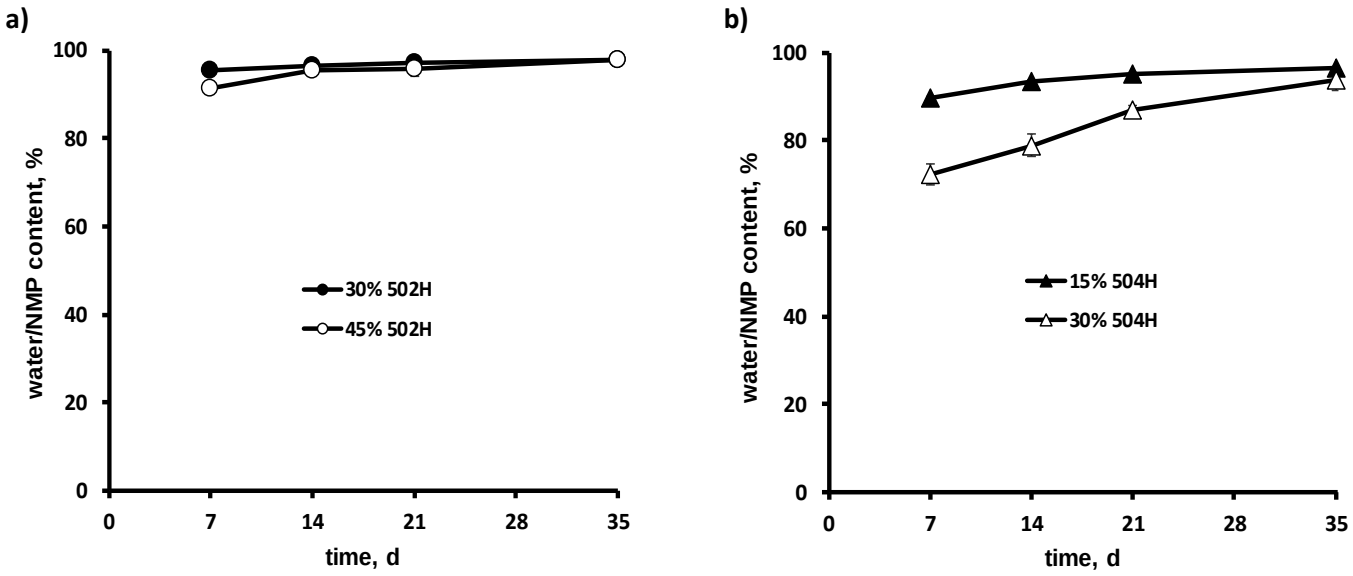

Figure 3.1.9: Effects of the PLGA concentration in the formulation on the dynamic changes in the water/NMP content of implants formed *in-situ* upon exposure to 2.25 mL phosphate buffer pH 7.4: a) PLGA 502H and b) PLGA 504H. The formulations contained 0.25 % dexamethasone. Mean values +/- standard deviation are indicated (n=3).

Furthermore, the smaller central implant cavities at higher initial PLGA concentrations resulted in lower increases in the systems' wet mass and lower water contents, irrespective of the PLGA polymer molecular weight (Figures 3.1.8 and 9). Figures 3.1.10 to 12 illustrate the dynamic changes in the polymer molecular weight (Mw) of the PLGA, the pH of the surrounding bulk fluid and the dry mass loss kinetics of the systems. Importantly, the smaller central implant cavities observed at higher initial polymer concentrations lead to accelerated ester chain cleavage (Figure 3.1.10: open symbols always below filled symbols). This can be attributed to an increase in the importance of autocatalytic effects in these systems: Water is present throughout the implants, thus, polymer chain cleavage occurs in the entire polymer matrices. The generated (water-soluble) shorter chain acids slowly diffuse into the surrounding bulk fluid, where they are (at least partially) neutralized. In addition, bases from the surrounding phosphate buffer diffuse into the implants and neutralize (at least partially) the generated acids. However, the rate at which the acids are generated within the implants can be higher than the rate at which they are neutralized. Consequently, the micro-pH can locally drop [10–14], resulting in pH gradients within the implants. Since hydrolytic ester bond cleavage is catalyzed by protons, PLGA degradation is accelerated at locations with low pH

values [15,16]. The importance of such autocatalytic effects strongly depends on the systems' dimensions and porosity [17,18].

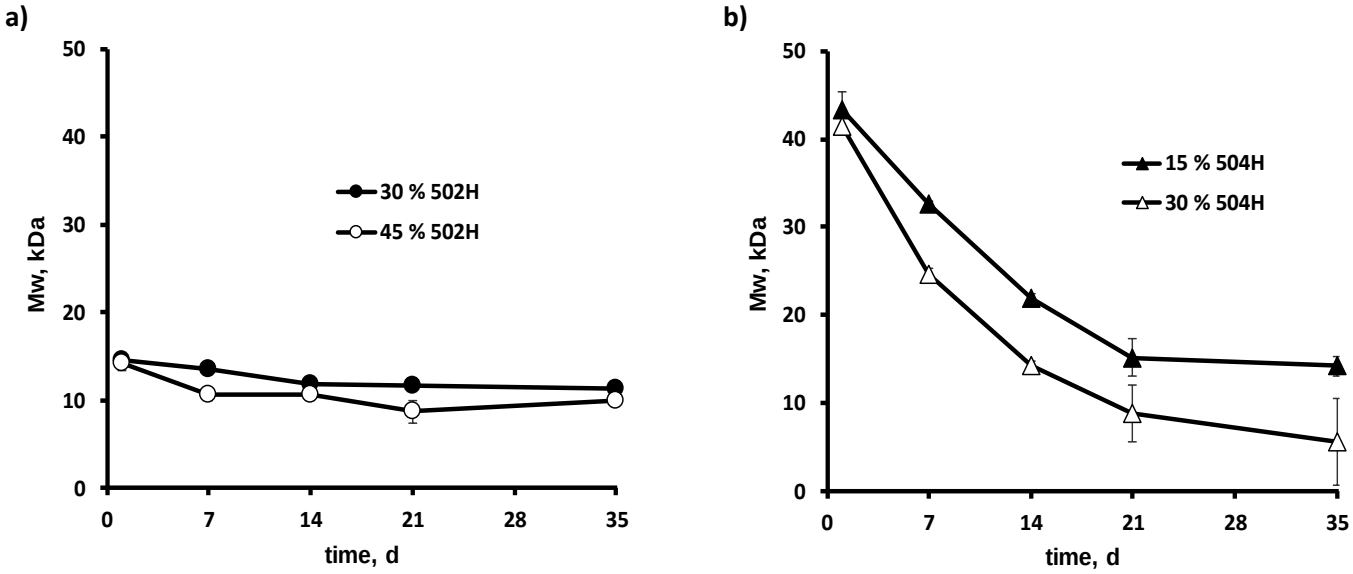

Figure 3.1.10: Impact of the PLGA concentration in the formulation on PLGA degradation in implants formed *in-situ* upon exposure to 2.25 mL phosphate buffer pH 7.4: a) PLGA 502H and b) PLGA 504H. The formulations contained 0.25 % dexamethasone. Mean values +/- standard deviation are indicated (n=3).

With increasing polymer concentration in the liquid formulation the thickness of the polymer "shells" increases (Figure 3.1.7), hence, autocatalysis is likely more pronounced. The experimentally measured PLGA degradation kinetics shown in Figure 3.1.10 clearly confirm this hypothesis: The polymer backbone is more rapidly cleaved at higher PLGA concentrations (open vs. filled symbols). Interestingly, this faster PLGA degradation at higher polymer concentrations is not reflected in the drug release kinetics (Figure 3.1.6), demonstrating the dominance of the thickness of the PLGA shells (the lengths of the diffusion pathways through the polymeric matrices) in this case.

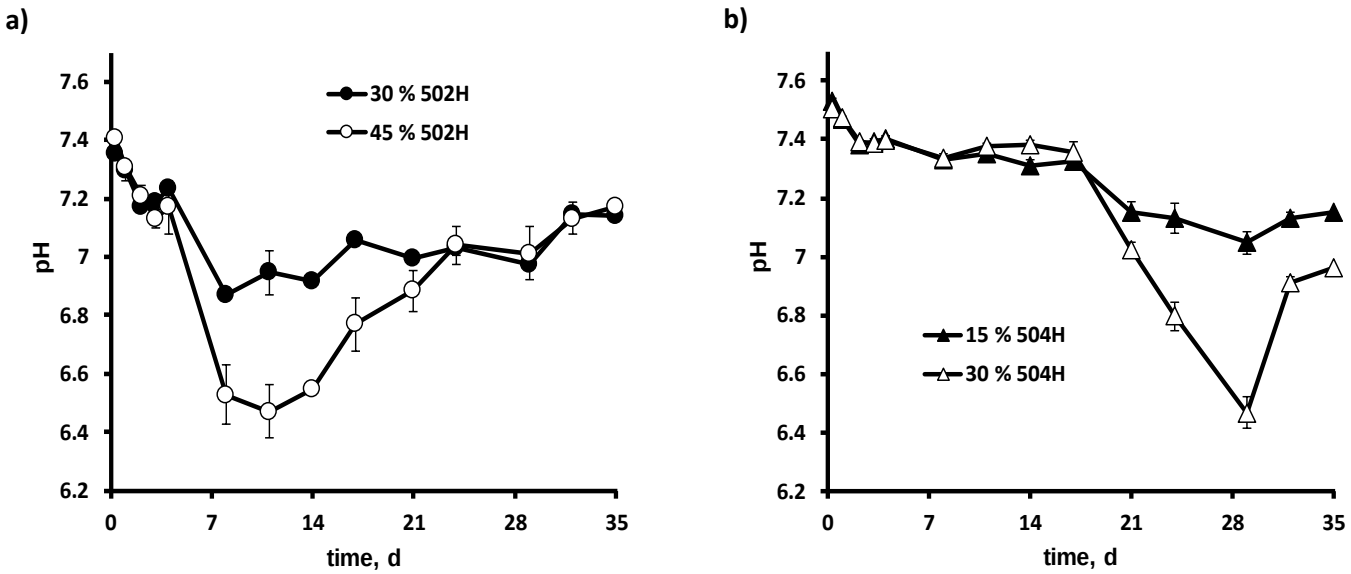

Figure 3.1.11: Effects of the PLGA concentration in the formulation on the dynamic changes in the pH of the release medium surrounding implants formed *in-situ* upon exposure to 2.25 mL phosphate buffer pH 7.4: a) PLGA 502H and b) PLGA 504H. The formulations contained 0.25 % dexamethasone. Mean values +/- standard deviation are indicated (n=3).

Furthermore, the diffusion of the short chain acids out of the implants into the surrounding bulk fluid can lead to a decrease in pH of the latter. As it can be seen in Figure 3.1.11, decreasing pH values of the release medium were indeed observed in all cases. At higher polymer concentrations the "pH drops" were much more pronounced than in the case of lower PLGA concentrations, irrespective of the polymer molecular weight. This can probably be attributed to the fact that thicker polymer "shells" are created at high PLGA concentrations, resulting in more pronounced autocatalytic effects (since the generated short chain acids more slowly diffuse out and bases from the release medium more slowly diffuse in, due to the longer diffusion pathways to be overcome). The potential consequences of (slight) acidifications of the surrounding environment in vivo should be addressed in future studies. The fact that dexamethasone is an anti-inflammatory drug might help minimizing tissue irritation, but caution should be taken when speculating on these aspects based on in vitro data.

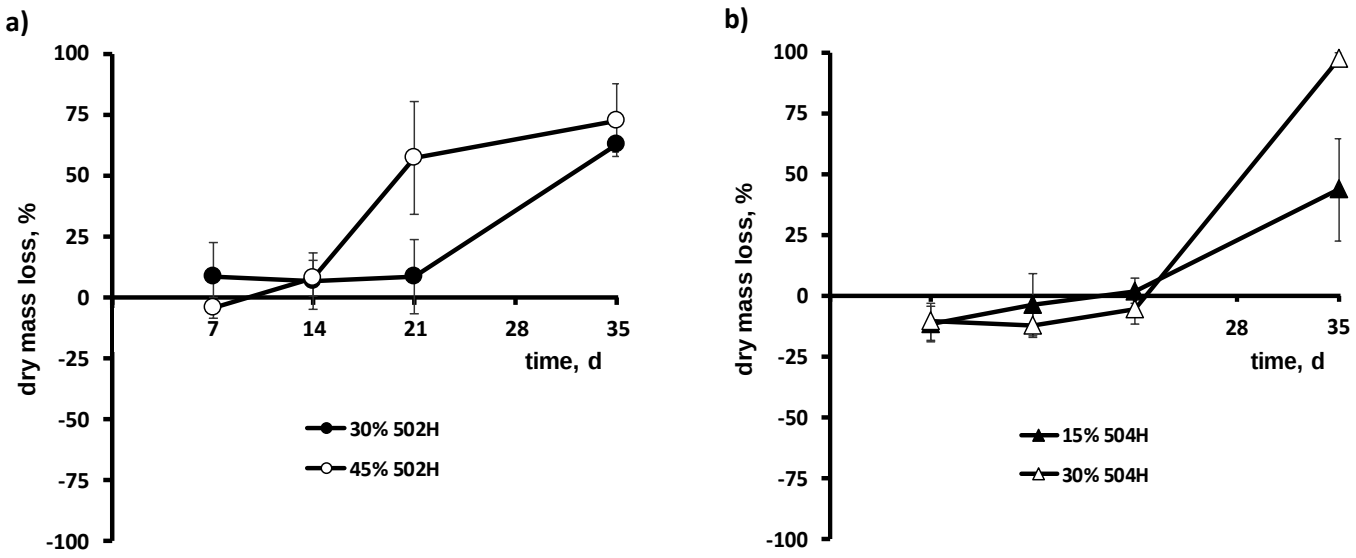

Figure 3.1.12: Impact of the PLGA concentration in the formulation on the dry mass loss of implants formed *in-situ* upon exposure to 2.25 mL phosphate buffer pH 7.4: a) PLGA 502H and b) PLGA 504H. The formulations contained 0.25 % dexamethasone. Mean values +/- standard deviation are indicated (n=3).

Comparing the dynamic changes in the pH values of the surrounding bulk fluids in the case of implants based on Resomer RG 502H and Resomer RG 504H (Figure 3.1.11 a vs. 11b), it can be seen that the "pH drops" occur at later time points in the case of the longer chain PLGA. This can at least partially be attributed to the fact that the initial polymer molecular weight was higher, thus, more time is needed to generate short chain, water-soluble acids, which can diffuse out. Interestingly, the "*clear* pH drops" in the bulk fluid observed at higher polymer concentrations (open symbols in Figures 3.1.11a,b) are followed by distinct increases in the systems' dry mass loss (open symbols in Figures 3.1.12a,b): The dry mass loss nicely reflects the leaching of the shorter chain (water-soluble) acids out of the implants into the release medium.

3.1.5 Conclusion

In-situ forming PLGA-based implants offer an interesting potential for ocular dexamethasone delivery. Importantly, the systems can be expected to be rather robust with respect to variations in the vitreous humor volumes encountered in vivo. Depending on the initial drug loading, drug saturation effects *within* the implants and in the surrounding aqueous medium can play an important role for the control of dexamethasone release. The polymer molecular weight as well as the PLGA concentration in the liquid formulations determine *how* the macromolecules precipitate as well as the extent and rate of system swelling. These are key features, being decisive for the mobility of water, drug, polymer degradation products and bases within the system. For example, they affect the thickness of the polymer shell, water content of the system and importance of local drops in the micro-pH (and, thus, autocatalysis). The inner implant structure and conditions for mass transport within the *in-situ* forming implants determine polymer degradation and drug release.

In the future, the toxicity of the solvent NMP for the ocular tissue as well as the potential consequences of local drops in pH due to leaching of PLGA degradation products should be studied in vivo. It would also be interesting to investigate the effects of the monomer ratio (lactic acid to glycolic acid) of the PLGA as well as the impact of potential additives, altering the formation of the implants and the conditions for mass transport. Such formulation changes might be used to adjust desired release kinetics for given drugs and drug doses during specific target release periods.

Part 2: Often neglected: PLGA/PLA swelling orchestrates drug release - HME implants

The aim of this study was to prepare different types of implants by hot melt extrusion (HME) and to characterize the systems thoroughly before and after exposure to the release medium (phosphate buffer pH 7.4, 37 °C). The lactic acid:glycolic acid ratio was varied (50:50, 75:25, 100:0) as well as the type of monomer (PLGA, PLA). All investigated polymers were amorphous. Dexamethasone was chosen as drug, since it does not act as a plasticizer for PLGA, and is neither acidic nor basic (and does, thus, not accelerate polyester hydrolysis). The idea was to limit the complexity of the underlying drug release mechanisms. Based on these experimental results the role of polymer swelling was to be better understood for the control of drug release from PLGA/PLA-based implants.

3.2.1 Morphology

Table 3.2.1 shows the practical drug loadings and initial dimensions of the investigated implants. All specimen were white, had a smooth surface and uniform appearance. Pictures of representative examples are shown in the top row of Figure 3.2.1.

Table 3.2.1: Dimensions and drug loadings of the investigated dexamethasone implants. Mean values +/- standard deviations are indicated (n=3).

Polymer \ Theoretical drug loading		1 %	2.5 %	5 %	7.5 %	10 %	15 %
PLGA (RG 502H)	Diameter (mm)	1.2 ± 0.0	1.4 ± 0.0	1.3 ± 0.1	1.2 ± 0.1	1.2 ± 0.1	1.2 ± 0.1
	Length (mm)	5.8 ± 0.0	5.8 ± 0.2	5.9 ± 0.2	5.7 ± 0.2	5.8 ± 0.4	5.8 ± 0.3
	Practical drug loading (%)	0.8 ± 0.0	2.3 ± 0.1	4.7 ± 0.1	7.2 ± 0.0	9.1 ± 0.0	13.9 ± 0.3
PLGA (RG 752H)	Diameter (mm)	1.2 ± 0.0	1.1 ± 0.0	1.2 ± 0.0	1.4 ± 0.0	1.2 ± 0.1	1.1 ± 0.0
	Length (mm)	5.4 ± 0.2	5.7 ± 0.1	5.3 ± 0.6	5.6 ± 0.2	5.7 ± 0.2	5.9 ± 0.2
	Practical drug loading (%)	0.9 ± 0.1	2.6 ± 0.1	4.7 ± 0.0	7.3 ±0.1	9.9 ± 0.3	15.0 ± 0.2
PLA (R 202H)	Diameter (mm)	1.2 ± 0.1	1.3 ± 0.1	1.4 ± 0.1	1.3 ± 0.1	1.4 ± 0.0	1.3 ± 0.1
	Length (mm)	5.8 ± 0.1	5.6 ± 0.2	5.7 ± 0.0	5.6 ± 0.3	5.6 ± 0.3	5.6 ± 0.4
	Practical drug loading (%)	1.0 ± 0.1	2.3 ± 0.0	4.8 ± 0.3	7.5 ± 0.1	9.7 ± 0.1	14.8 ± 0.2

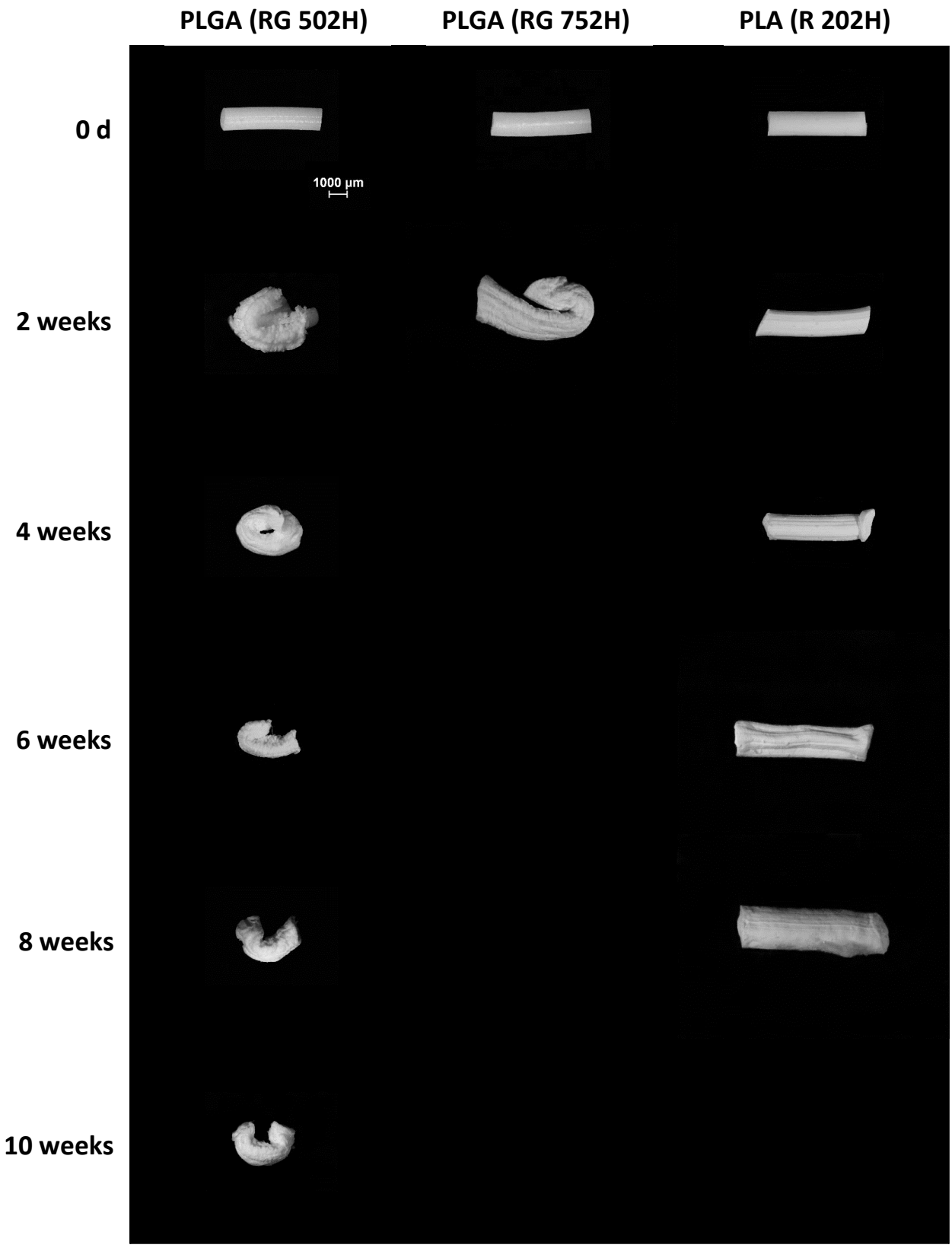

Figure 3.2.1: Macroscopic pictures of implants before and after exposure to phosphate buffer pH 7.4 (in the latter case after freeze drying). The implants contained 10 % dexamethasone. In the case of PLGA RG 752H, the implants became too fragile to be handled after 4 weeks.

3.2.2 PLGA (RG 502H)-based implants

Figure 3.2.2a illustrates the *relative* dexamethasone release rates from implants based on PLGA (RG 502H) (on the right-hand side a zoom on the first 2 weeks is shown). The drug loading was varied from 1 to 15 %. As it can be seen, the relative release rate decreased with increasing initial drug content. This can be attributed to the difference in the 100 % reference value for complete release, since the *absolute* drug release rates were similar prior to drug exhaustion for all drug loadings (Figure 3.2.2b).

Furthermore, during major time periods about constant drug release rates were observed. This might serve as an indication for the fact that limited drug solubility effects *within* the implants are of major importance, combined with perfect sink conditions in the surrounding bulk fluid. Upon water penetration into the systems, the drug is probably only partially dissolved, because the amounts of water within the implants are limited and since the solubility of dexamethasone in aqueous media is low (e.g. 77 +/- 4 µg/mL at 37 °C in phosphate buffer pH 7.4). Thus, dissolved and non-dissolved drug co-exist within the systems. Importantly, only dissolved drug is available for diffusion (non-dissolved drug cannot diffuse). Hence, irrespective of the initial drug content of the implants, saturated dexamethasone solutions likely exist *within* the systems. Released dissolved dexamethasone molecules are rapidly replaced by the partial dissolution of the non-dissolved drug excess. Combined with perfect sink conditions in the surrounding, well-stirred release medium, this results in similar drug concentration gradients in all cases (roughly "*solubility – 0"*). In addition, since the polymer and drug are the same in all cases (and the drug loadings limited), also the drug permeability is likely similar. Consequently, the resulting *absolute* drug diffusion rates (= *absolute* drug release rates) are similar (as long as saturated drug solutions are provided within the implants) (Figure 3.2.2b).

Once all non-dissolved drug excess within the implants is exhausted, released *dissolved* drug molecules are no more replaced and the dexamethasone concentration in the system decreases with time. This leads to decreasing drug concentration gradients (the driving forces for diffusion), and hence, to decreasing absolute and relative drug release rates (Figures 3.2.2a and b). Drug release "levels off", and complete drug release is achieved. With increasing initial drug content, this "drug exhaustion and leveling off" effect occurs at later time points.

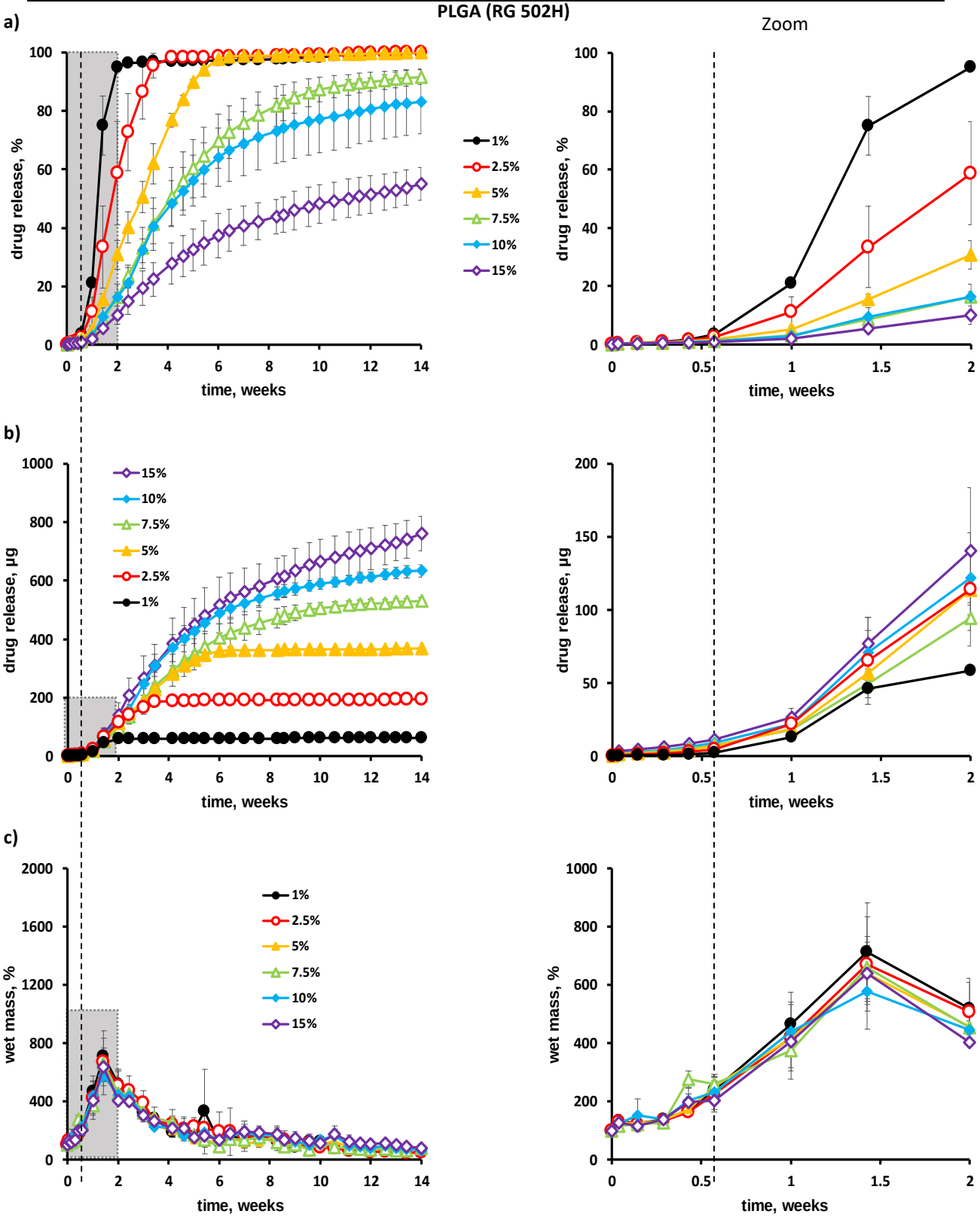

Figure 3.2.2: Impact of the initial drug loading of PLGA (RG 502H)-based implants (indicated in the diagrams) on the resulting: a) *relative* dexamethasone release kinetics, b) *absolute* dexamethasone release kinetics, and c) dynamic changes in the systems' wet mass after exposure to phosphate buffer pH 7.4. Mean values +/- standard deviations are indicated (n=3). On the right-hand side, zooms on early time points are shown (marked in grey on the left-hand side).

Figure 3.2.2c shows the dynamic changes in the implants' wet mass upon exposure to the release medium. Clearly, the wet mass substantially increased up to 1.5 weeks (irrespective of the drug loading), and then decreased again. The initial increase in wet mass is due to the penetration of water into the system, the subsequent decrease results from implant erosion and drug release. Interestingly, a lag time of about 4 d was observed for the onset of drug release (Figure 3.2.3a), irrespective of the initial drug loading. This corresponds to the time point when the water content of the implants substantially increased (Figure 3.2.2c). Hence, it seems that the drug "has to wait" for significant amounts of water to enter the system, before being released. Initially, dexamethasone is effectively trapped within the polymeric matrix. The amounts of water present within the system are not sufficient to allow for noteworthy drug dissolution and diffusion. Only once substantial amounts of water come in, important drug amounts can dissolve and diffuse out (the mobility of the polymer chains increases with increasing water content, resulting in increased drug mobility). This is consistent with the experimentally measured water contents of the implants upon exposure to the release medium (Figure 3.2.3a): After 1 week the implants consist of more than 80 % water. Clearly, a drug can be expected to have a noteworthy mobility in a polymeric system with such a high water content.

Figure 3.2.3b shows the likely reason for this substantial increase in the water content of the PLGA (RG 502H)-based implants after about 4 d: The polymer molecular weight (Mw) decreased from initially about 13-14 kDa to about 8 kDa. Initially, the polymer chains were rather long and, thus: (i) more hydrophobic, and (ii) more intensively mutually entangled. Note that in the case of PLGA with –COOH end groups, the polymer backbone is hydrophobic and the end groups are hydrophilic. The limited amounts of water penetrating into the implants at early time points start cleaving the ester bonds (Figure 3.2.3b). The newly created –COOH groups render the macromolecular network more hydrophilic. In addition, the degree of polymer chain entanglement decreases. As soon as a critical threshold value is reached (roughly around 8 kDa), the hydrophilicity of the PLGA chains becomes sufficiently high to allow substantial amounts of water to enter the system. In addition, the degree of polymer chain entanglement has decreased to such an extent that the network becomes more easily "expandable" (which is also a pre-requisite for substantial swelling). Furthermore, the presence of water-soluble degradation products can be expected to build up a steadily increasing osmotic pressure within the implants, attracting water into the system [19]. The consequence is tremendous implant swelling, e.g. the wet mass increased up to 600-800 % (Figure 3.2.2c). Note that since the chain

length is not 100 % uniform, it is preferable to consider a threshold value “range” rather than a single threshold “value”.

The experimentally measured dry mass loss kinetics and dynamic changes in the pH of the surrounding bulk fluid are consistent with these hypotheses: The substantial decrease in polymer molecular weight is accompanied by the release of water-soluble, short chain acids into the release medium, leading to a clear drop in the pH of the bulk fluid after 4-7 d (Figure 3.2.3d). Furthermore, this time point corresponds to the onset of substantial dry mass loss of the implants (Figure 3.2.3c).

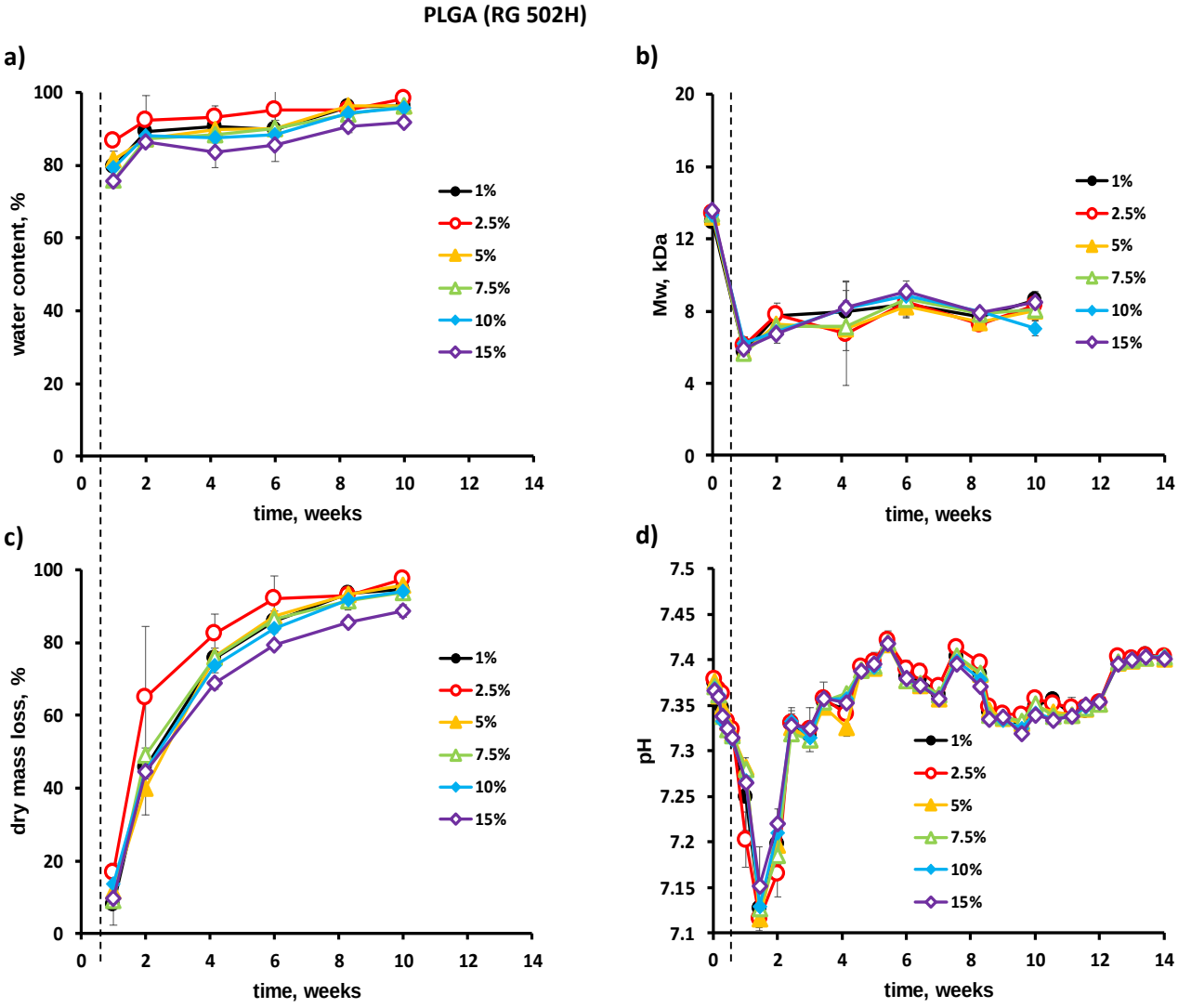

Figure 3.2.3: Impact of the initial drug loading of PLGA (RG 502H)-based implants (indicated in the diagrams) on the dynamic changes in the: a) water content, b) polymer molecular weight, c) dry mass of the systems upon exposure phosphate buffer pH 7.4, and d) pH of the release medium. Mean values +/- standard deviations are indicated (n=3).

3.2.3 PLGA (RG 752H)-based implants

Figures 3.2.4a and b show the *relative* and *absolute* dexamethasone release rates from PLGA (RG 752H)-based implants. In this case, the lactic acid:glycolic acid ratio was 75:25 (compared to 50:50 in the previous section).

Importantly, the same phenomena were observed as in the case of PLGA (RG 502H)-based implants (essentially only the onset of the different events was shifted to later time points):

- During the first 10 d the relative and absolute release rates were close to zero, because the drug was effectively trapped within the polymeric systems: The water contents were limited at this stage (Figure 3.2.5a), resulting in low polymer permeability and limited amounts of water available for drug dissolution (only dissolved drug being able to diffuse). Note that the type of preparation technique (hot melt extrusion) assured non-porous implant surfaces (data not shown). Thus, water and drug transport through pores/cracks with direct surface access was negligible.
- However, the limited amounts of water that could penetrate into the implants caused polymer degradation right from the beginning (Figure 3.2.5b).
- After about 10 d, the polymer molecular weight decreased to the critical polymer molecular weight threshold range around 8 kDa (Figure 3.2.5b): This rendered the PLGA sufficiently hydrophilic to allow for substantial swelling: Important amounts of water came in (Figure 3.2.5a). For example, the implants contained 85 % water after 2 weeks. Thus, the drug could dissolve and became mobile within the polymeric systems: This caused the onset of dexamethasone release.
- Also, short chain acids (which were generated upon PLGA degradation) dissolved in the incoming water and became sufficiently mobile at this time point to diffuse out of the system (due to concentration gradients), into the surrounding bulk fluid: Consequently, the pH of the release medium significantly decreased after 10 d (Figure 3.2.5c).
- Due to the loss of short chain degradation products and due to drug release, the dry mass loss of the implants set on (Figure 3.2.5d).
- Interestingly, these phenomena were virtually independent of the initial drug content (only the 100 % reference value for complete drug release was different). This can at least in part be explained by the fact that dexamethasone is not acting as a plasticizer for PLGA [20] nor is it an acidic or a base (and, thus, does not accelerate ester hydrolysis). Furthermore, the drug loading was relatively limited (1-15 %).

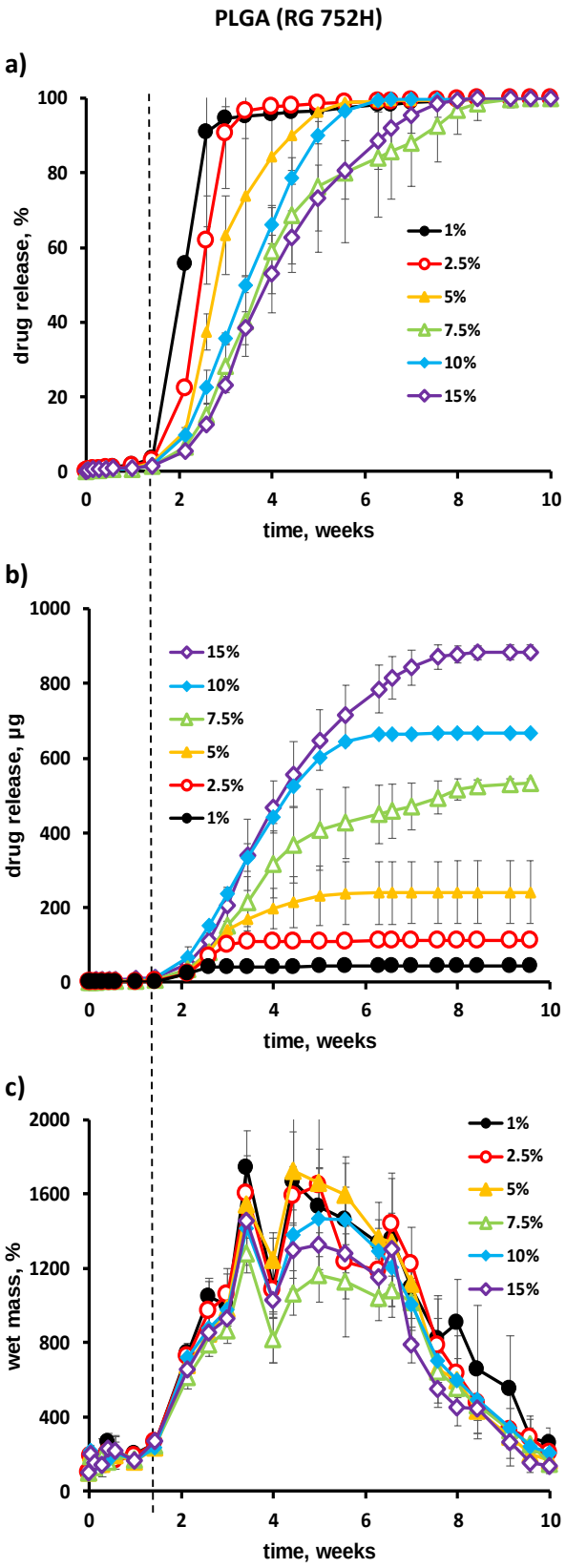

Figure 3.2.4: Impact of the initial drug loading of PLGA (RG 752H)-based implants (indicated in the diagrams) on the resulting: a) *relative* dexamethasone release kinetics, b) *absolute* dexamethasone release kinetics, and c) dynamic changes in the systems' wet mass after exposure to phosphate buffer pH 7.4. Mean values +/- standard deviations are indicated (n=3).

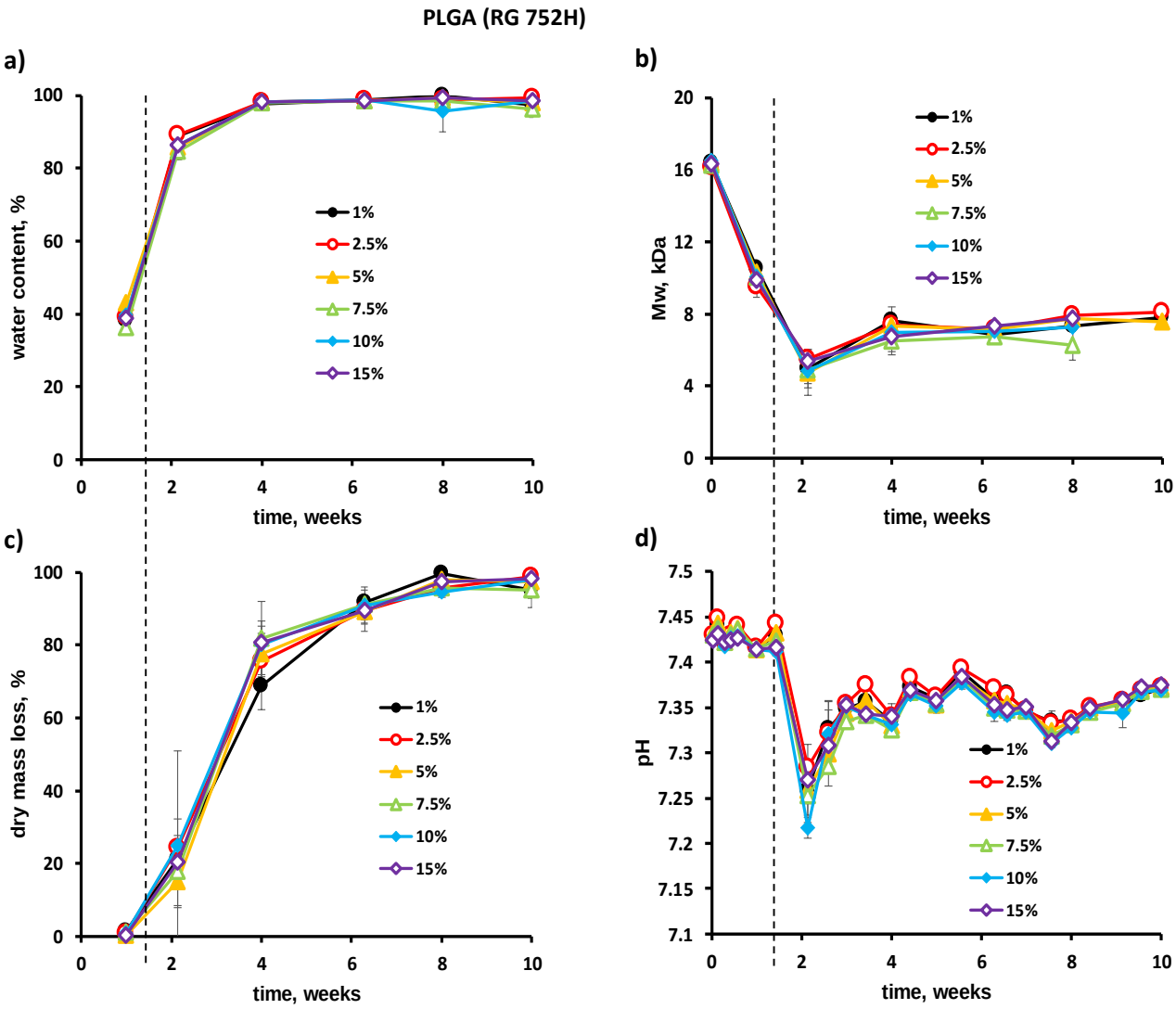

Figure 3.2.5: Impact of the initial drug loading of PLGA (RG 752H)-based implants (indicated in the diagrams) on the dynamic changes in the: a) water content, b) polymer molecular weight, c) dry mass of the systems upon exposure phosphate buffer pH 7.4, and d) pH of the release medium. Mean values +/- standard deviations are indicated (n=3).

The fact that most of these phenomena set on at later time points compared to PLGA (RG 502H)-based implants can at least partially be explained by the fact that: (i) the initial polymer molecular weight was higher (16 vs. 13 kDa), (ii) PLGA (RG 752H) contains more lactic-acid units than PLGA (RG 502H): This renders the polymer more hydrophobic (thus, it is more "difficult" for the water to come in) and slows down the ester bond cleavage. Consequently, the critical polymer molecular weight of around 8 kDa is reached at a later time point (Figure 3.2.5b vs. Figure 3.2.3b), and the onset of system swelling is delayed.

Note that the water content of the implants approached 100 % after 4 weeks (Figure 3.2.5a). Hence, drug mobility can be expected to substantially increase. This explains why the remarkable increase in system dimensions (volume increase up to 1700 %: Figure 3.2.4c; pictures in Figure 3.2.1) did not significantly slow down drug release: The increase in the mobility of dissolved dexamethasone molecules can be expected to "roughly" compensate the increase in the lengths of the diffusion pathways.

3.2.4 PLA (R 202H)-based implants

Figures 3.2.6a and b show the *relative* and *absolute* dexamethasone release rates from PLA (R 202H)-based implants, with an initial drug loading of 1 to 15 %. Again, a clear lag time was observed, coinciding with the lag time for implant swelling (Figure 3.2.6c). As with PLGA (RG 502H) and PLGA (RG 752H), also in the case of PLA (R 202H), the following phenomena occurred:

- Upon contact with the release medium, limited amounts of water penetrated into the implants, causing PLA degradation from the beginning (Figure 3.2.7b).
- As soon as the critical threshold range around 8 kDa was reached (after about 6 weeks), substantial implant swelling set on (Figures 3.2.7b and 6c).
- The tremendous increase in the water content of the system (approaching 100 %, Figure 3.2.7a) allowed for drug dissolution and diffusion. Note that during the first 6 weeks, even up to 60 % water content of the implants did not allow for noteworthy drug release (Figures 3.2.6a and 7a). This value is consistent with those observed with PLGA (RG 502H)- and PLGA (RG 752H)-based implants (e.g., Figures 3.2.3a and 5a).
- In the highly swollen implants also the generated water-soluble short chain acids dissolved and were released into the surrounding bulk fluid, leading to a drop in the pH of the release medium (Figure 3.2.7d) and (together with drug release) to the onset of substantial dry mass loss of the implants (Figure 3.2.7c).

Again, no noteworthy impact of drug loading was observed. Interestingly, and in contrast to PLGA (RG 502H)- and PLGA (RG 752H)-based implants, the cylindrical geometry of the systems was kept during at least 8 weeks (Figure 3.2.1). This might at least partially be attributable to the slower polymer degradation (Figures 3.2.3b, 5b and 7b): The longer the polymer chains, the more they are mutually entangled and the higher is the mechanical stability of the system. The observed deformation of the PLGA (RG 502H)- and PLGA (RG 752H)-based implants during drug release can be attributed to the fact that the implants became deformable and adapted their shape to the geometry of the bottoms of the Eppendorf vials (shaken at 80 rpm).

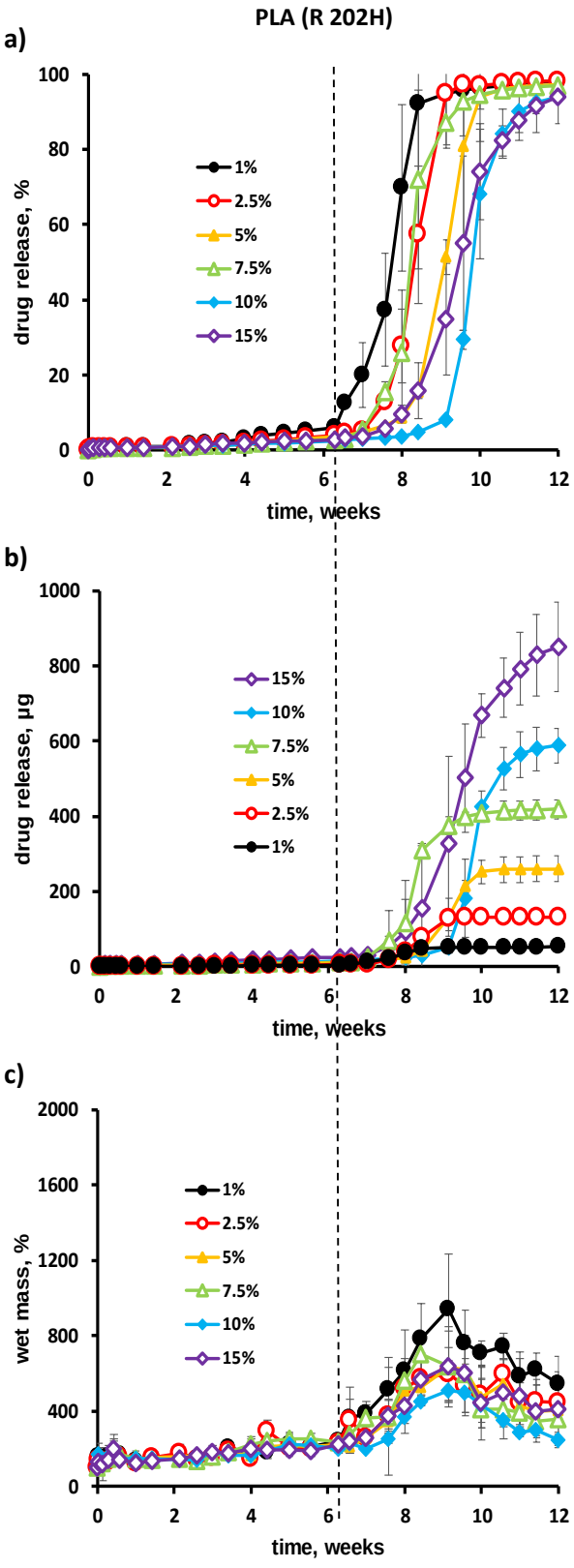

Figure 3.2.6: Impact of the initial drug loading of PLA (R 202H)-based implants (indicated in the diagrams) on the resulting: a) *relative* dexamethasone release kinetics, b) *absolute* dexamethasone release kinetics, and c) dynamic changes in the systems' wet mass after exposure to phosphate buffer pH 7.4. Mean values +/- standard deviations are indicated (n=3).

Furthermore, the onset time point for substantial polymer swelling was delayed compared to (RG 502H)- and PLGA (RG 752H)-based implants (Figures 3.2.2c, 4c and 6c). This can probably at least partially be explained by the fact that PLA (R 202H) contains only lactic acid units, while PLGA contains lactic and glycolic acid units: The additional methyl group in the lactic acid units causes sterical hindrance for hydrolytic ester bond cleavage and renders the system more hydrophobic. Both effects slow down polymer degradation.

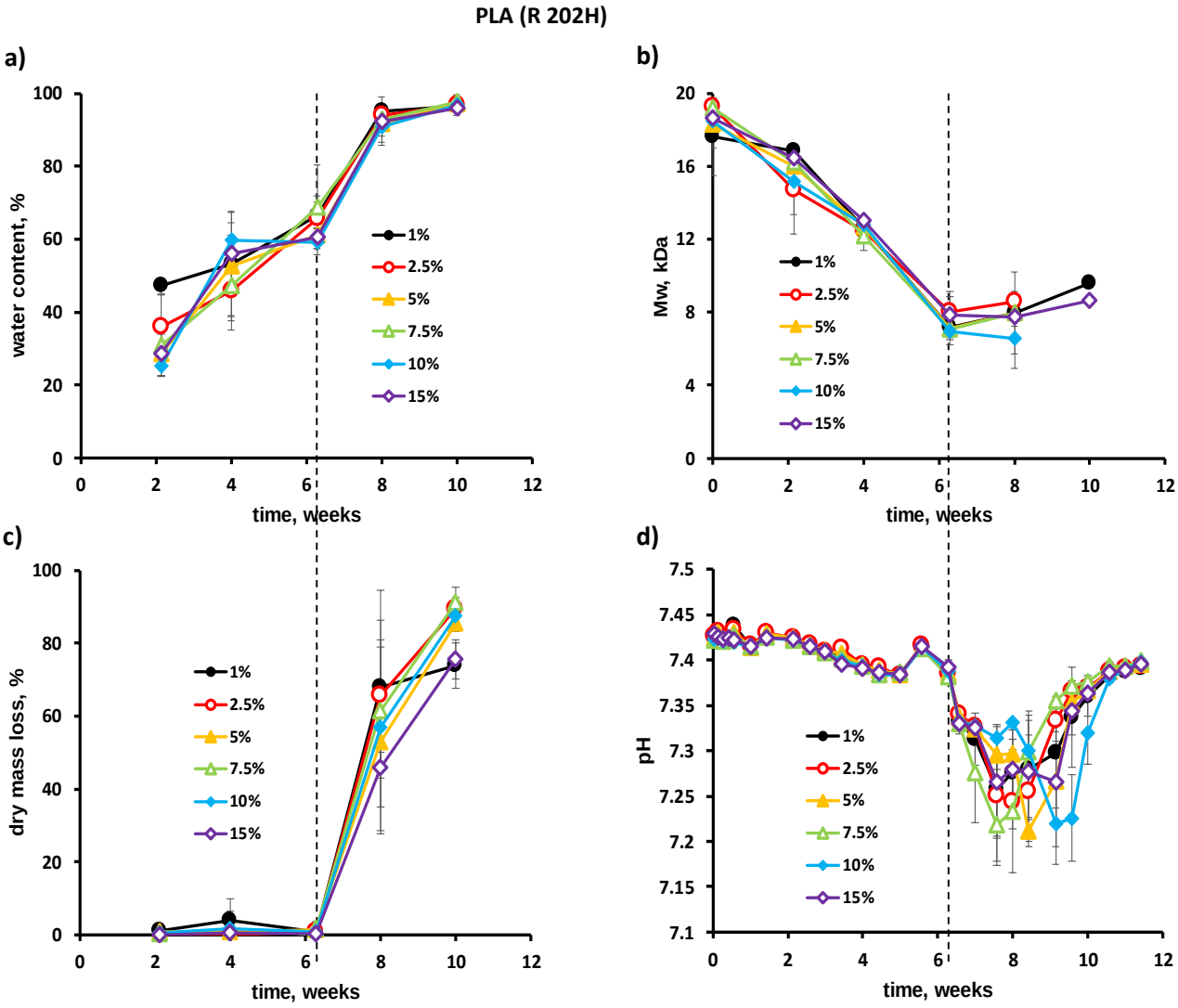

Figure 3.2.7: Impact of the initial drug loading of PLA (R 202H)-based implants (indicated in the diagrams) on the dynamic changes in the: a) water content, b) polymer molecular weight, c) dry mass of the systems upon exposure phosphate buffer pH 7.4, and d) pH of the release medium. Mean values +/- standard deviations are indicated (n=3).

Comparing Figures 3.2.2a, 4a and 6a, it can be seen that the slope of the drug release curves (once dexamethasone release had started) increased in the following ranking order: PLGA (RG 502H) < PLGA (RG 752H) < PLA (R 202H). This is in good agreement with the observed dry mass loss rates of the implants (once dry mass loss had started), which increased in the same ranking order (Figures 3.2.3c, 5c and 7c). The exact reasons for these differences are not yet fully understood. They are likely attributable to the differences in the polymeric structures (type of monomers and monomer ratio) [21]. Potential partial explanations might include the following: In the case of PLGA (RG 502H)-based implants, the resulting water contents even in the fully swollen states are lower compared to PLGA (RG 752H)- and PLA (R 202H)-based systems (Figures 3.2.3a, 5a and 7a). This leads to lower drug and short chain acid mobility. In the case of PLGA (RG 752H) and PLA (R 202H), the water contents in the fully swollen state are close to 100 % (Figures 3.2.5a and 7a). However, the pathways to be overcome are much longer in the case of PLGA (RG 752H)-based implants compared to PLA (R 202H)-based systems, as evidenced by the very high wet mass values (Figure 3.2.4c vs. 6c). Please note that PLGA (RG 752H)-based implants became too fragile to be handled after 4 weeks. This is why no pictures could be taken (Figure 3.2.1), but they increased tremendously in dimensions (visual observation). Longer pathways lead to slower release rates.

3.2.5 The orchestrating role of PLGA/PLA swelling for drug release

The hypothesized drug release mechanisms for the 3 types of PLGA/PLA-based implants are schematically illustrated in Figure 3.2.8. They are valid for all investigated polymers types and drug loadings.

Initially, the drug is effectively trapped within the polymeric matrix. Upon contact with aqueous fluids, limited amounts of water penetrate into the implants (the water contents of the latter does not exceed 60 %). This is because of the hydrophobicity of the PLGA/PLA chains and their intensive entanglement. The amounts of water entering the implants at this stage are not sufficient to allow for significant drug dissolution and mobility: The drug is still effectively trapped and release into the surrounding bulk fluid is negligible. However, the limited amounts of water entering the implants upon exposure to the release medium are sufficient to cause polymer degradation throughout the devices. Hence, the polymer molecular weight decreases and the PLGA/PLA chains become more hydrophilic and less entangled. Also, water-soluble degradation products build up a steadily increasing osmotic pressure, attracting water into the system.

Once a critical threshold range (around 8 kDa) is reached, substantial polymer swelling sets on: The newly created –COOH end groups, lower polymer chain entanglement and generated osmotic pressure lead to water contents exceeding 80-90 % in the implants. Obviously, this represents fundamentally altered conditions for drug release: Considerable amounts of water are now available for drug dissolution and the mobility of dissolved drug molecules is dramatically increased. Due to concentration gradients, the drug diffuses out of the implants into the surrounding bulk fluid: Drug release sets on.

In brief, polymer swelling "orchestrates" drug release: It enables drug release by fundamentally changing the conditions for drug dissolution and diffusion.

As also the mobility of the generated shorter chain acids substantially increases upon PLGA/PLA swelling, also they can diffuse out into the release medium. The loss of these compounds as well as the loss of the drug result in the onset of the dry mass loss of the implants. The time point at which polymer swelling sets on depends on the type of PLGA/PLA.

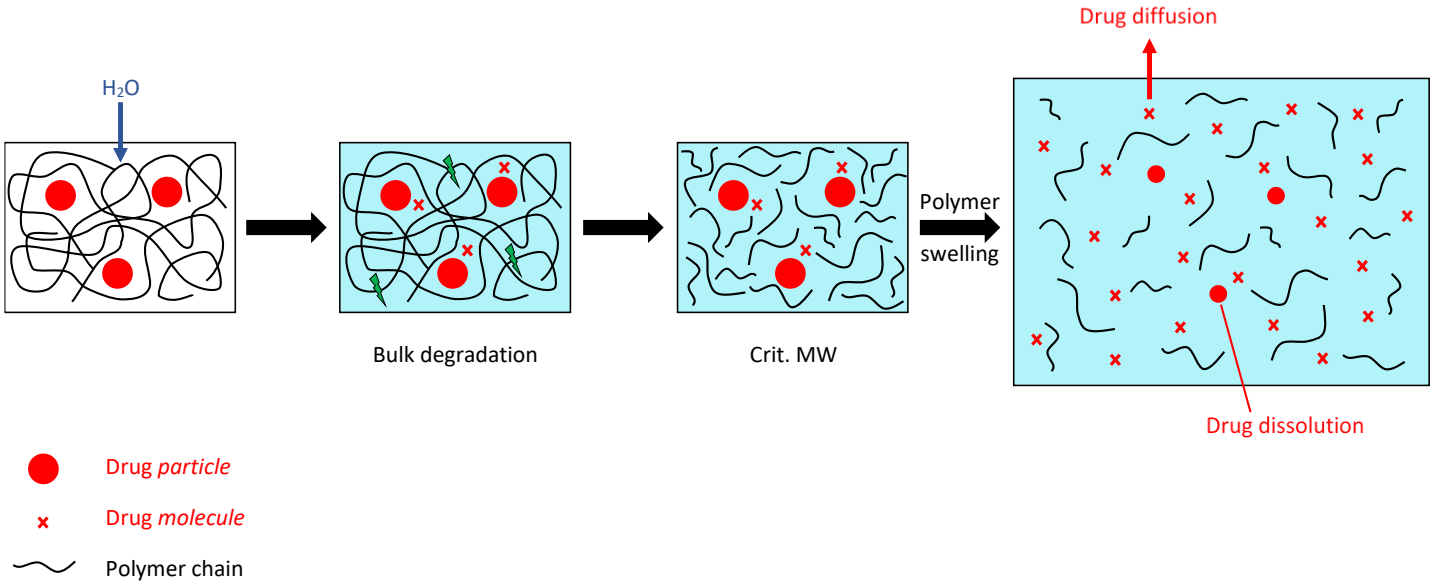

Figure 3.2.8: Schematic presentation of the involved mass transport phenomena involved in the control of drug release from the investigated PLGA/PLA-based implants. Polymer swelling "orchestrates" drug release: after a certain lag time, it fundamentally changes the conditions for drug dissolution and diffusion, and drug release sets on.

3.2.6 Conclusion

PLGA/PLA swelling seems to control the conditions for drug dissolution and diffusion in hot melt extruded implants: Initially, the polymers are too hydrophobic to allow for substantial water penetration into the system. Hence, the drug is not sufficiently mobile to be released. But the limited amounts of water that penetrate into the implants cleave the polyesters. Since the polymer end groups are hydrophilic (-COOH terminated), the PLGA/PLA becomes more hydrophilic over time. Once a critical threshold range around 8 kDa is reached, tremendous amounts of water come in (the water content exceeds 80-90 %). This fundamentally changes the environment of the drug: The latter can dissolve and becomes mobile in the highly swollen implants: Drug release starts. In the future, it will be interesting to study the impact of the type of preparation technique and device design (e.g. geometry and dimensions) on this "orchestrating" role of PLGA/PLA swelling for drug release, which is often neglected.

Part 3: Coloring of PLGA implants to better understand drug release mechanisms

The aim of this study was to use different types of dyes and a colored vitamin to get insight into the underlying mass transport mechanisms from PLGA-based implants. Methylene blue was used as water-soluble dye to stain the release medium. Riboflavin was selected as water-soluble, colored vitamin and incorporated into the implants. And Sudan-III-red was chosen as poorly water-soluble dye and also incorporated into different types of PLGA-based implants. The latter were prepared by hot melt extrusion (HME) or formed *in-situ*, upon injection of a PLGA solution in NMP into phosphate buffer pH 7.4.

3.3.1 Pre-formed (HME) implants

Figure 3.3.1 shows macroscopic pictures of PLGA implants prepared by hot melt extrusion (HME), before and after exposure to a 0.01 % methylene blue solution in phosphate buffer pH 7.4. Surfaces are shown on the left-hand side, cross-sections (obtained by cutting with a heated blade) on the right-hand side. The implants were initially vitamin- and dye-free (opaque cylinders, top row). After exposure to the bulk fluid at 37 °C, the implants were removed at predetermined time points (as indicated) and freeze dried. Note that this latter step at least partially alters the morphology of the systems. Thus, some caution needs to be paid when drawing conclusions based on these pictures. However, it can clearly be seen that the blue dye progressively penetrates into the implants. Importantly, its molecular weight is much higher than that of water (320 vs. 18 Da). Hence, water penetration can be expected to be faster than methylene blue penetration into the PLGA implants.

As it can be seen on the right-hand side of Figure 3.3.1, a shell of swollen PLGA is formed upon contact with the aqueous bulk fluid. Water is known to act as a plasticizer for PLGA [22,19,23]. Consequently, the amorphous polymer “PLGA Resomer RG 502H” (50:50 lactic acid:glycolic acid) undergoes a glassy to rubbery phase transition. Furthermore, the PLGA chains are initially relatively long and hydrophobic. Thus, water penetration into the system is limited and delayed: As it can be seen in Figure 3.3.1 (right-hand side), the thickness of the swollen PLGA shell increases only slowly: On day 3, most of the implant core is still non-swollen. This corresponds to a limited increase in the implants’ wet weight during the first 3 d of exposure to the bulk fluid (blue curve in Figure 3.3.2a).

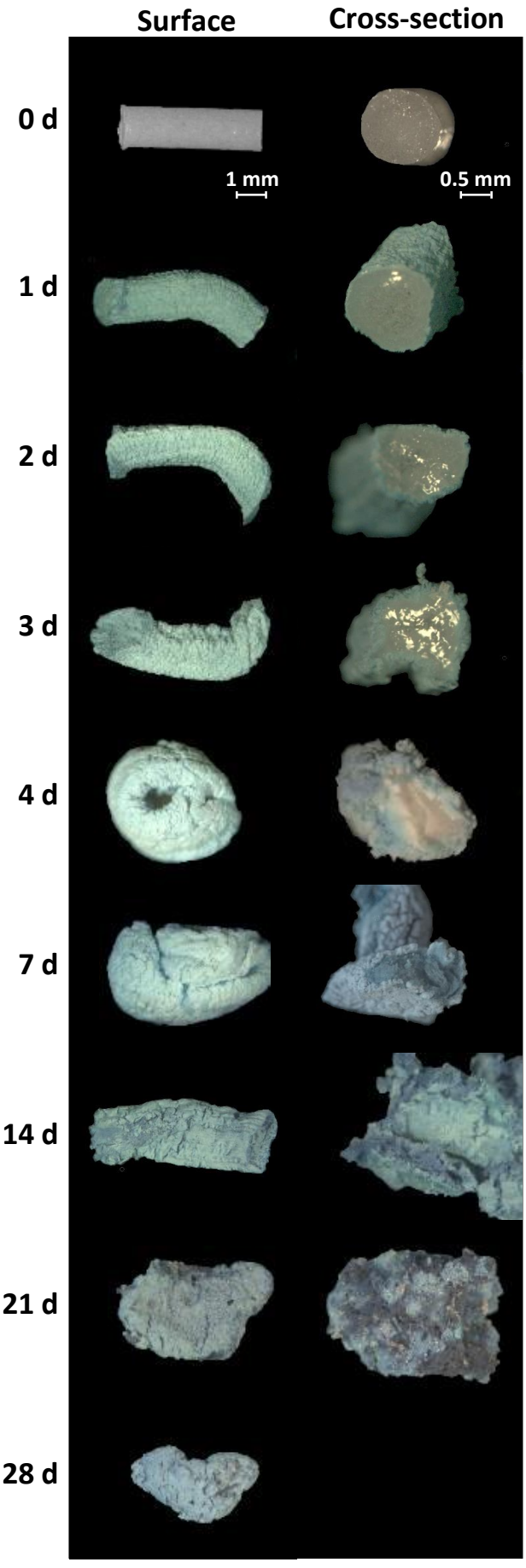

(caption on next page)

Figure 3.3.1: Macroscopic pictures of HME implants (initially vitamin/dye-free) upon exposure to a 0.01 % methylene blue solution in phosphate buffer pH 7.4 for different time periods (as indicated), and subsequent freeze drying. Surfaces are shown on the left-hand side, cross-sections on the right-hand side.

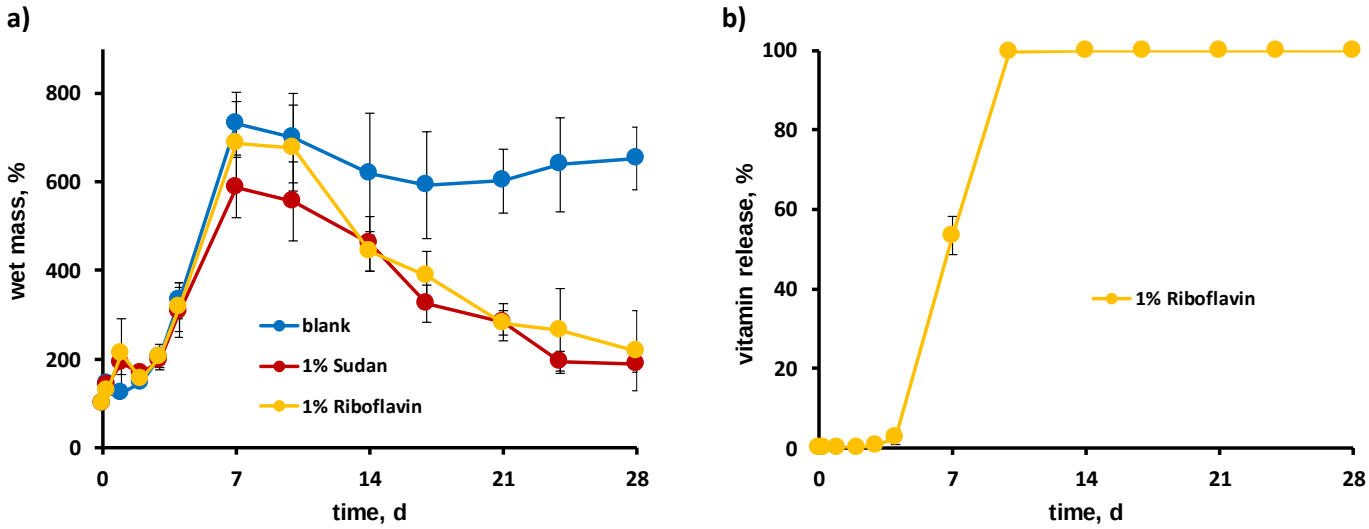

Figure 3.3.2: a) Dynamic changes in the wet mass of HME implants (blank, or loaded with 1 % riboflavin or Sudan-III-red, as indicated), upon exposure to the aqueous bulk fluids. b) Riboflavin release from HME implants (1 % drug loading) in phosphate buffer pH 7.4. Mean values ± standard deviation are indicated (n = 3).

Importantly, afterwards the system takes up *substantial* amounts of water (Figure 3.3.3a). This coincides with the disappearance of the non-swollen implant core and an important increase in system size (Figure 3.3.1). A similar type of swelling behavior (lag time, followed by a substantial increase in the systems' wet weight) has recently also been reported for other types of HME implants, based on PLGA 50:50 (lactic acid:glycolic acid), PLGA 75:25 (lactic acid:glycolic acid) as well as on poly(lactic acid) (PLA) (Part 2). A likely explanation for this behavior is the following: At early time points, the polymeric network is dense, highly entangled and hydrophobic. Thus, the amounts of water that can penetrate into the implants is limited. Nevertheless, small amounts of water can enter the system and start polymer degradation by ester bond cleavage throughout the device ("bulk erosion") [24]. Consequently, the PLGA polymer molecular weight decreases. Since the newly created end groups are hydrophilic (-COOH), the polymer becomes more and more hydrophilic. In addition, the degree of polymer chain entanglement decreases and, thus, the mechanical resistance to substantial system swelling decreases.

Also, water-soluble degradation products are generated, creating a steadily increasing osmotic pressure within the implants. As soon as the system is sufficiently hydrophilic and flexible (e.g. less entangled), implant swelling sets on. This starts at the implants' surface (since the water concentration is highest), but is limited until - after a certain lag time (here about 3 d) – the entire implant starts to substantially swell (Figures 3.3.1 and 2a). The presence of a mechanical stable, non-swollen implant core can also be expected to avoid substantial entire implant swelling, due to steric hindrance. Once the entire implant started swelling, the water content of the system increases tremendously. These very high amounts of water allow the entrapped drug to dissolve and diffuse through the highly swollen system. Briefly, PLGA swelling plays an "orchestrating" role for the control of drug release, determining the onset of noteworthy drug dissolution and diffusion (Part 2). The experimental results obtained in this study using methylene blue to stain the release medium confirm this theory: As it can be seen in Figure 3.3.1, a drug can be expected to be able to dissolve and to be much more mobile in the highly swollen implant (e.g. after 7 d exposure) compared to the relatively dry and non-swollen implant cores during the first 3 d.

Note that the dark blue regions observed at later time points in Figure 3.3.1 are likely artifacts created during freeze drying: Probably, water-filled cavities are formed at these stages. Since methylene blue is water-soluble, it can be expected to be present in these cavities. Upon freeze drying the water is removed, and the dye precipitates.

Figure 3.3.3 shows macroscopic pictures of surfaces and cross-sections of PLGA HME implants, initially containing 1 % riboflavin. This vitamin has a yellow color. The two pictures at the top illustrate the initial homogenous distribution of riboflavin throughout the implants, before exposure to the release medium. Upon contact with phosphate buffer pH 7.4, a swollen PLGA shell forms at the implants' surface, steadily growing. However, the water uptake during the first 3 d remains very limited (Figure 3.3.2a), and a non-swollen core is clearly visible (as in the case of the blank implants exposed to an aqueous methylene blue solution). In this non-swollen implant core, the amount of water available for riboflavin dissolution is very limited and the mobility of dissolved vitamin molecules (or ions) can be expected to be very low. This is why riboflavin release is negligible during the first 3 d (Figure 3.3.2b). But once the critical PLGA polymer molecular weight is reached, substantial amounts of water penetrate into the system (Figure 3.3.2a), and the entire implant becomes highly hydrated (Figure 3.3.3).

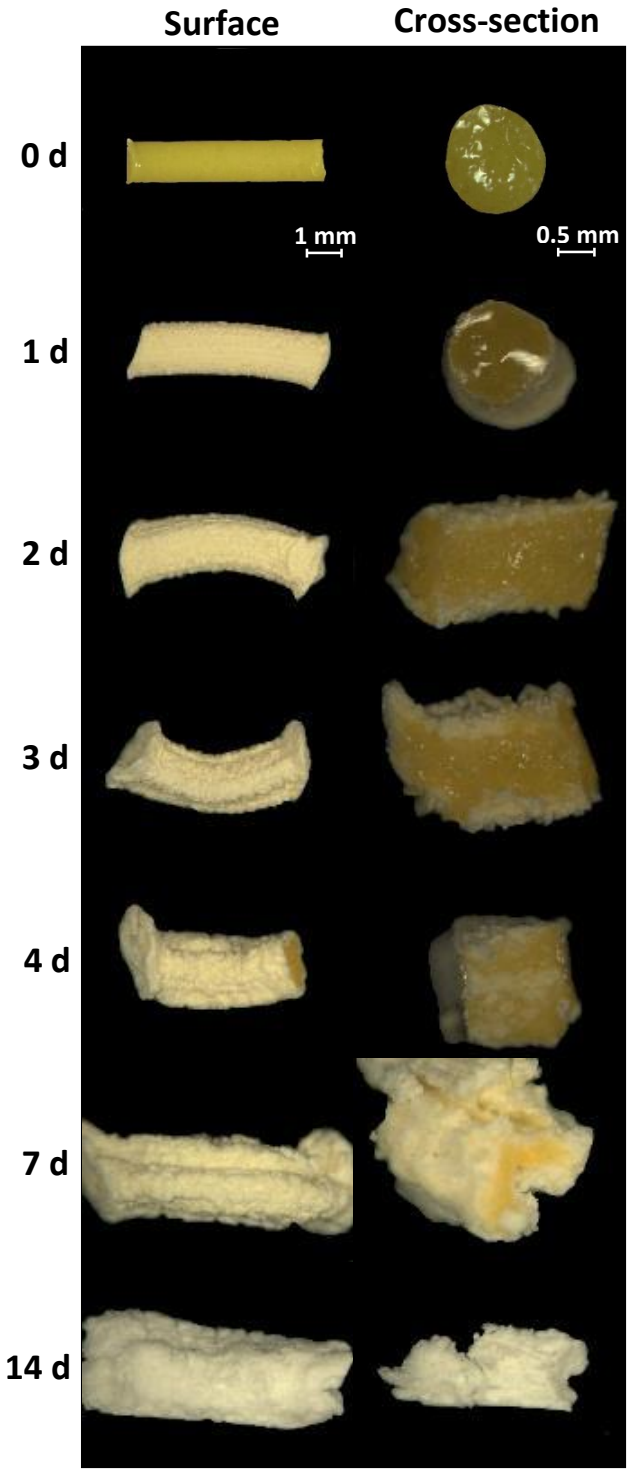

Figure 3.3.3: Macroscopic pictures of HME implants loaded with 1 % riboflavin upon exposure to phosphate buffer pH 7.4 for different time periods (as indicated), and subsequent freeze drying. Surfaces are shown on the left-hand side, cross-sections on the right-hand side.

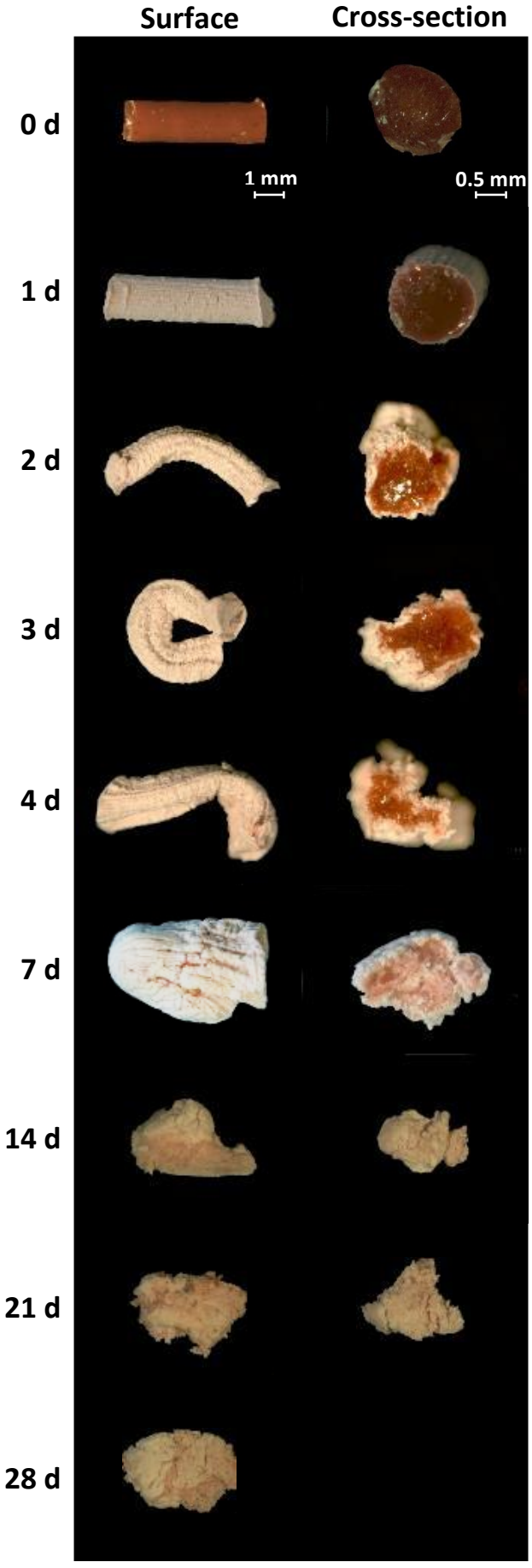

(caption on next page)

Figure 3.3.4: Macroscopic pictures of HME implants loaded with 1% Sudan-III-red upon exposure to phosphate buffer pH 7.4 (containing 0.02% Tween 80) for different time periods (as indicated), and subsequent freeze drying. Surfaces are shown on the left-hand side, cross-sections on the right-hand side.

Under these conditions, the vitamin can dissolve (solubility in phosphate buffer pH 7.4 at 37° C = 165.0 ± 1 µg/mL, but due to acidic micro-climates a much higher local solubility within the implants can be expected). Once dissolved, the vitamin molecules/ions diffuse out of the system in the surrounding bulk fluid, due to concentration gradients. Note that after 7 d exposure to the bulk fluid, the inner parts of the implants were still dark yellow (Figure 3.3.4, right-hand side), whereas the outer regions were bright yellow. This nicely illustrates the vitamin concentration gradients within the systems (which are the driving forces for diffusion).

In addition, Sudan-III-red was used to color HME implants: a poorly water-soluble, lipophilic dye. The two pictures at the top of Figure 3.3.4 show the homogenous initial distribution of this compound in the PLGA implants prior to exposure to the aqueous bulk fluid. In this case, 0.02% Tween 80 was added to the phosphate buffer, to allow for complete dye release within a couple of weeks under the given experimental conditions. Note that the presence of this surfactant might alter the velocity of some of the involved mass transport processes to a certain extent (e.g. water penetration into the system). However, this potential impact is likely limited, as it can be seen in the following: Analogous to the blank and riboflavin-loaded HME implants (Figures 3.3.1-3), during the first 3 d, a swollen polymer shell formed at the cylinders' surface, while the systems' core remained non-swollen. Again, after this lag time, substantial implant swelling set on (Figure 3.3.2a), allowing for Sudan-III-red release into the surrounding bulk fluid. As in the case of riboflavin, vitamin/dye concentration gradients from the core in the direction of the surfaces of the implants were observed, e.g. after 7 d. Thus, also in this case, the "orchestrating" role of PLGA swelling for the control of drug/vitamin/dye release from HME implants could be confirmed visually.

3.3.2 *In-situ* forming implants

Figure 3.3.5 shows pictures of surfaces and cross-sections of blank PLGA implants that formed *in-situ*, upon injection of a solution of "Resomer RG 502H" in N-methyl-pyrrolidone (NMP) into phosphate buffer pH 7.4 containing 0.01 % methylene blue (37 °C). The polymer concentration in the NMP solution was 30 or 45 % (left- and right-hand side), respectively. At predetermined time points, the implants were withdrawn from the bulk fluid and freeze-dried. Again, note that this drying process created artifacts. The cross-sections were obtained by manual breaking, the dashed curves indicate the presence of hollow cavities in the freeze-dried implants. Clearly, cavities were formed at the center of the implants, irrespective of the polymer concentration in the liquid formulations. This can be explained as follows: Initially, the PLGA is dissolved in the NMP. Upon contact with the aqueous phosphate buffer solution, water diffuses into the NMP formulation and NMP diffuses into the aqueous bulk fluid (water and NMP being miscible). Consequently, the solubility of the PLGA in the formulation decreases (not being soluble in water). The decrease in polymer solubility is most important at the interface "formulation – aqueous bulk fluid", since the water content is highest and the NMP content lowest. Consequently, a PLGA shell forms at this interface (Part 1). This shell grows inwards: in the direction of the core of the *in-situ* forming implant. At a certain time point, all PLGA has precipitated and a hollow center remains (the amount of polymer in the formulation is insufficient to entirely fill the implant). The central cavity is initially mainly filled NMP/water mixtures, later with mainly water (in which short chain polymer degradation products, buffer salts and methylene blue are dissolved). At a PLGA content of 45 % in the liquid NMP formulation, more polymer is available to fill the implant compared to the formulations containing only 30 % PLGA. Consequently, the PLGA "walls" of the respective implants are thicker (pictures on the right-hand side in Figure 3.3.5 compared to pictures on the left-hand side). One of the consequences of the thicker implant walls is a lower water penetration rate into the system (dashed vs. solid blue curve in Figure 3.3.6a). Another consequence is a slower methylene blue penetration into the thicker PLGA walls of implants prepared with 45 compared to 30 % polymer content (cross-sections in Figure 3.3.5). [Again, note that water can be expected to be more mobile than the dye, due to the difference in molecular weight.] It has previously been shown that the thicker PLGA implant walls resulting from higher polymer concentrations also lead to more pronounced autocatalytic effects and accelerated PLGA degradation (Part 1).

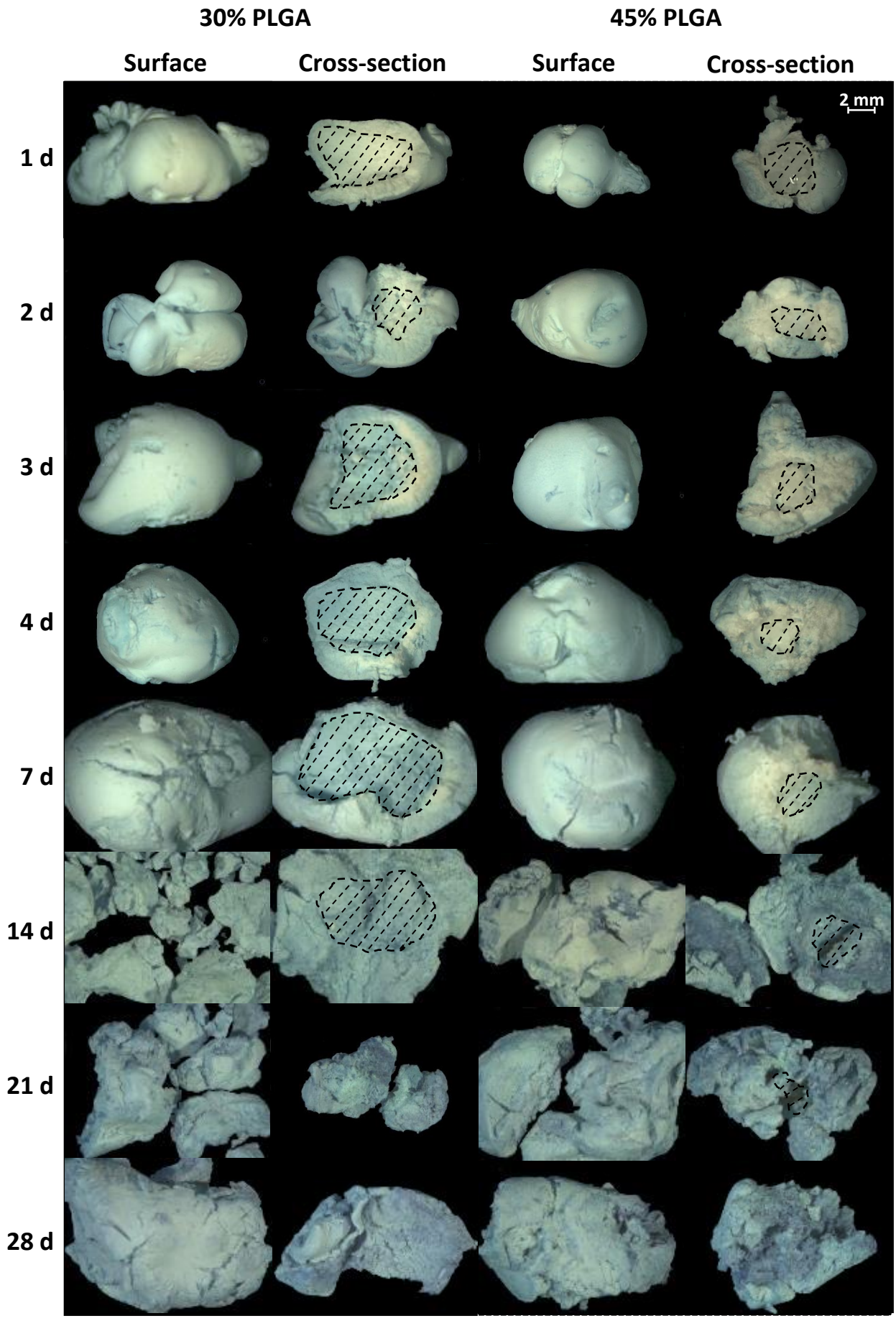

(caption on next page)

Figure 3.3.5: Macroscopic pictures of (vitamin/dye-free) implants formed *in-situ* upon exposure to a 0.01 % methylene blue solution in phosphate buffer pH 7.4, and subsequent freeze drying. The time periods of exposure are indicated on the left-hand side. Surfaces and cross-sections are shown. The liquid formulations contained 30 or 45 % PLGA RG 502H (left- and right-hand side).

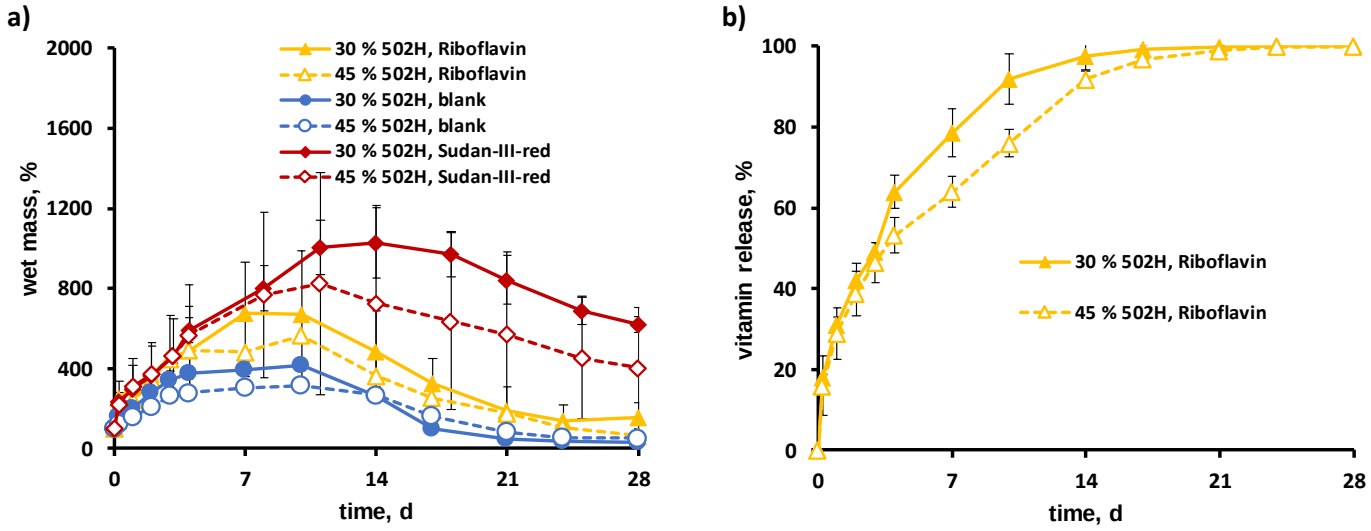

Figure 3.3.6: a) Dynamic changes in the wet mass of *in-situ* forming implants: blank, or loaded with 1 % riboflavin or Sudan-III-red (as indicated) upon exposure to aqueous bulk fluids. b) Riboflavin release from *in-situ* forming implants (1 % vitamin loading) in phosphate buffer pH 7.4. The liquid formulations contained 30 or 45 % PLGA RG 502H (as indicated). Mean values ± standard deviation are indicated (n = 3).

Surfaces and cross-section of *in-situ* formed implants loaded with 1 % riboflavin are shown in Figure 3.3.7. The PLGA content of the NMP solution was 30 and 45 % (left- and right-hand side). Again, a clear difference in implant wall thickness was observed, confirming the above described hypotheses. Furthermore, the implants' central cavities were initially dark yellow, because the water (at early time points also NMP) was (were) removed during freeze drying, leading to artificial riboflavin precipitation. The thicker PLGA walls also slowed down vitamin release: As it can be seen in Figure 3.3.6b, riboflavin release was slower at 45 % polymer content of the NMP formulation compared to 30 %. This is also consistent with the cross-sections overserved after 14 d (Figure 3.3.7, difference in the intensity of the yellow color in the implants), and with the reduced water uptake rates and extents of the implants at higher PLGA concentrations (dashed vs. solid yellow curves in Figure 3.3.6a).

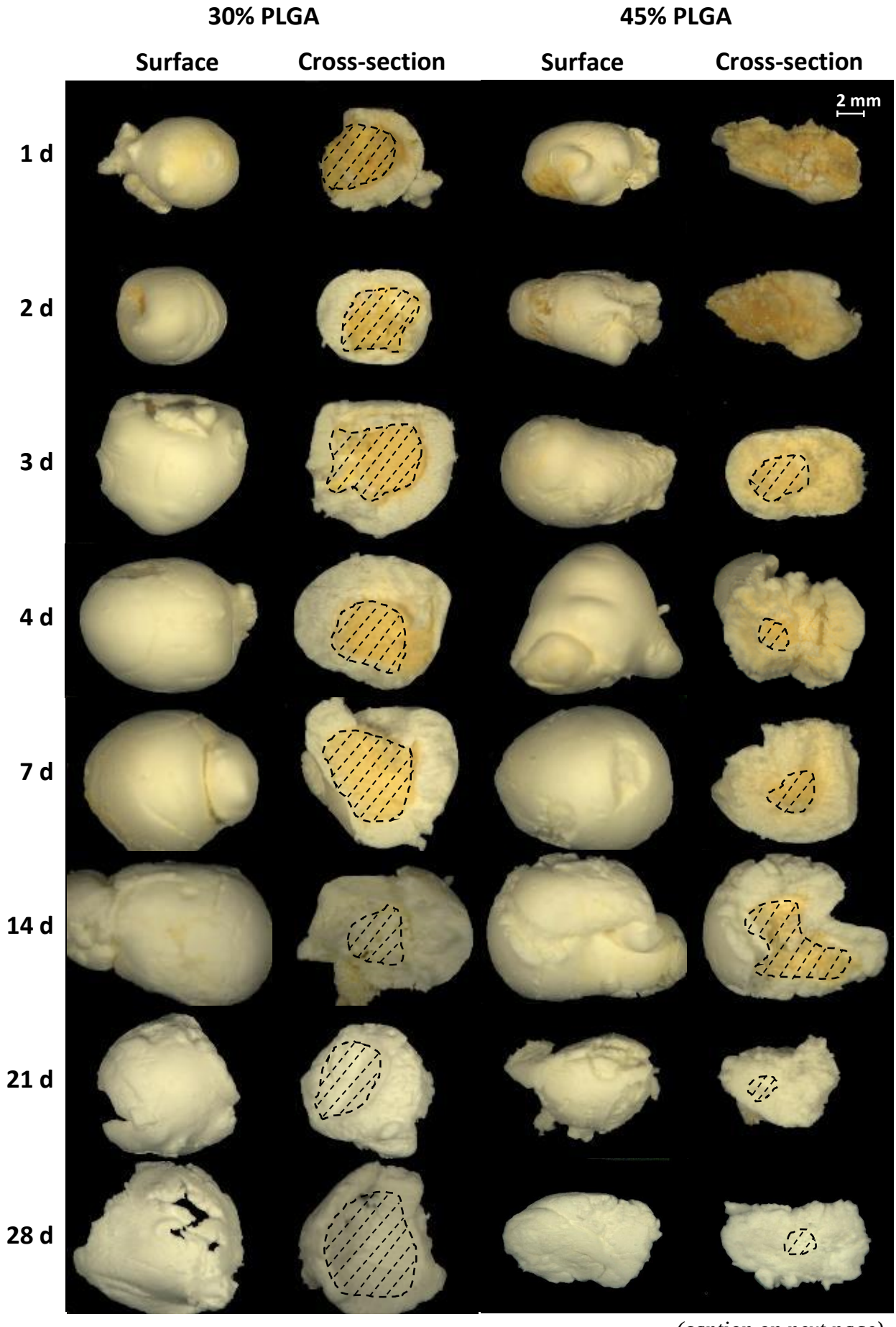

(caption on next page)

Figure 3.3.7: Macroscopic pictures of implants loaded with 1 % riboflavin formed *in-situ* upon exposure to phosphate buffer pH 7.4, and subsequent freeze drying. The time periods of exposure are indicated on the left-hand side. Surfaces and cross-sections are shown. The liquid formulations contained 30 or 45 % PLGA RG 502H (left- and right-hand side).

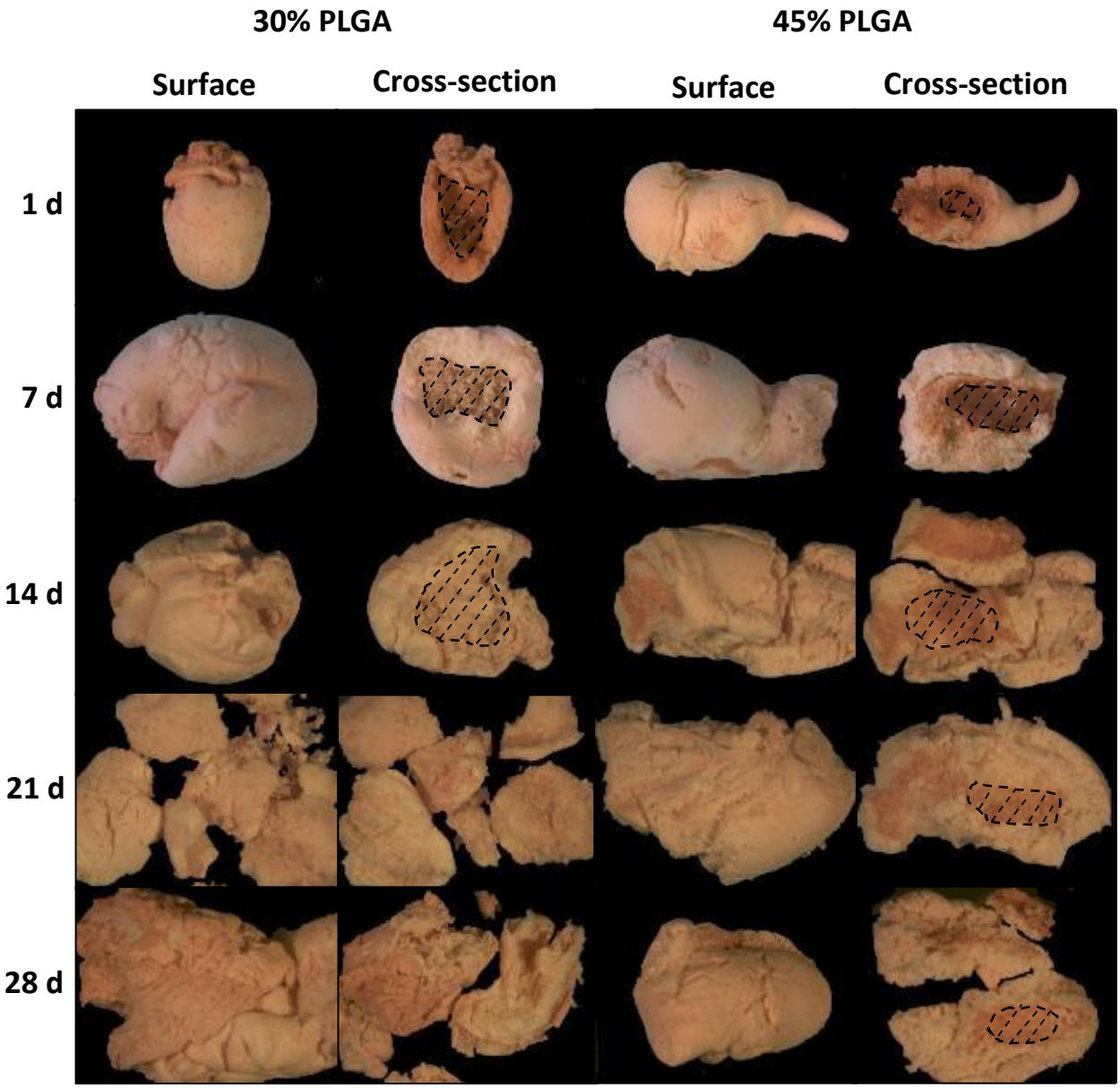

Figure 3.3.8: Macroscopic pictures of implants loaded with 1 % Sudan-III-red formed *in-situ* upon exposure to phosphate buffer pH 7.4, and subsequent freeze drying. The time periods of exposure are indicated on the left-hand side. Surfaces and cross-sections are shown. The liquid formulations contained 30 or 45 % PLGA RG 502H (left- and right-hand side).

These tendencies were further confirmed with *in-situ* forming implants loaded with Sudan-III-red: Figure 3.3.8 shows surfaces and cross-sections of implants formed upon injection of a solution of PLGA (30 or 45 %) and dye (1 %) in NMP into phosphate buffer pH 7.4 (containing 0.02% Tween 80 to facilitate the release of this poorly water-soluble dye under the given experimental conditions). The thicker implants walls obtained with formulations containing 45 % PLGA slowed down dye release, as indicated by the red color remaining for longer time periods within these implants compared to systems obtained with formulations containing only 30 % PLGA. Again, the thicker walls also reduced the extent and the rate at which water penetrated into the implants (dashed vs. solid red curves in Figure 3.3.6a).

Thus, in all cases, the use of dyes in the formulations or in the release medium as well as the use of a colored vitamin could help visualizing the mechanisms of *in-situ* implant formation and help to better understand the impact of the composition of the liquid formulations on the key properties of the implants, including their swelling and release behavior.

3.3.3 Conclusion

The results obtained in this study with dyes and a colored vitamin allowed getting further insight into the mechanisms controlling drug release from PLGA-based implants. In the case of preformed, hot melt extruded implants, the orchestrating role of PLGA swelling for the control of drug release could be visualized. In the case of *in-situ* forming implants based on solvent exchange, the impact of the liquid formulation's composition on the systems' key properties could be better understood. This knowledge can help facilitating: (i) the optimization of PLGA-based implants (and most likely also of other biodegradable controlled release dosage forms), and (ii) the explanation of sometimes surprising tendencies observed with PLGA-based drug delivery systems in vitro and in vivo.

Part 4: *In-situ* forming PLGA implants: How additives affect swelling and drug release

The aim of this study was to investigate the effects of adding small amounts of a variety of additives [crosslinked poly(acrylic acid), poly(ethylene glycol), hydroxypropyl methylcellulose, stearic acid and acetyltributyl citrate] on the key features of *in-situ* forming PLGA implants loaded with dexamethasone. N-methyl-pyrrolidone (NMP) was used as water-miscible solvent. The implants formed upon exposure to phosphate buffer pH 7.4. Dynamic changes in the implants' wet mass were measured gravimetrically, the pH of the release medium was monitored as well as NMP leaching and drug release. In addition, the implants' inner and outer morphology was studied, using optical and scanning electron microscopy.

3.4.1 Carbopol

In the case of Carbopol, only 0.5, 1 and 3 % additive were investigated, since formulations containing 5 % Carbopol were too viscous to be injected. The percentages refer to the total formulation mass (polymer + drug + additive + NMP). As it can be seen in Figure 3.4.1 (top row), the addition of these small amounts of Carbopol (PLGA content = 40 %) fundamentally altered the morphology of the *in-situ* formed implants. Optical macroscopy pictures of cross-sections of systems formed after 3 d exposure to the release medium and subsequent freeze-drying are shown (the cross-sections were obtained by manual breaking). In the case of 1 % Carbopol content, highly porous (and fragile) systems were observed. At 3 % Carbopol content, the implants already started disintegrating into smaller fragments at this time point. Importantly, this disintegration was already observed prior to the freeze-drying. In contrast, much denser (and mechanically stronger) implants were formed in the absence of Carbopol (picture at the very top in Figure 3.4.1). Note that some caution needs to be paid, since freeze-drying can create artefacts.

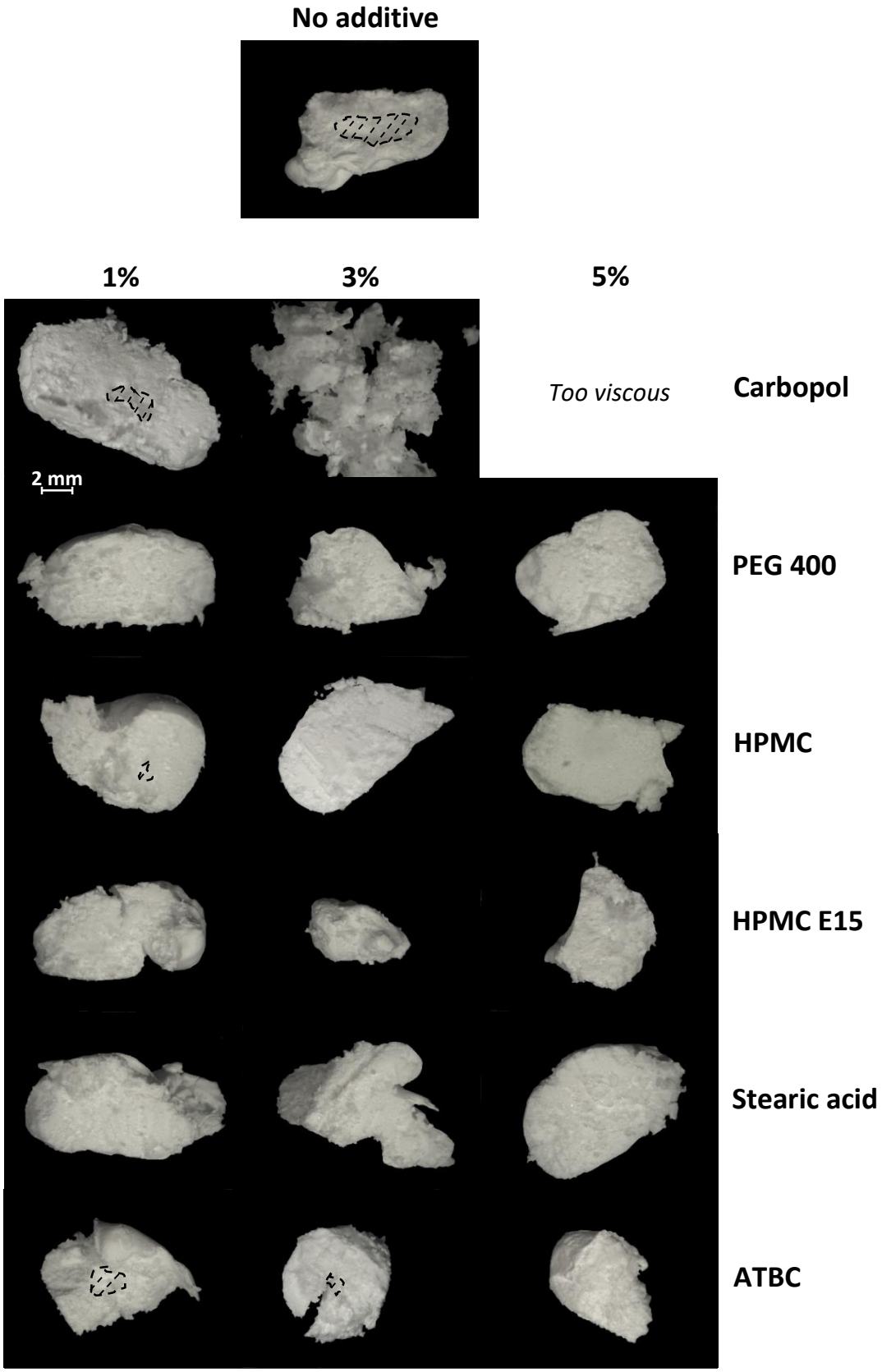

Figure 3.4.1: Macroscopic pictures of cross-sections of *in-situ* formed implants after 3 d exposure to phosphate buffer pH 7.4 (and subsequent freeze-drying). Optionally different concentrations of additives were added (as indicated). The dashed curves indicate the presence of hollow cavities. Note that formulations containing 5 % Carbopol were too viscous to be injected.

The impact of the addition of Carbopol can be explained by the hydrophilicity of this cross-linked poly(acrylic acid) and its considerable swelling capacity in water at neutral pH: The polymer attracts important amounts of water into the system (Figure 3.4.2a), accelerating implant disintegration (Figure 3.4.1). Consequently, drug release is facilitated (Figure 3.4.2b): the drug is more mobile and the diffusion pathways to be overcome are shorter (since the systems disintegrate into smaller fragments). Also, the neutralization of the short chain acids generated upon PLGA degradation can be expected to be faster in these highly porous and rapidly disintegrating implants. Hence, the importance of autocatalytic effects is likely reduced, resulting in less pronounced drops in the pH of the release medium (Figure 3.4.2c). Furthermore, the addition of 3 % Carbopol slightly accelerated the leaching of NMP into the surrounding bulk fluid (Figure 3.4.2d). The impact of the addition of 3 % Carbopol on the inner and outer morphology of implants formed after 3 d contact with the release medium and subsequent freeze-drying, observed by scanning electron microscopy, is illustrated in Figure 3.4.3. Again, care should be taken, because the freeze-drying of the highly swollen systems likely created artefacts. Furthermore, the addition of up to 3 % Carbopol had only a very limited effect on the glass transition temperature (Tg) of the implants formed *in-situ* after 3 d exposure to the release medium (Figure 3.4.4, the Tg of the respective Carbopol free implants was 46.5 ± 0.2 °C).

In brief, the addition of small amounts of Carbopol substantially increased the implant porosity and accelerated implant disintegration, but the resulting increase in the drug release rate was only slight/moderate.

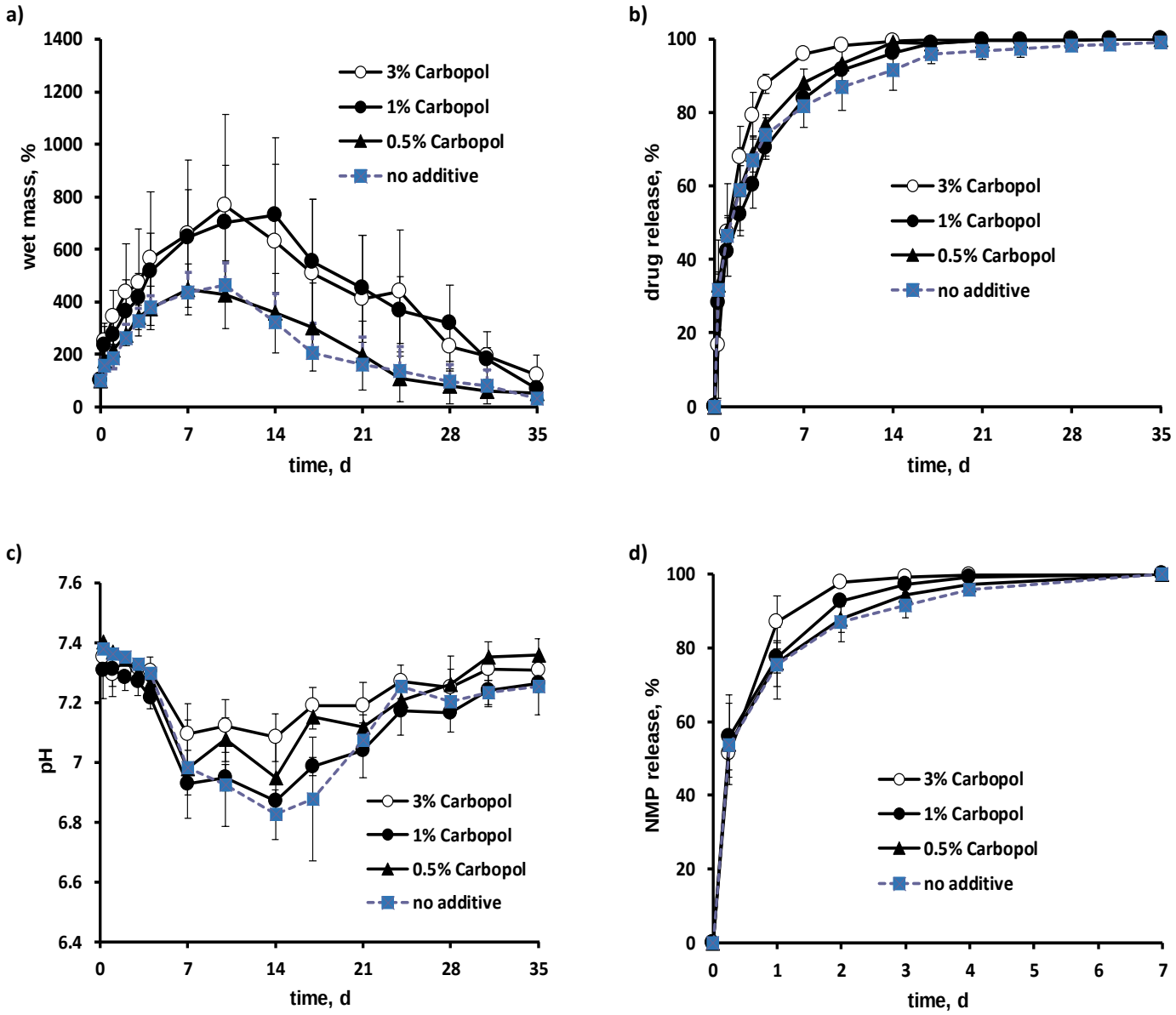

Figure 3.4.2: Impact of the addition of different amounts of Carbopol on the: a) wet mass, b) drug release, c) pH of the release medium, and d) NMP release of/from *in-situ* forming implants upon exposure to phosphate buffer pH 7.4 at 37 °C. Mean values +/- standard deviation are indicated (n=3).

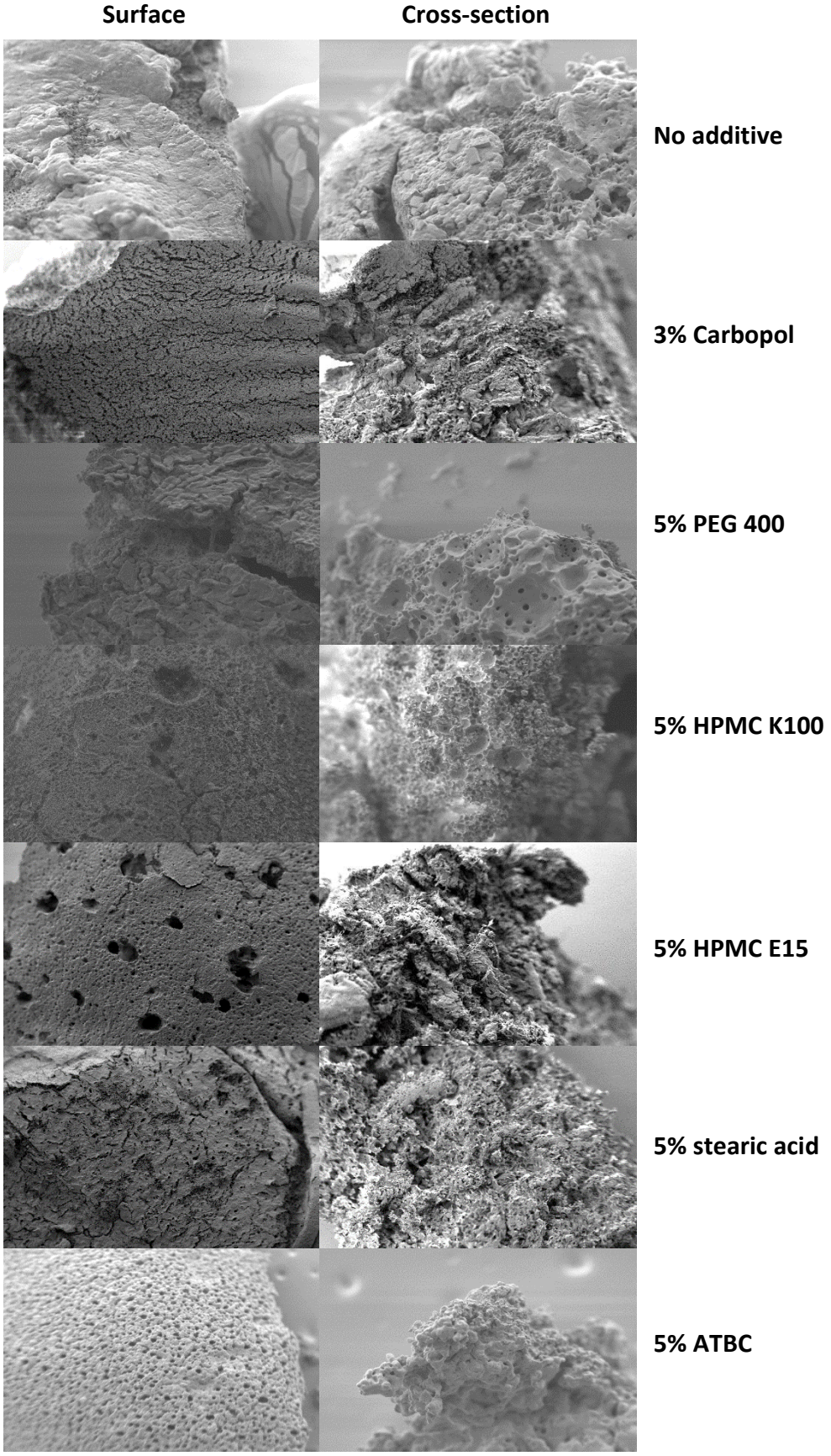

Figure 3.4.3: SEM pictures of surfaces and cross-sections of *in-situ* formed implants after 3 d exposure to phosphate buffer pH 7.4 (upon freeze-drying). Optionally different concentrations of additives were added (as indicated).

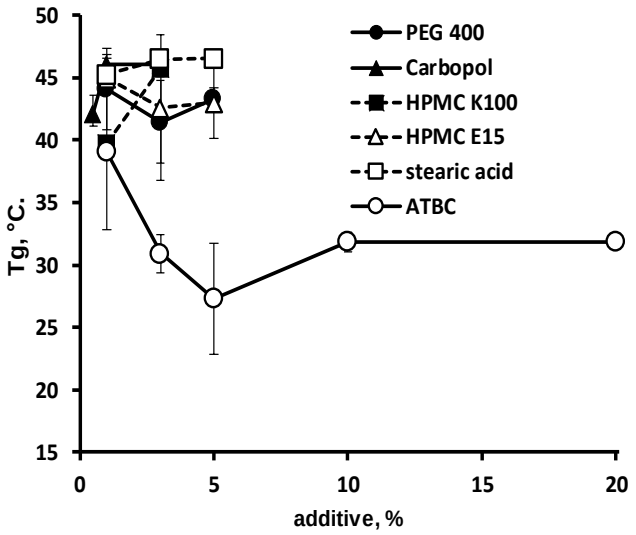

Figure 3.4.4: Impact of the addition of different amounts of additives (indicated in the diagram) on the glass transition temperature (Tg) of *in-situ* formed implants formed after 3 d exposure to phosphate buffer pH 7.4 and subsequent freeze-drying. Mean values +/- standard deviation are indicated (n=3).

3.4.2 PEG 400

Figure 3.4.1 (second row from the top) shows optical macroscopy pictures of cross-sections of *in-situ* formed implants after 3 d exposure to the release medium and subsequent freeze-drying. The systems initially contained 1, 3 or 5 % PEG 400. Importantly, PEG 400 is a water-soluble liquid, and known to act as a plasticizer for PLGA [25]. Since the glass transition temperature (Tg) of the implants formed in this study after 3 d exposure to the release medium (and subsequent freeze-drying) were rather similar to the Tg of PEG free implants obtained under the same conditions, it can be hypothesized that major parts of the PEG rapidly leached out into the surrounding bulk fluid during implant formation. This is consistent with the numerous pores that are visible in cross-sections of freeze-dried implants (Figure 3.4.3). However, again, note that artefact creation during freeze-drying is likely to occur and conclusions should be viewed with caution. As it can be seen in Figure 3.4.4, the impact of the addition of up to 5 % PEG had only a slight effect (if at all) on the resulting dexamethasone release kinetics, NMP leaching and dynamic changes in the pH of the bulk fluid. There was a slight to moderate increase in the implants' swelling after 7 d, but drug release was almost complete at this stage.

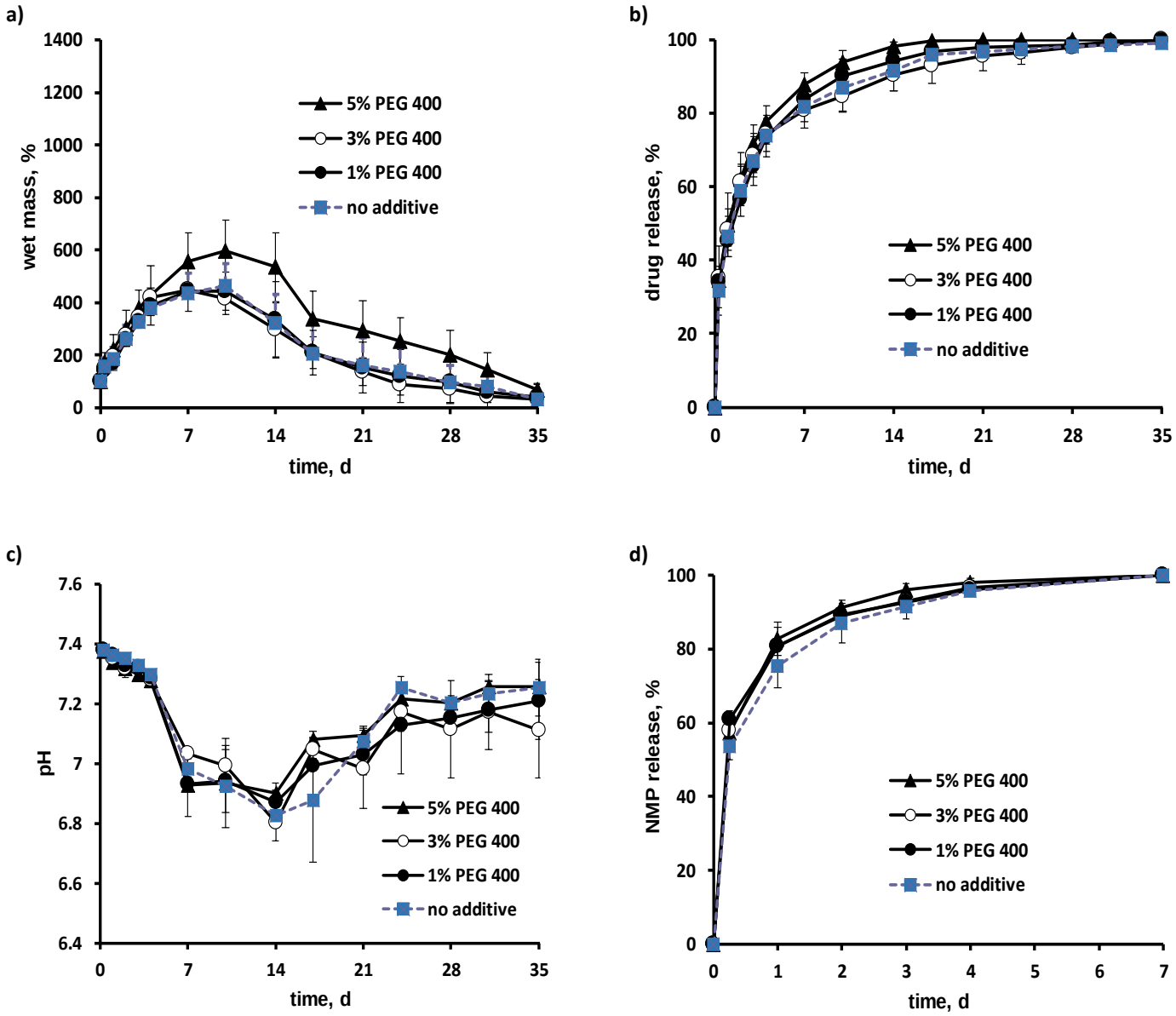

Figure 3.4.5: Effects of the addition of different amounts of PEG 400 on the: a) wet mass, b) drug release, c) pH of the release medium, and d) NMP release of/from *in-situ* forming implants upon exposure to phosphate buffer pH 7.4 at 37 °C. Mean values +/- standard deviation are indicated (n=3).

Thus, the addition of small amounts of PEG 400 to the investigated *in-situ* forming implant formulations was only limited, probably due to rapid PEG leaching into the release medium during implant formation.

3.4.3 HPMC

The impact of the addition of 1, 3 and 5 % HPMC K100 or HPMC E15 (differing in their chain length) on the morphology, swelling and drug release kinetics of/from the investigated *in-situ* forming implants is shown in Figures 3.4.1, 3, 5 and 6. The macroscopic pictures of cross-sections of freeze-dried implants (Figure 3.4.1) indicate relatively dense and intact implants, compared to the Carbopol containing formulations described above. Interestingly, various small holes were visible on the systems' surfaces observed by SEM (Figure 3.4.3). If these holes are not artefacts, they might indicate that HPMC eventually partially precipitated during implant formation at the *aqueous bulk fluid – implant formulation* interface, and subsequently dissolved. But this is just a hypothesis. Being hydrophilic, the presence of the HPMC can be expected to attract more water into the PLGA-based implants (Figures 3.4.5a and 6a), facilitating acid neutralization (generated upon polyester cleavage) and decreasing the importance of the pH drop in the bulk fluid (Figures 3.4.5c and 6c). The impact on NMP release was only very minor, irrespective of the investigated HPMC chain length (Figures 3.4.5d and 6d). Importantly, there is only a slight increase in the dexamethasone release rate in all cases (Figures 3.4.5b and 6b). This effect can at least partially be attributed to the increased water content of the systems (Figures 3.4.5a and 6a). Note that Do et al. recently reported on slightly *de*creasing drug release rates from *in-situ* forming PLGA Resomer RG 502 H-based implants containing doxycycline or metronidazole upon HPMC addition [7,26]. However, the HPMC content in the Do reports was substantially higher. Also, the fact that the glass transition temperature (Tg) of the freeze-dried implants obtained after 3 d exposure to the release medium did not show any substantial difference to HPMC free systems, indicates that the HPMC either already leached out into the bulk fluid and/or phase separated from the PLGA.

Hence, also the addition of small amounts of HPMC did not fundamentally alter the dexamethasone release kinetics and only moderately affected system swelling.

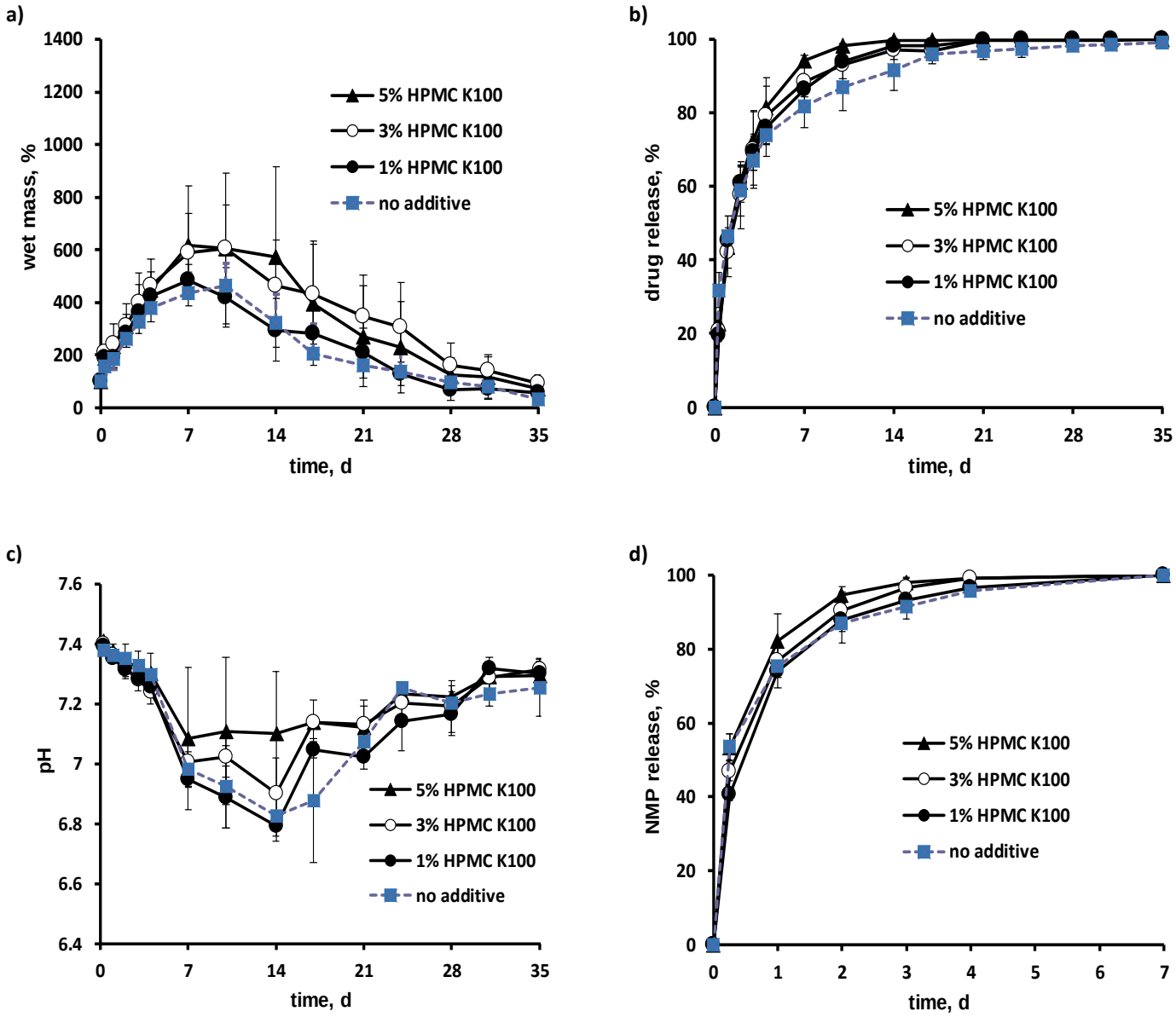

Figure 3.4.6: Impact of the addition of different amounts of HPMC K100 on the: a) wet mass, b) drug release, c) pH of the release medium, and d) NMP release of/from *in-situ* forming implants upon exposure to phosphate buffer pH 7.4 at 37 °C. Mean values +/- standard deviation are indicated (n=3).

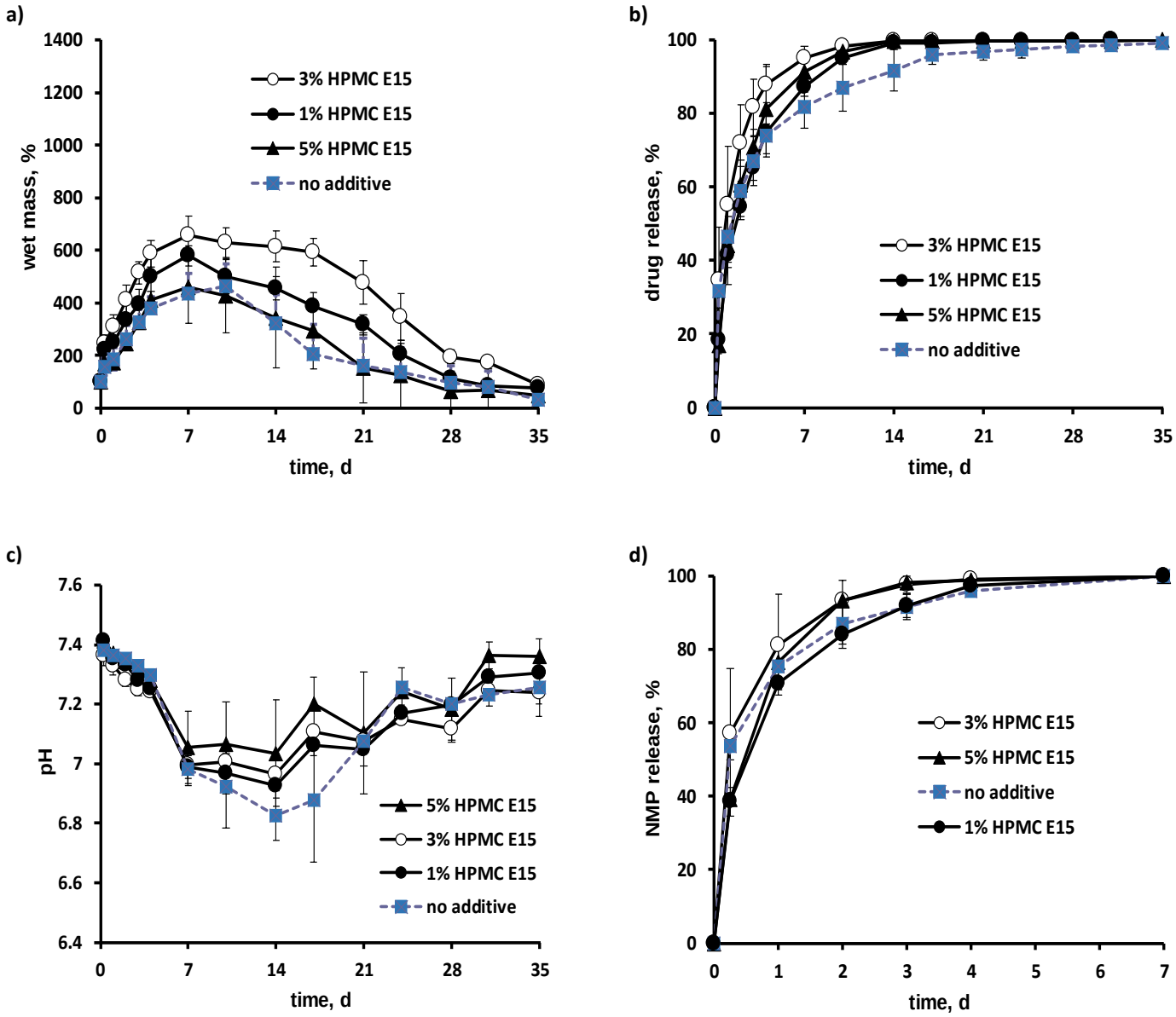

Figure 3.4.7: Effects of the addition of different amounts of HPMC E15 on the: a) wet mass, b) drug release, c) pH of the release medium, and d) NMP release of/from *in-situ* forming implants upon exposure to phosphate buffer pH 7.4 at 37 °C. Mean values +/- standard deviation are indicated (n=3).

3.4.4 Stearic acid

Stearic acid is a saturated fatty acid which is not soluble in water. The addition of 1, 3 or 5 % of this lipophilic compound to the *in-situ* forming implant formulations had a relatively limited impact on the macroscopic morphology of cross-sections of implants formed after 3 d exposure to phosphate buffer pH .4 and subsequent freeze-drying (Figure 3.4.1). The SEM pictures of surfaces (Figure 3.4.3) might indicate that phase separation took place at the *formulation – release medium* interface, but again, great caution should be paid, due to the risk of artefact creation upon sample drying. Interestingly, the wet mass of the implants substantially increased at the highest investigated stearic acid content (5 %), but to a much lesser extent at lower stearic acid contents. The exact reasons for this behavior are not clear, potential plasticizing effects are unlikely (Figure 3.4.4). Importantly, the impact on drug release was limited in all cases, probably because the increasing length of the diffusion pathways was compensated by the increasing amounts of water in the system (water being mandatory for drug dissolution and leading to increased drug mobility). Furthermore, there was is a slight increase in the NMP leaching rate and a slight impact on the dynamic changes in the pH of the release medium upon stearic acid addition (Figure 3.4.8).

Thus, also the presence of up to 5 % lipophilic stearic acid had only a limited effect on dexamethasone release from the investigated *in-situ* forming implants.

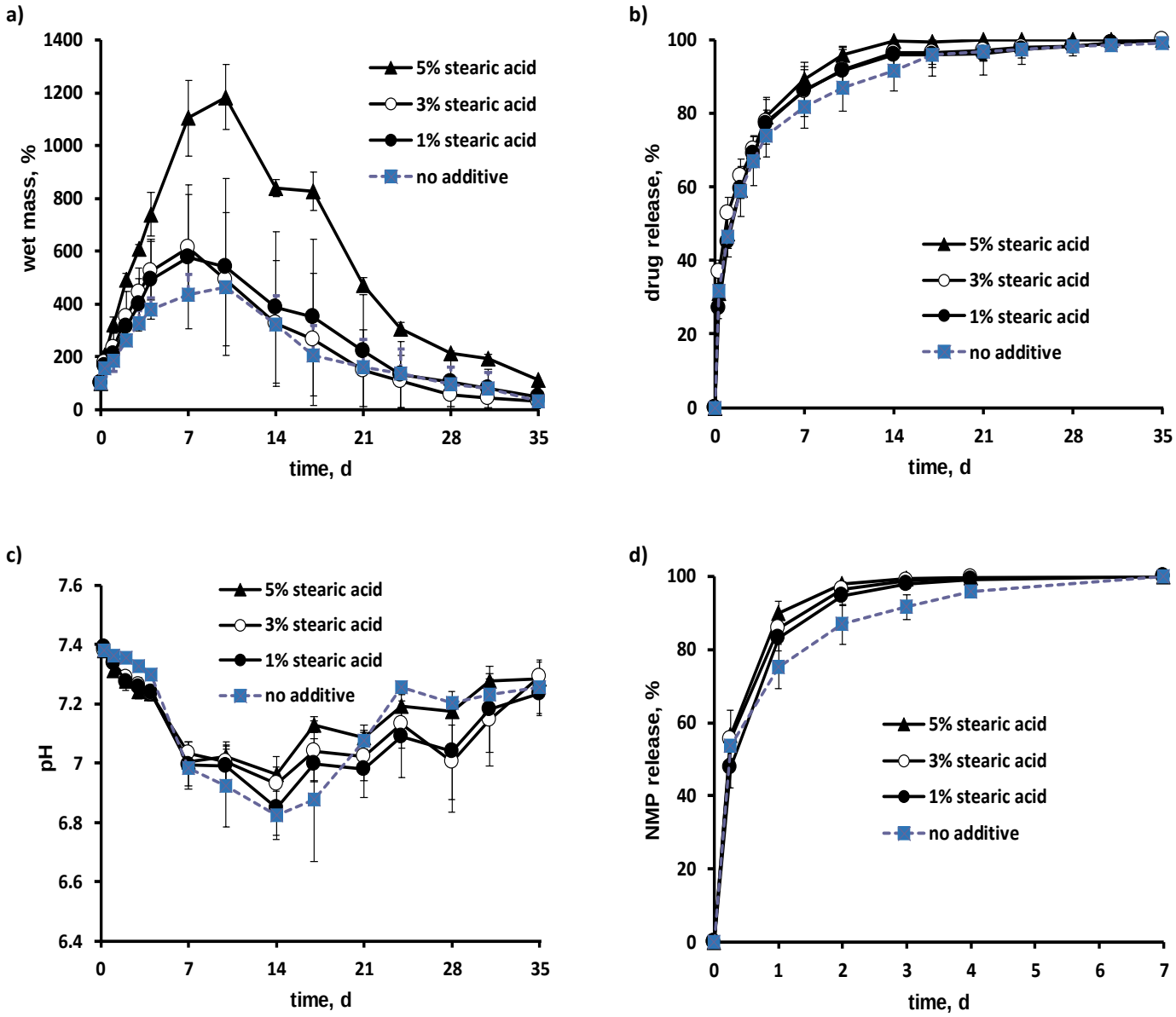

Figure 3.4.8: Impact of the addition of different amounts of stearic acid on the: a) wet mass, b) drug release, c) pH of the release medium, and d) NMP release of/from *in-situ* forming implants upon exposure to phosphate buffer pH 7.4 at 37 °C. Mean values +/- standard deviation are indicated (n=3).

3.4.5 ATBC

ATBC is a liquid with very limited solubility in water. Importantly, it acts as plasticizer for PLGA: As it can be seen in Figure 3.4.4, the glass transition temperature (Tg) of the implants formed after 3 d exposure to the release medium and subsequent freeze-drying, decreased upon ATBC addition. But this was only the case up to about 5 % ATBC. Afterwards, a plateau was reached. Hence, a few percent of ATBC can be expected to be more or less homogenously distributed throughout the PLGA phase. This renders the implants more hydrophobic and reduces their swelling (Figure 3.4.9a). However, higher ATBC contents do not further decrease the Tg of the polymeric phase. Thus, they might phase separate. Interestingly, at 10 and 20 % initial ATBC contents, implant swelling substantially increased (Figure 3.4.9a). The exact reasons for this behavior are unclear. Importantly, at all ATBC loadings the resulting dexamethasone release rates were slightly/moderately slower compared to implants free of ATBC (Figure 3.4.9b). This is at least partially likely due to increased implant hydrophobicity, increased diffusion pathway lengths and plasticizing effects, the relative importance of these phenomena depending on the ATBC content. NMP leaching was not strongly affected. Also the impact of ATBC addition on the dynamic changes in the pH of the release medium were limited. The same was true for the macroscopic morphology of cross-sections of freeze-dried implants: Figure 3.4.1 shows examples for 1-3 % ATBC content. The SEM pictures of surfaces of implants formed upon 3 d exposure to the release medium (and subsequent freeze-drying) showed numerous tiny pores, which might be artefacts or indicate phase separation.

So, ATBC was the only additive in this study, which slightly *de*creased the resulting dexamethasone release rate from the investigated PLGA implants forming *in-situ*. It was also the only additive, which decreased the swelling of the implants, at low ATBC contents.

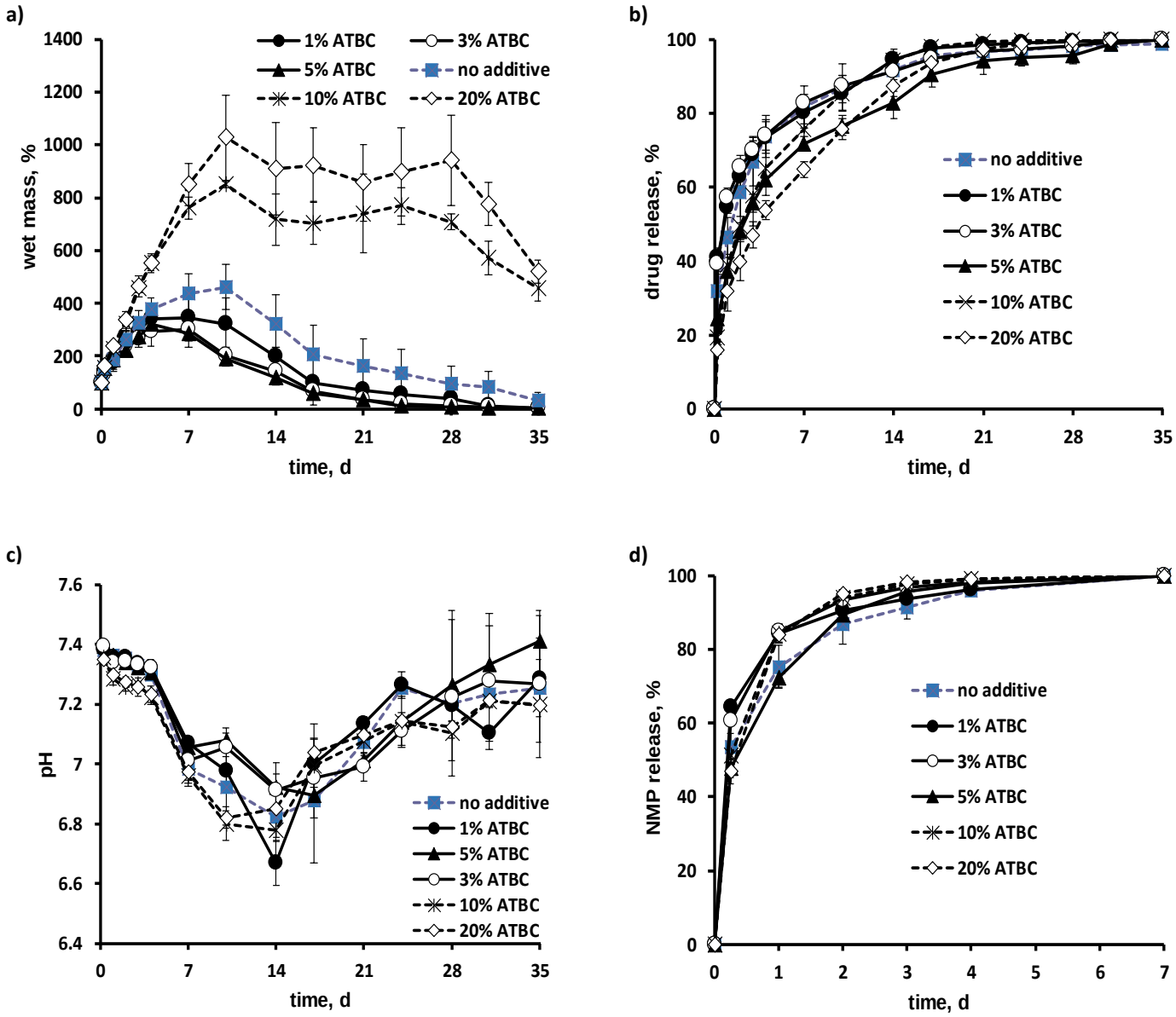

Figure 3.4.9: Effects of the addition of different amounts of ATBC on the: a) wet mass, b) drug release, c) pH of the release medium, and d) NMP release of/from *in-situ* forming implants upon exposure to phosphate buffer pH 7.4 at 37 °C. Mean values +/- standard deviation are indicated (n=3).

3.4.6 Conclusion

Interestingly, the addition of very different types of additives (Carbopol, PEG 400, HPMC, stearic acid and ATBC) partially had pronounced effects on the morphology and swelling kinetics of the investigated *in-situ* forming PLGA implants. For instance, Carbopol containing systems rapidly disintegrated. However, the impact on dexamethasone release was relatively limited in all cases. Generally, the release rate increased when additives were present, only in the case of ATBC the release rate slightly decreased. The observed rather limited impact of the various additives on drug release might at least partially be attributed to the fact that water-soluble compounds can rapidly leach into the aqueous release medium during implant formation, and to phase separation effects in the case of lipophilic additives.

References

[1] L. Bennett, Other Advances in Ocular Drug Delivery, in: R.T. Addo (Ed.), Ocul. Drug Deliv. Adv. Chall. Appl., Springer International Publishing, 2016: pp. 165–185. doi:10.1007/978-3-319-47691-9_10.

[2] C.B. Toris, M.E. Yablonski, Y.-L. Wang, C.B. Camras, Aqueous humor dynamics in the aging human eye, Am. J. Ophthalmol. 127 (1999) 407–412. doi:10.1016/S0002-9394(98)00436-X.

[3] A. Urtti, Challenges and obstacles of ocular pharmacokinetics and drug delivery, Adv. Drug Deliv. Rev. 58 (2006) 1131–1135. doi:10.1016/j.addr.2006.07.027.

[4] A. Chan, L.-S. Leung, M.S. Blumenkranz, Critical appraisal of the clinical utility of the dexamethasone intravitreal implant (Ozurdex®) for the treatment of macular edema related to branch retinal vein occlusion or central retinal vein occlusion, Clin. Ophthalmol. Auckl. NZ. 5 (2011) 1043–1049. doi:10.2147/OPTH.S13775.

[5] J. Siepmann, F. Siepmann, Mathematical modeling of drug delivery, Int. J. Pharm. 364 (2008) 328–343. doi:10.1016/j.ijpharm.2008.09.004.

[6] J. Siepmann, F. Siepmann, Modeling of diffusion controlled drug delivery, J. Controlled Release. 161 (2012) 351–362. doi:10.1016/j.jconrel.2011.10.006.

[7] M.P. Do, C. Neut, E. Delcourt, T. Seixas Certo, J. Siepmann, F. Siepmann, In situ forming implants for periodontitis treatment with improved adhesive properties, Eur. J. Pharm. Biopharm. 88 (2014) 342–350. doi:10.1016/j.ejpb.2014.05.006.

[8] M.P. Do, C. Neut, H. Metz, E. Delcourt, K. Mäder, J. Siepmann, F. Siepmann, In-situ forming composite implants for periodontitis treatment: How the formulation determines system performance, Int. J. Pharm. 486 (2015) 38–51. doi:10.1016/j.ijpharm.2015.03.026.

[9] M.P. Do, C. Neut, H. Metz, E. Delcourt, J. Siepmann, K. Mäder, F. Siepmann, Mechanistic analysis of PLGA/HPMC-based in-situ forming implants for periodontitis treatment, Eur. J. Pharm. Biopharm. 94 (2015) 273–283. doi:10.1016/j.ejpb.2015.05.018.

[10] A. Brunner, K. Mäder, A. Göpferich, pH and Osmotic Pressure Inside Biodegradable Microspheres During Erosion1, Pharm. Res. 16 (1999) 847–853. doi:10.1023/A:1018822002353.

[11] A.G. Ding, S.P. Schwendeman, Determination of water-soluble acid distribution in poly(lactide-co-glycolide), J. Pharm. Sci. 93 (2004) 322–331. doi:10.1002/jps.10524.

[12] L. Li, S.P. Schwendeman, Mapping neutral microclimate pH in PLGA microspheres, J. Controlled Release. 101 (2005) 163–173. doi:10.1016/j.jconrel.2004.07.029.

[13] A.G. Ding, S.P. Schwendeman, Acidic Microclimate pH Distribution in PLGA Microspheres Monitored by Confocal Laser Scanning Microscopy, Pharm. Res. 25 (2008) 2041–2052. doi:10.1007/s11095-008-9594-3.

[14] A. Schädlich, S. Kempe, K. Mäder, Non-invasive in vivo characterization of microclimate pH inside in situ forming PLGA implants using multispectral fluorescence imaging, J. Controlled Release. 179 (2014) 52–62. doi:10.1016/j.jconrel.2014.01.024.

[15] I. Grizzi, H. Garreau, S. Li, M. Vert, Hydrolytic degradation of devices based on poly(dl-lactic acid) size-dependence, Biomaterials. 16 (1995) 305–311. doi:10.1016/0142-9612(95)93258-F.

[16] L. Lu, C.A. Garcia, A.G. Mikos, In vitro degradation of thin poly(DL-lactic-co-glycolic acid) films, J. Biomed. Mater. Res. 46 (1999) 236–244.

[17] J. Siepmann, K. Elkharraz, F. Siepmann, D. Klose, How Autocatalysis Accelerates Drug Release from PLGA-Based Microparticles: A Quantitative Treatment, Biomacromolecules. 6 (2005) 2312–2319. doi:10.1021/bm050228k.

[18] D. Klose, F. Siepmann, K. Elkharraz, S. Krenzlin, J. Siepmann, How porosity and size affect the drug release mechanisms from PLGA-based microparticles, Int. J. Pharm. 314 (2006) 198–206. doi:10.1016/j.ijpharm.2005.07.031.

[19] N. Faisant, J. Siepmann, J.P. Benoit, PLGA-based microparticles: elucidation of mechanisms and a new, simple mathematical model quantifying drug release, Eur. J. Pharm. Sci. 15 (2002) 355–366. doi:10.1016/S0928-0987(02)00023-4.

[20] H. Gasmi, J.-F. Willart, F. Danede, M.C. Hamoudi, J. Siepmann, F. Siepmann, Importance of PLGA microparticle swelling for the control of prilocaine release, J. Drug Deliv. Sci. Technol. 30 (2015) 123–132. doi:10.1016/j.jddst.2015.10.009.

[21] T.G. Park, Degradation of poly(d,l-lactic acid) microspheres: effect of molecular weight, J. Controlled Release. 30 (1994) 161–173. doi:10.1016/0168-3659(94)90263-1.

[22] N. Passerini, D.Q.M. Craig, An investigation into the effects of residual water on the glass transition temperature of polylactide microspheres using modulated temperature DSC, J. Controlled Release. 73 (2001) 111–115. doi:10.1016/S0168-3659(01)00245-0.

[23] P. Blasi, S.S. D'Souza, F. Selmin, P.P. DeLuca, Plasticizing effect of water on poly(lactide-co-glycolide), J. Controlled Release. 108 (2005) 1–9. doi:10.1016/j.jconrel.2005.07.009.

[24] F. von Burkersroda, L. Schedl, A. Göpferich, Why degradable polymers undergo surface erosion or bulk erosion, Biomaterials. 23 (2002) 4221–4231. doi:10.1016/S0142-9612(02)00170-9.

[25] L.P. Tan, S.S. Venkatraman, P.F. Sung, X.T. Wang, Effect of plasticization on heparin release from biodegradable matrices, Int. J. Pharm. 283 (2004) 89–96. doi:10.1016/j.ijpharm.2004.06.022.

[26] M.P. Do, C. Neut, H. Metz, E. Delcourt, K. Mäder, J. Siepmann, F. Siepmann, In-situ forming composite implants for periodontitis treatment: How the formulation determines system performance, Int. J. Pharm. 486 (2015) 38–51. doi:10.1016/j.ijpharm.2015.03.026.

GENERAL CONCLUSION AND FUTURE PERSPECTIVES

General Conclusion

Diseases affecting the posterior segment of the eye, such as age-related macular degeneration, diabetic retinopathy and uveitis, can potentially be sight-threatening. For an effective treatment of these diseases, drugs have to reach the retina in the back of the eye. With eye drops, only a very small part of the administered drug dose (approximately 0.001 – 0.0004 %) is generally found inside the vitreous. Thus, often intraocular injections are required. However, molecules with a low molecular weight like dexamethasone can freely diffuse in the vitreous humor and can cross the blood-retinal barrier. This leads to a short intravitreal half-live of just a few hours for example. To reduce the administration frequency and sustain the drug release, biodegradable implants offer an interesting potential. Poly(lactic-co-glycolic) acid (PLGA) and poly(lactic acid) (PLA) are frequently used to control the drug release due to their good biocompatibility and biodegradability. In-situ forming implants (ISFIs) and pre-formed implants prepared via hot melt extrusion (HME) both offer interesting possibilities for a sustained release in the vitreous. The drug release, swelling and degradation behavior of both types of systems were studied in more detail as well as the influence of different additives to ISFIs. A good understanding of the underlying mechanism can facilitate the development of innovative implants with controlled drug release profiles.

In the *first part* of this PhD thesis, different formulations of in-situ forming implants containing PLGA and N-methyl pyrrolidone (NMP) were prepared to control the delivery of dexamethasone. The influence of the volume of the release medium used for in vitro testing, the initial drug content, the molecular weight of the polymer and the polymer concentration was studied. The systems were characterized with respect to their morphology, dynamic changes of wet and dry mass upon exposure to the release medium, pH of the surrounding bulk fluid, molecular weight of the PLGA and water/NMP content when being exposed to phosphate buffer pH 7.4. The volume of the release medium showed no significant influence on the implants' characteristics. The ISFIs can be expected to be rather robust to different vitreous humor volumes in vivo. Interestingly, at an initial drug loading of 7.5%, the drug solubility inside the implants and in the surrounding bulk fluid has a limiting effect on the drug release. Additionally, the PLGA molecular weight has a high influence of the swelling behavior of the system. A longer polymer chain is less hydrophilic and thus, the water penetration into the system is reduced. Furthermore, the polymer concentration is decisive for the swelling behavior and the precipitation of the implants. All ISFIs were hollow inside, however, the size of the cavities was dependent on the PLGA concentration. This affected drug release and polymer degradation. A

thicker implant wall hinders the diffusion of the drug and acids, that are generated during the hydrolytic ester cleavage, and increases autocatalytic effects.

In the *second part* of this PhD thesis, two different types of PLGA and one type of PLA were used to prepare pre-formed implants containing dexamethasone via hot melt extrusion (HME). The molecular weight of the different polymers remained comparable, whereas the amount of lactic acid:glycolic acid ratio was varied (50:50, 75:25, 100:0). Additionally, different dexamethasone loadings (from 1 to 15 %) were studied. To characterize the implants, the drug release, the dynamic changes in wet and dry mass, the molecular weight of the polymer and the pH of the surrounding medium were examined. Interestingly, the polymer swelling is crucial for the drug release. At early time points, only limited amounts of water penetrate into the systems (the macromolecules are highly entangled). A small amount of water inside the implants can only dissolve a limited amount of the drug. Even though the amount of water is low, it already initiates the biodegradation of the polymer chain. The macromolecules decrease in size and become less entangled. The formed acids inside the implant lead to an increase in osmotic pressure and more water diffuses into the system. When a critical polymer molecular weight threshold (around 8kDa) is reached, the implant swelling increases substantially. A higher amount of water can dissolve greater amounts of the drug, thus initiates the drug release after a certain lag time. To conclude, the polymer swelling "orchestrates" the drug release.

To further corroborate the impact of the polymer swelling and drug release mechanisms of PLGA-based pre-formed implants (prepared by HME) and *in-situ* forming implants prepared with NMP, different dyes were used in the *third part* of this PhD thesis. To illustrate the water penetration, methylene blue was used to stain the release medium. Riboflavin with its yellow color was used as a water-soluble "model drug" whereas Sudan-III-red was used as a poorly water-soluble dye. For the pre-formed implants, the "orchestrating" role of the water penetration as shown in part two could be visualized. Initially, the implant swelling is limited and insufficient to dissolve the drug. Thus, during the first days there is no noteworthy drug release. As soon as the water content increases and large amounts of water are found inside the implants, the drug release begins. For in-situ forming implants, the results show that a higher polymer concentration and smaller macrovoid slows down the methylene blue penetration (and consequently the water penetration) into the implants. Therefore, the vitamin release decreases as well. This confirms the findings of part one.

The *fourth part* of this PhD thesis studies the impact of different types of additives on important characteristics of in-situ forming implants prepared with PLGA, NMP and dexamethasone. Additives used in this study were crosslinked poly(acrylic acid) (Carbopol), poly(ethylene glycol) (PEG 400), hydroxypropyl methylcellulose (HPMC K100, HPMC E15), stearic acid and acetyltributyl citrate (ATBC). The concentration of the additives were varied between 1 and 5 % (or up to 20 % in case of ATBC). Dynamic changes in the implants' wet mass, dexamethasone release, pH of the release medium and NMP leaching were monitored upon exposure to phosphate buffer pH 7.4. Additionally, the morphology of the implants was studied using optical and scanning electron microscopy. The morphology and swelling kinetics of the *in-situ* forming implants were in some cases significantly altered, depending on the additive. However, the dexamethasone release was mostly unaffected. Generally, the presence of additives increased the drug release slightly, whereas ATBC had the opposite effect and slightly decreased it. The predominantly limited effect on the drug release might be caused by rapid leaching of the water-soluble additives into the release medium and the impact of lipophilic additives might be limited due to phase separation effects.

In conclusion, the impact of different parameters, such as polymer molecular weight and concentration, on the swelling behavior and the drug release of ISFIs were shown. With the aid of additives those can be further influenced. Moreover, the "orchestrating" role of implant swelling on the drug release of pre-formed implants was demonstrated and further corroborated with the aid of dyes.

Future perspectives

In order to further elaborate the findings of this thesis, future studies should include the following points:

- Size reduction of the systems
    - Decreasing the substantial swelling behavior for ISFIs using additives or other solvents to limit potential visual obstruction
    - Reduction of the length and diameter of pre-formed implants using a smaller die to decrease the required needle size and, thus, the pain during the injection
- Reduction of the burst release of ISFIs
    - Influence the implant formation in order to limit the significant drug release during the first days using other solvents or additives
- Sterilization
    - Influence of γ-irradiation on the PLGA molecular weight, release kinetics and implant formation in case of ISFIs or surface morphology in case of pre-formed implants
- In-vivo studies
    - Studying the biocompatibility of NMP for intravitreal injections
    - Studying the influence of pH drops in the vitreous
    - Evaluation of the drug release, swelling and degradation behavior *in-vivo*

Abstract

PLGA IMPLANTS FOR OCULAR DRUG DELIVERY

Until today, the treatment of posterior eye diseases, such as age-related macular degeneration, diabetic retinopathy and uveitis, remains challenging. The eye with its different ocular barriers is well protected from external factors. Those barriers also reduce the bioavailability of drugs to the vitreous. After a topical administration, only a limited amount (0.001 – 0.0004 %) reaches the vitreous. This is caused by for example reflexive blinking, tear dilution and a low corneal permeability of the drug. After a systemic or oral administration, the blood-aqueous and the blood-retinal barrier hinder the drug from entering and only around 2 % of the administered drug is found in the vitreous. In order to reach therapeutic concentrations, a high dose has to be given which in turn increases the risk for systemic side effects. The most efficient way to treat posterior diseases remains the intravitreal injection. However, small lipophilic molecules like dexamethasone can easily diffuse through the retina and the blood-ocular barriers and, thus, have a limited half-life of just a few hours. Since many of the posterior diseases are chronic, a frequent intravitreal injection would be necessary. Every intravitreal injection bears the risks for retinal detachment, hemorrhage, and other side effects. Biodegradable implants for intravitreal administration can prolong the drug release and in turn decrease the side effects. Poly(lactic-co-glycolic acid) (PLGA) is a widely used polymer that is biocompatible and biodegradable. It can also sustain the drug release from a few days up to several months. In this study, *in-situ* forming implants (ISFI) and pre-formed implants prepared via hot melt extrusion were studied in depth. The aim of this work was (i) to study the impact of the volume of the release medium, polymer type and concentration as well as drug content of different ISFI, (ii) to evaluate the drug release, swelling and degradation behavior of pre-formed implants prepared with different drug loadings and polymer types, (iii) to visualize the drug release and water uptake of ISFI and pre-formed implants using colored model drugs and (iv) to investigate the effect of varying amounts of different additives on key features of ISFI. This knowledge can help to manufacture implants with different release profiles. Our studies show that ISFI are rather robust regarding different volumes of the vitreous humor that could be encountered in vivo. However, the polymer molecular weight and polymer concentration have a strong influence on the morphology and swelling behavior of the implants. Consequently, the degradation and drug release are affected. For pre-formed implants the swelling "orchestrates" the drug release. In the beginning only limited amounts of water can diffuse into the implants. Thus, only insignificant amounts of the drug are dissolved and can be released. When the PLGA starts to degrade, the polymer becomes more hydrophilic and bigger amounts of water can penetrate. This polymer swelling facilitates drug dissolution and diffusion and initiates the drug release. The studies using colored model drugs corroborate the role of water penetration and drug dissolution for pre-formed implants. Concerning ISFI, it visualized the importance of the polymer concentration on the resulting inner implant structure and consequently the water uptake and drug release. The swelling behavior and morphology of ISFI could also be significantly altered using different additives. The overall effect on the drug release was limited.

Key words: PLGA, implant, swelling, diffusion, dissolution, drug release mechanism